

MAS Thesis

Analysis of Hydroclimatic Trends in the Aconcagua basin, central Chile

Lilian REYES CARBAJAL

Master of Advances Studies in Water resources Management and
Engineering
EPF Lausanne - ETH Zurich

Supervisors
Dr. Francesca Pellicciotti
Dr. Peter Molnar

Abstract

In this study, trends in streamflow, precipitation and temperature at the seasonal timescale for the period of record 1970-1992 are analysed for the Aconcagua River basin in central Chile. In this mountainous watershed, glaciers and snow covers are of critical importance for water resources, and for this reason studies of variations in the hydroclimatic variables become relevant. Data of daily resolution are used with the purpose to explain changes that may not be detected in data with higher resolution. In this sense, this study complements the work by Pellicciotti et al., (2006) using monthly data. The Mann-Kendall nonparametric test is used to identify the significant trends. Trends in streamflow are examined together with changes in precipitation and temperature. Analysis of atmospheric circulation indices such as El Niño Southern Oscillation (ENSO) is also carried out. In addition, glacier coverage is related to the observed trends in the basin.

The main identified trend although not significant is the decreasing trend in summer runoff in the upper section of the watershed, where snow and glacier melting is an important source of water. Trends in precipitation are not sufficient to explain the observed trend in runoff, since precipitation is in general increasing but not in a significant manner.

The reduction of summer streamflow may be explained by the glacier retreat in the region that was reported in previous studies. This is also suggested by the significant positives trends in temperature which were observed in this work.

Correlation with Sea Surface Temperature shows an increase in precipitation in winter and spring during El Niño events, generating peaks in winter runoff and accumulation of snow that increases the snowmelt in spring and summer.

Contents

Abstract	i
Contents	ii
List of Figures	iv
List of Tables	vii
1. INTRODUCTION		1
1.1 Motivation	1
1.2 Goals	2
1.3 Methodology	2
1.4 Literature review	3
1.5 Overview	4
1.6 Abbreviations	5
2. STUDY SITE		
2.1 Climate	6
2.1.1 Warm Mediterranean	6
2.2.2 Cold climate of the Andes Mountains	7
2.2 Hydrogeology	8
2.3 Population	8
2.4 Activities and extractive water uses	9
2.4.1 Activities	9
2.4.2 Water uses	9
3. DATA PROCESSING		10
3.1 Data availability	10
3.2 Data base quality	12
3.3 Data Filling Procedure	13
3.3.1 Streamflow	13
3.3.1.1 Linear interpolation	13
3.3.1.2 Scaling Replacement Method	13
3.3.1.3 Data variability	16
3.3.2 Precipitation	18
3.3.3 Temperature	23
4. TREND ANALYSIS		
4.1 Parameters or indices	26
4.1.1 Streamflow	26
4.1.2. Precipitation	27
4.1.3 Temperature	27
4.2 Time series analysis	28
4.2.1 Streamflow	28
4.2.2.1 Station 14	31
4.2.2.2 Station 16	32
4.2.2.3 Station 17	33

4.2.2.4 Station 18	34
4.2.2 Precipitation	35
4.2.2.1 Station 18	38
4.2.2.2 Station 25	39
4.2.2.3 Station 26	40
4.2.2.4 Station 27	41
4.2.2.5 Station 29	42
4.2.2.6 Station 34	43
4.2.3 Temperature	44
4.2.3.1 Station 29	45
4.3 Trend Analysis Statistics ...	46
4.3.1 Method	46
4.3.2 Streamflow	47
4.3.3 Precipitation	49
4.3.4 Temperature	51
 5. CORRELATION ANALYSIS WITH LARGE-SCALE CIRCULATION PATTERNS	 52
5.1 Correlation with Streamflow	53
5.2 Correlation with Precipitation	55
5.3 Correlation with Temperature	57
 6 GLACIER COVERAGE	 58
 7. DISCUSSION	 62
 8. CONCLUSION	 64
 APPENDIX	 66
A1. Parameters of the Scaling replacement method for streamflow gaps	66
A2. Parameters of the Scaling replacement method for temperature gaps	68
A3. Mann- Kendall Test- Code Matlab	69
 BIBLIOGRAPHY	 70

List of figures

Figure a: Mean seasonal streamflow and mean precipitation total at station 14 in year 1986.

Figure 1: Aconcagua basin location in Chile

Figure 2: Main cities in the Aconcagua watershed

Figure 3: Distribution of the population in the Aconcagua river basin. Below each community the total number of inhabitants is indicated

Figure 4: Spatial distribution of streamflow and meteorological stations in the Aconcagua basin

Figure 5: Streamflow at Station 19 for year 1970

Figure 6: Runoff data filling procedure

Figure 7: Data gap at a runoff station and the scaling replacement parameters

Figure 8: Spatial distribution of the streamflow stations used for the Analysis

Figure n° 9: (a) Scatter plot between daily streamflow between station 14 and station 16. (b) Between station 14 and station 17. (c) Between station 14 and 18. (d) Between station 16 and 17. (e) Between station 16 and 18. (f) Between station 17 and 18. The cross correlation coefficient r is shown for each plot.

Figure 10: Frequency of daily streamflow at station 14 for period 1970-2003. (a) Summer. (b) Autumn. (c) Winter. (d) Spring. (BFD): Before filling data. (AFD): After filling data.

Figure 11: Frequency of daily streamflow at station 16 for period 1970-2003. (a) Summer. (b) Autumn. (c) Winter. (d) Spring. (BFD) Before filling data. (AFD) After filling data.

Figure 12: Frequency of daily streamflow at station 17 for period 1970-2003. (a) Summer. (b) Autumn. (c) Winter. (d) Spring. (BFD) Before filling data. (AFD) After filling data.

Figure 13: Frequency of daily streamflow at station 18 for period 1970-2003. (a) Summer. (b) Autumn. (c) Winter. (d) Spring. (BFD) Before filling data. (AFD) After filling data.

Figure 14: Station 18 correlated with station 29 used to fill its data, ($r_1=r^2$). (a) Autumn. (b) Winter. (c) Spring

Figure 15: Station 25 correlated with station 27 used to fill its data, ($r_1=r^2$). (a) Autumn. (b) Winter. (c) Spring

Figure 16: Station 26 correlated with station 30 used to fill its data, ($r_1=r^2$). (a) Autumn. (b) Winter. (c) Spring

Figure 17: Station 27 correlated with station 29 used to fill its data, ($r_1=r^2$). (a) Autumn. (b) Winter. (c) Spring

Figure 18: Station 29 correlated with station 27 used to fill its data, ($r_1=r^2$). (a) Autumn. (b) Winter. (c) Spring

Figure 19: Station 34 correlated with station 29 used to fill its data, ($r_1=r^2$). (a) Autumn. (b) Winter. (c) Spring

Figure 20: Frequency of daily temperature maximum at station 29 for period 1970-2003.
(a) Summer. (b) Autumn. (c) Winter. (d) Spring. (BFD): Before filling data. (AFD): After filling data.

Figure n° 21: Frequency of daily temperature minimum at station 29 for period 1970-2003.
Summer. (b) Autumn. (c) Winter. (d) Spring. (BFD): Before filling data. (AFD): After filling data.

Figure 22: Seasonal average of streamflow aercentiles throughout the record 1970-2003 for stations 14, 16, 17 and 18 (a) Percentile 0. (b) Percentile 25. (c) Percentile 50. (d) Percentile 75. (e) Percentile 90. (f) Percentile 100.

Figure 23: Streamflow series at station 14. The data is presented for the percentiles P0, P25, P50, P75, P90 and P100 (a) SUMMER (b) AUTUMN (c) WINTER (d) SPRING

Figure 24: Streamflow series at station 16. The data is presented for the percentiles P0, P25, P50, P75, P90 and P100 (a) SUMMER (b) AUTUMN (c) WINTER (d) SPRING

Figure 25: Streamflow series at station 17. The data is presented for the percentiles P0, P25, P50, P75, P90 and P100 (a) SUMMER (b) AUTUMN (c) WINTER (d) SPRING

Figure 26: Streamflow series at station 18. The data is presented for the percentiles P0, P25, P50, P75, P90 and P100 (a) SUMMER (b) AUTUMN (c) WINTER (d) SPRING

Figure 27: Precipitation parameters in stations 18, 25,26,27,29 and 34. (a) Seasonal Precipitation Totals, averaged for period 1970-2003. (b) Seasonal frequency of dry days, averaged for period1970-2003. (c) Seasonal maximum precipitation averaged for record 1970-2003

Figure 28: Precipitation series at station 18. The data is presented for Ptotal, Pmax and Freq (P=0). (a) AUTUMN. (b)WINTER (c) SPRING.

Figure 29: Precipitation series at station 25. The data is presented for Ptotal, Pmax and Freq (P=0). (a) AUTUMN. (b)WINTER (c) SPRING.

Figure 30: Precipitation series at station 26. The data is presented for Ptotal, Pmax and Freq (P=0). (a) AUTUMN. (b)WINTER. (c) SPRING

Figure 31: Precipitation series at station 27. The data is presented for Ptotal, Pmax and Freq (P=0). (a) AUTUMN. (b)WINTER. (c) SPRING

Figure 32: Precipitation series at station 29. The data is presented for Ptotal, Pmax and Freq (P=0). (a) AUTUMN. (b)WINTER. (c) SPRING

Figure 33: Precipitation series at station 34. The data is presented for Ptotal, Pmax and Freq (P=0). (a) AUTUMN. (b)WINTER. (c) SPRING

Figure 34: Temperature parameters at station 29 averaged for period 1970-2003. (a) Temperature maximal, minimal and Diurnal Range. (b) Frequency of $T_{min} > 0$

Figure 35: Temperature series at station 29 for the SUMMER season. Data is presented for temperature maximum, minimum, the diurnal range and frequency of $T_{min} > 0$. (a) SUMMER. (b) AUTUM. (c) WINTER. (d) SPRING

Figure 36: Trend test statistics Z at 5% of significance level for seasonal streamflow series for the period of record 1970-1992. The sign of Z indicates trend direction. (a) Station 14, (b) Station 16, (c) Station 17, (d) Station 18. No statistically significant trends

Figure 37: Trend test statistics Z for seasonal precipitation series for the period of record 1970-1992. The sign of Z indicates trend direction. (a) Station 18, (b) Station 25, (c) Station 26, (d) Station 27. (e) Station 29, (f) Station 34. No trends are statistically significant at the 5% significance level.

Figure 38: Trend test statistics Z for seasonal temperature series in station 29 for the period of record 1970-1992. The sign of Z indicates trend direction. The arrows indicate significant trends at 5% of significance level.

Figure 39: Time series of standardised 5 months running means of the Sea Surface Temperature (SST) for “Niño 3” and of standardised monthly streamflow percentiles: P0, P50 and P100 for period of record 1970-1992. (a) Station 14. (b) Station 16. (c) Station 17. (d) Station 18. El Niño events are indicated by the red curves above the threshold $+0.5^{\circ}\text{C}$

Figure 40: Time series of standardised 5 months running means of the Sea Surface Temperature (SST) for “Niño 3” and of standardised monthly precipitation parameters: $\text{Freq}(P=0)$ and P_{total} for period of record 1970-1992. (a) Station 18. (b) Station 25. (c) Station 26. (d) Station 27. (e) Station 29. (f) Station 34. El Niño events are indicated by the red curves above the threshold $+0.5^{\circ}\text{C}$

Figure 41: Time series of standardised 5 months running means of the Sea Surface Temperature (SST) for “Niño 3” and of standardised monthly temperature parameters: T_{min} and T_{max} for period of record 1970-1992 in station 29. El Niño events are indicated by the red curves above the threshold $+0.5^{\circ}\text{C}$

Figure 42 Watershed of streamflow stations 14, 16, 17 and 18

Figure 43: Histogram of altitude in the watershed of station 14

Figure 44: Histogram of altitude in the watershed of station 16. Minimum, maximum and mean altitudes of the areas covered by glaciers are indicated

Figure 45: Histogram of altitude in the watershed of station 17.

Figure 46: Histogram of altitude in the watershed of station 18. Minimum, maximum and mean altitudes of the areas covered by glaciers are indicated

List of tables

Table 1: Water Use per Type of Activity in the Aconcagua Basin

Table 2: Streamflow stations

Table 3: Meteorological stations

Table 4: Number of missing years within the period 1970 and 2003 for streamflow and meteorological stations

Table 5: Streamflow stations used for the analysis

Table 6: Meteorological stations used for the analysis

Table 6-a: Scaling replacement equation and parameters

Table 7: Cross correlation matrix of runoff stations

Table 8: Seasonal Variance for station 14, 15, 16 and 17, computed before and after the filling data process for the period 1970 to 2003

Table n° 9: Linear regression parameter A_i and correlation coefficient (r^2) for autumn winter and spring at all the precipitation stations

Table 10: Cross correlation matrix of temperature stations

Table 11: Variance of minimum and maximum temperature at station 29 for period 1970-2003.

Table n°12: Indices used in streamflow trend analysis

Table 13: Indices used in precipitation trend analysis

Table 14: Indices Used in Temperature trend Analysis

Table 15: Seasonal runoff percentage at the analysed stations. Period 1970-2003

Table 16: Mean, maximum and minimum value of the streamflow percentiles (m^3s^{-1}) throughout the record 1970-2003

Table 17: Seasonal percentage of precipitation totals in the analysed stations. Period 1970-2003

Table 18: Mean, maximum and minimum value of precipitation parameters for the period 1970-2003

Table 19: Mean, Maximum and Minimum value of Temperature Parameters for the period 1970-2003

Table 20 Lag-1 autocorrelation coefficients of the seasonal streamflow series at stations 14, 16, 17 and 18 for period of record 1970-1992

Table 21: Trend test statistics Z at 5% of significance level for seasonal streamflow series. Period of record 1970-1992

Table 22: Seasonal lag-1 autocorrelation coefficient of precipitation series at stations 18, 25, 26, 27, 29 and 34 for the period of record 1970-1992

Table 23: Trend test statistics Z at 5% of significance level for seasonal precipitation series period of record 1970-1992

Table 24: Seasonal lag-1 autocorrelation coefficient of temperature series in 29. Period of record 1970-1992

Table 25: Trend test statistics Z at 5% of significance level for seasonal temperature series. Period of record 1970-1992

Table 26: Correlation coefficients between mean seasonal streamflow percentiles: P0, P50, P100 and seasonal standardised Sea Surface Temperature (SST) for “Niño 3”. Period of record 1970-1992

Table 27: Correlation coefficients between mean seasonal precipitation parameters: Freq. (P=0) and Ptotal and seasonal standardised Sea Surface Temperature (SST) for “Niño 3”. Period of record 1970-1992

Table 28: Correlation coefficients between mean seasonal temperature parameters: Tmin and Tmax and seasonal standardised Sea Surface Temperature (SST) for “Niño 3”. Period of record 1970-1992

Table 29: Properties of the Streamflow stations Watershed

Table 30: Properties of Glaciers in Watershed of stations 16 and 18

CHAPTER 1

INTRODUCTION

1.1 Motivation

Water resources originating from high mountains are a crucial source of water in large regions of the world. This MAS thesis being part of a larger project investigation aimed to assess past and future impacts on climatic variations on water resources from highly glacierised basins is focusing its attention on the Aconcagua River Basin in central Chile. The Aconcagua is one of the major basins in Chile with growing population developing agriculture and industry then growing potential for conflicts on water allocation in case water scarcity.

The water availability in the basin changes seasonally. In summer (DJF) and spring (SON) when amount of runoff is largest it comes exclusively from snow and ice melt because precipitation is very low (fig. a), whereas in winter (JJA) and autumn (MAM) streamflow in the basin is low and comes from precipitation.

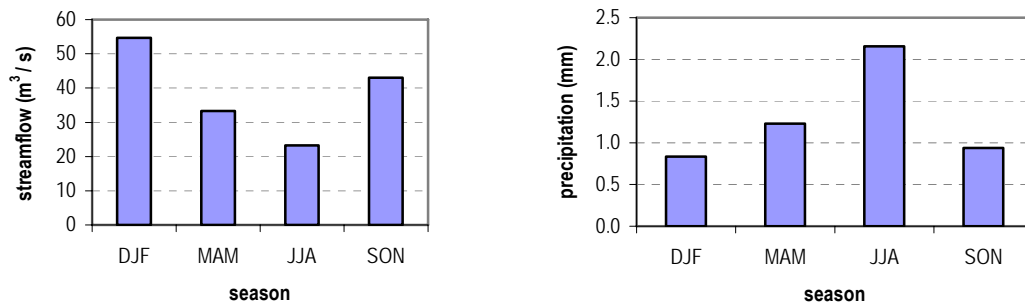


Figure a: Mean seasonal streamflow and mean precipitation total at station 14 in year 1986.

In addition, evidence provided by some recent studies has shown that glaciers in the area are shrinking and the snowline is retreating upwards, a fact that may affect seriously the water availability in summer and spring. For those reasons, the detection of trends in instrumental records of hydroclimatic variables such as air temperature, precipitation and streamflow becomes relevant as a climate variability study for the water resources in the basin. Large scale circulation patterns like Souther Oscilation and its relationship with the precipitation and runoff regime is also an important factor and is taken into account.

1.2 Goals

The goals of this master thesis are:

1. To identify significant trends in observed streamflow, precipitation and temperature data and their occurrence in time and space in the Aconcagua river basin, with attention to its upper section
2. To analyse the connection between observed changes in streamflow, precipitation and air temperature
3. To analyse the connection between significant trends and their occurrence with sub-basin characteristics, in particular glacier coverage
4. To analyse the correlation between hydroclimatic variables and global indices representative of large-scale circulation patterns that are active in the region like El Niño– Southern Oscillation (ENSO)

1.3 Methodology

The first step was to choose the stations to be investigated, and to check the data quality and quantity.

The second step consisted in filling the gaps or discontinuities observed in the selected stations; and to correct errors in data. The techniques used were linear interpolation and scaling replacement method.

The third step was to choose the variables to be analysed. For streamflow they were defined as percentiles, for precipitation it was precipitation totals and frequency of dry days and for temperature minimum, maximum, as well as range and frequency of temperature minimum larger than zero.

The fourth step was to analyse for the presence of trends in the series using the non-parametric Mann-Kendall (MK) test. This test has been widely used in hydrological studies. Its advantages are that it is distribution-free, robust against outliers, and has a higher power than many other commonly used test (e.g., Hess et al., 2001).

The fifth step was to analyse the correlation between El Niño Southern Oscillation and streamflow, precipitation and temperature.

The sixth step consisted in the calculation of the glacier coverage and altitudes in the upper part of the basin and in the analysis of their relationship with the observed trends.

1.4 Literature review

The debate on climate variability and climate change relies heavily on the detection of trends (or lack thereof) in hydroclimatic variables such as air temperature, precipitation and streamflow. In many parts of the world, and in particular in the United States, Canada and Europe, numerous large-scale analyses of hydroclimatic trends have recently been conducted on precipitation and streamflow data at different time scales with the nonparametric Man-Kendal test (e.g. Lettenmaier et al., 1994; Karl & Knight, 1998; Lins & Slack, 1999; Zhang et al., 2001; Molnár & Ramírez, 2001; Burn & Hag Elnur, 2002; Kahya & Kalayci, 2004; Birsan et al., 2005). This is not the case for the South American continent, where analyses of trends in instrumental records of streamflow and precipitation are scarce (e.g. Rosenblüth et al., 1997). Nevertheless some studies on the Aconcagua basin can be found (e.g. Waylen & Caviedes, 1990; Montecinos & Aceituno, 2003), which however have focused on the impact of the El Niño – Southern Oscillation (ENSO) phenomenon on the interannual variability of precipitation and streamflow and not on trends analysis.

The first watershed-based analysis of streamflow and precipitation trends in the Aconcagua River was conducted by Pellicciotti (2006/ in press) using 5 streamflow and 9 precipitation stations in an annual, seasonal and monthly timescale for different periods of records. This study showed a decrease in streamflow in the upper section of the basin on annual and seasonal scales. Changes in precipitation were not sufficient to explain the observed trend in runoff, nevertheless a shift in precipitation seasonality was found together with an increasing trend in temperature at all temporal resolutions. It also appeared that monthly streamflow and precipitation are affected by ENSO events.

Impacts of the El Niño – Southern Oscillation (ENSO) were studied by (e.g. Aceituno, 1988; Waylen & Caviedes, 1990; Montecinos et al., 2000; Montecinos & Aceituno, 2003; Waylen & Poveda, 2002; Schneider & Gies, 2004). One of the main effects of ENSO in central Chile was shown to be an increase in annual precipitation during El Niño events, which results mainly from an increase in winter precipitation (e.g. Waylen & Caviedes, 1990; Montecinos et al., 2000; Montecinos & Aceituno, 2003). A decrease in rainfall during La Niña events, due to the strengthening of the anticyclone, has also been reported (Rubin, 1955; Aceituno, 1988; Rutllant & Fuenzalida, 1991).

On the other hand, evidence of glacier retreat and thinning in central Chile during the 20th century has been reported by Casassa (1995) and Rivera et al. (2002). Rivera et al. (2002) examined glacier surface and thickness variations for 95 Chilean glaciers, and concluded that a general

glacier recession has occurred in central Chile, with an average estimate of 12.8% of area less in the last 51 years from 1945-96. This result is in agreement with findings of previous studies on temperature trends (Rosenblüth et al., 1997, Carrasco et al. (2005), which have indicated statistically significant warming since the end of 19th century to the end of the 20th century in central Chile. For the same reasons, it is likely that also the extension and depth of the seasonal snow covers in the area have been decreasing, as it might be inferred also from the results of Carrasco et al., 2005, which have shown an increase of the snow line elevation in central Chile in the last quarter of the 20th century by 127 m. Glacier changes in the Aconcagua Basin, however, are difficult to document because of limited data (e.g. Rivera et al., 2002).

This thesis will build on the study of Pellicciotti, (2006) by using higher resolution daily data on a seasonal basis with the purpose to identify changes that may have not been clear with monthly data. The correlation with the El Niño – Southern Oscillation (ENSO) will be also analysed as well as the glacier coverage.

1.5 Overview

In the following, the content of this thesis report is briefly outlined:

Chapter 2 – Study Site In this chapter, the main characteristics of the Aconcagua basin are outlined, for instance its location, climate, geology, hydrogeology, population and activities or water uses. A summary of the most relevant information for this study is done on the basis of information by the Chilean Dirección General de Aguas (DGA)

Chapter 3 – Data Processing This chapter is an important preprocessing step before the trend analysis itself. Here the process to select the gauging stations with the most appropriate data is described as well as the methods to complete the records. As a first step the availability of the data provided by DGA was analysed, eliminating stations with more than one year of missing data within the record 1970-2003. The next step was to verify the data quality in the remaining stations, eliminating additional ones in this stage. Finally the discontinuities of data or gaps were filled in for the three climatic variables: streamflow, precipitation and temperature. The techniques used to complete data were linear interpolation, linear regression and scaling replacement method

Chapter 4 – Trend Analysis In this chapter the analysis of the presence of trends was conducted, using the Mann-Kendall (MK) test. The analysis for streamflow was done by percentiles 0, 25, 50, 75, 90 and 100. In the case of precipitation the variables were precipitation totals, the frequency of dry days and maximum precipitation. For temperature the variables were minimum temperature, maximum temperature, diurnal range and frequency of minimum temperature above 0°C. All analysis was conducted on a seasonal basis.

Chapter 5 – Correlation Analysis with Large-Scale Circulation Patterns In order to investigate the influence of global atmospheric circulation patterns on the hydroclimatic variables, correlation analysis between Sea Surface Temperature (SST) and the time series was carried out. In addition the standardised SST for the region Niño 3 was plotted with standardized time series for streamflow, precipitation and temperature in order to figure out the synchronism or relation of El Niño periods with the peaks or extreme events in the time series.

Chapter 6 – Glacier Coverage The drainage areas of the sub basins draining to the analysed streamflow stations were calculated in order to investigate the altitude distribution in the subbasins and those of the glacierized areas.

Chapter 7 – Discussion In this chapter the obtained trends in the time series for streamflow, precipitation and temperature are discussed looking into the relationship among them and as well as others factors like Sea Surface Temperature, El Nino Southern Oscillation and glacial coverage

Chapter 8 – Conclusion This chapter summarize the main conclusions of this master thesis

1.6 Abbreviations

DGA	Dirección General de Aguas (from While)
INE	Instituto Nacional de Estadísticas (from While)
DJF	Summer (December, January, February)
MAM	Autumn (March, April, May)
JJA	Winter (June, July, August)
SON	Spring (September, October, November)
P0	Percentile 0
P25	Percentile 25
P50	Percentile 50
P75	Percentile 75
P90	Percentile 90
P100	Percentile 100
Ptotals	Precipitation Totals
Freq (P=0)	Frequency of dry days
Pmax	Maximum precipitation
Tmin	Minimum temperature
Tmax	Maximum temperature
DR	Diurnal Range
Freq (Tmin>0)	Frequency of minimum temperature >0
SST	Sea Surface temperature
SO	Southern Oscillation
ENSO	El Niño Southern Oscillation
JMA	Japan Meteorological Agency
Wat14	Watershed of station 14
Wat16	Watershed of station 16
Wat17	Watershed of station 17
Wat18	Watershed of station 18

CHAPTER 2

STUDY SITE

The Aconcagua basin is located in the south part of Valparaíso Region, the number 5th in Chile; roughly 50 km north of the national capital Santiago (see Fig. 1). The total area of the watershed is 7 340 km² (representing 45% of Valparaíso Region) and the direction of flow is from east to west. The most important tributaries have their origins in the Andes Mountains at exceptional altitudes such as “Juncal peak” (6110 metres), “Alto de Los Leones” peak (5400 metres) and the “Aconcagua peak” (7021 metres)⁽¹⁾ (See Fig. 1).

The Aconcagua River is formed at 1430 metres by the junction of the Juncal River coming from the west and the Blanco River coming from the south east. From this junction until the outlet in the Concón bay at the Chilean sea, the river is 142 Km. long and considering the Juncal River the length reaches 177 km.⁽¹⁾ In the section between Blanco River and the Andes city a large tributary joins from the north, the Colorado River. Near San Felipe city the Estero Pocuro joins from the south and about 4 km. downstream the Putaendo River joins from the north.⁽¹⁾ Downstream of San Felipe city, others important tributaries can be mentioned such as: Estero Catemu, Estero La Vegas, El Melon and Estero Limanche (see fig. 2).

In the next sections the most relevant characteristics of the basin for this study are given.

2.1 Climate

Two climate types are observed in the Aconcagua basin: warm Mediterranean and cold climate in the high Andes

2.1.1 Warm Mediterranean

This climate present in almost all the basin and is characterized by dried prolonged periods in summer and spring and a differenced wet winter with extreme temperatures that can fall below 0°C. The autumn is also a wet season but much less rainy than winter.

Mean annual temperature is 15.2°C but with strong seasonal differences. In summer temperature increases above 27°C during the day. Mean annual precipitation at the coast is approximately 395 mm/year but in the central part of the basin it is 261 mm/year, presenting dryer areas and less

(1)Source: Dirección General de Aguas

amount of precipitation because of its relief. At higher elevations precipitation increases to 467 mm/year⁽¹⁾.

2.2.2 Cold climate of the Andes Mountains

This climate is found at the highlands above 3000 metres in the Andes, low temperatures and solid precipitation are characteristic of this climate permitting the snow accumulation and glacier coverage in the mountains.

Chile's seasons are reversed to that the Northern hemisphere, summer is from December to February, autumn from March to May, winter from June to August and spring from September to November. In general, for both types of climates, registered amounts of precipitation are largest during the winter season.

Basin-average annual runoff at the coast side of the basin is over 50 mm/year and in the central part (Andes city) the values are less than 20 mm/year⁽¹⁾. Higher values are present in summer and spring as a result of glaciers and snow melt. Lower flows during autumn and winter; this is a special behaviour of the upper part of the watershed above 1000 metres altitude where the regimen of the Aconcagua River is nival. At lower elevations the regime becomes mixed; nivo-pluvial with high flows in winter and spring due to rainfall and snow melt and with a dry season in summer and autumn. The evaporation in the central part (Quillota city) is about 1 361 mm/year and in upper parts (above Andes city) around 2 209 mm/year. The predominant wind direction is SW⁽¹⁾.

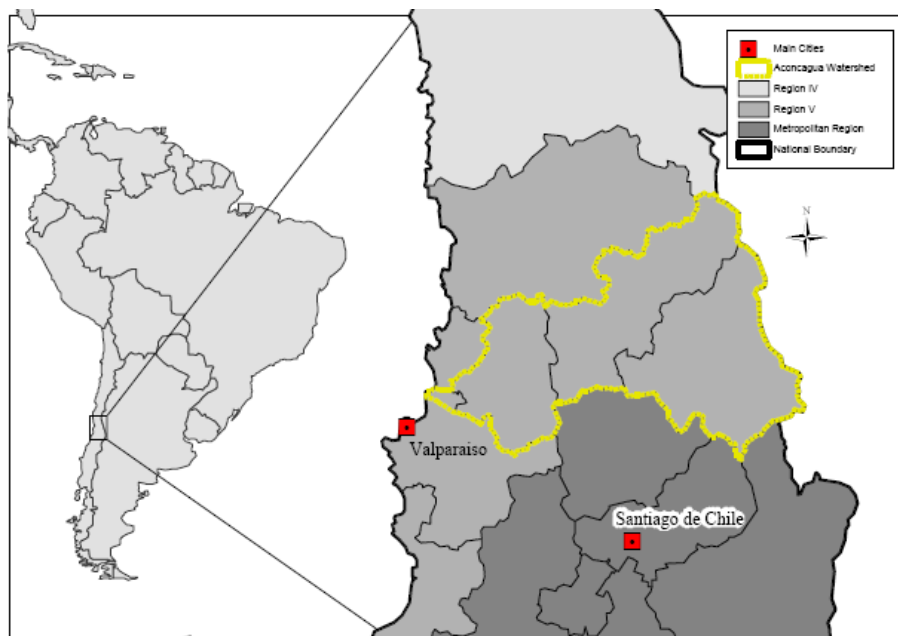


Figure 1: Aconcagua basin location in Chile

(1)Source: Dirección General de Aguas

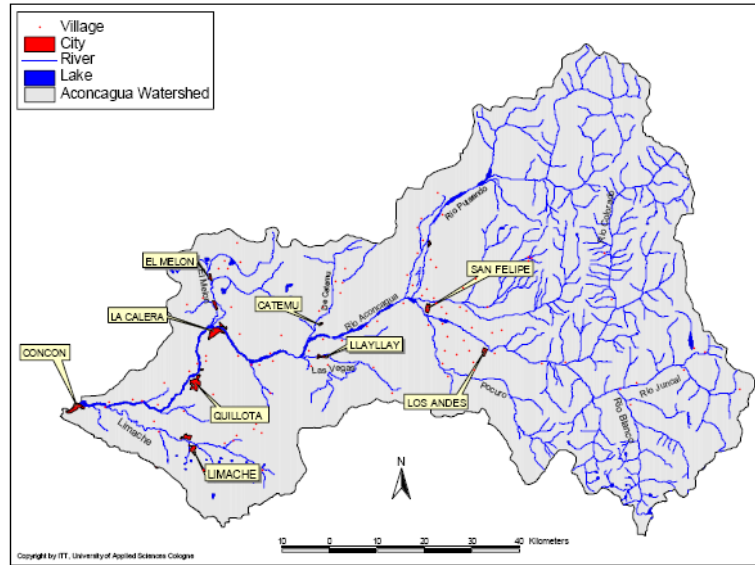


Figure 2: Main cities in the Aconcagua watershed

2.2 Hydrogeology

Groundwater aquifers are located only around the course of the rivers Aconcagua and Putaendo. The water in the aquifers flows in direction of the river streamflow. The rest of the catchment area does not have aquifers since the soil permeability is too low or almost null.

2.3 Population

The total population of the basin is 485 614. The most populated localities are Quillota, San Felipe, Los Andes and La Calera (see Fig. 3). The highest population can be found in the urban centres around the course of the main river ⁽²⁾.

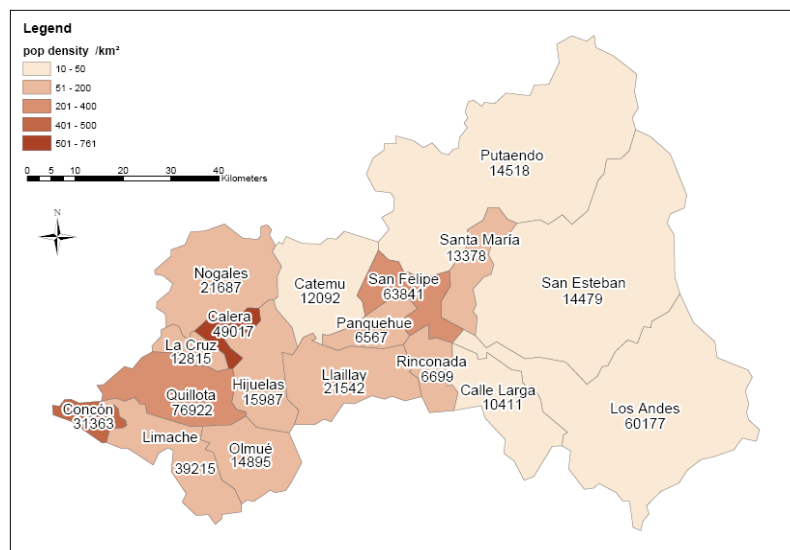


Figure 3: Distribution of the population in the Aconcagua river basin. Below each community the total number of inhabitants is indicated

(2) Data source: INE 2002; INE, Instituto Nacional de Estadísticas, 2001b. Compendio de Estadísticas, INE, Santiago

2.4 Activities and extractive water uses

2.4.1 Activities

The most important activities in the watershed are agriculture, mining and industry. The first one is mainly carried out in the localities San Felipe, Los Andes and La Calera. Cereals are the main product. About the mine industry, the most important is copper exploitation in the vicinity of Andes and Catemu. Another exploited material is limestone that is mined for cement production in La Calera community. Others kind of industries developed in the region are food, meat and fish processing, chemical, cement and canning.

2.4.2 Water Uses

The water use is according to the developed activities in the basin and is summarized in table 1.

Table 1: Water Use per Type of Activity in the Aconcagua Basin

Sectors	Demand ⁽¹⁾
Irrigation	429 175 000 m ³ /year (1997)
Fresh water	129 423 744 m ³ /year
Industrial activities	636 40800 m ³ /year (1997)
Mining	39 248 280 m ³ /year
Hydropower generation	No available information

(1) Source: Dirección General de Aguas

CHAPTER 3

DATA PROCESSING

3.1 Data availability

Daily data was provided by the Chilean Direccion General de Aguas (DGA) for streamflow, precipitation and temperature. Twelve stations for streamflow were given, which had a spatial distribution over the whole basin (see fig. 4) and are listed in table 2. For precipitation, fifteen stations were available with similar distribution and density (see fig. 4). Only four stations had temperature measurements. In table 3 meteorological stations and record lengths are presented.

Table 2: Streamflow stations

Name of Station	DGA number	Period
Rio Putaendo en Resguardo Los Patos	7	1970-2003
Rio Aconcagua en San Felipe	8	1970-2003
Estero Catemu en Puente Santa Rosa	9	1986-2003
Estero Las Vegas en Desembocadura	11	1970-2001
Rio Aconcagua en Romeral	12	1970-2003
Canal Las Vegas en Bocatoma	13	1970-2003
Rio Aconcagua en Chacabuquito	14	1970-2003
Rio Colorado en Colorado	15	1970-2003
Rio Juncal en Juncal	16	1970-2003
Rio Aconcagua en Rio Blanco	17	1970-2003
Rio Blanco en Rio Blanco	18	1970-2003
Estero Pocuro en El Sifon	19	1970-2003

Table 3: Meteorological stations

PRECIPITATION		
Name of Station	DGA number	Period
Resguardo Los Patos	18	1970-2003
El Tartaro	20	1990-2003
Jahuel	24	1989-2003
San Felipe	25	1970-2003
Catemu	26	1970-2003
Los Andes	27	1970-2003
Lo Rojas	28	1970-2003
Vilcuya (*)	29	1970-2003 (1970-2003)*
Rabuco	30	1970-2003
Las Chilcas	31	1990-2003
Quillota (*)	33	1978-2003 (1977-2003)*
Riecillos	34	1970-2003
Los Aromos (*)	37	1974-2003 (1981-2003)*
Quebrada Alvarado	41	1990-2003
Embalse Lliu-Lliu (*)	45	1978-2003 (1979-2003)*

(*) Stations where temperature was also recorded

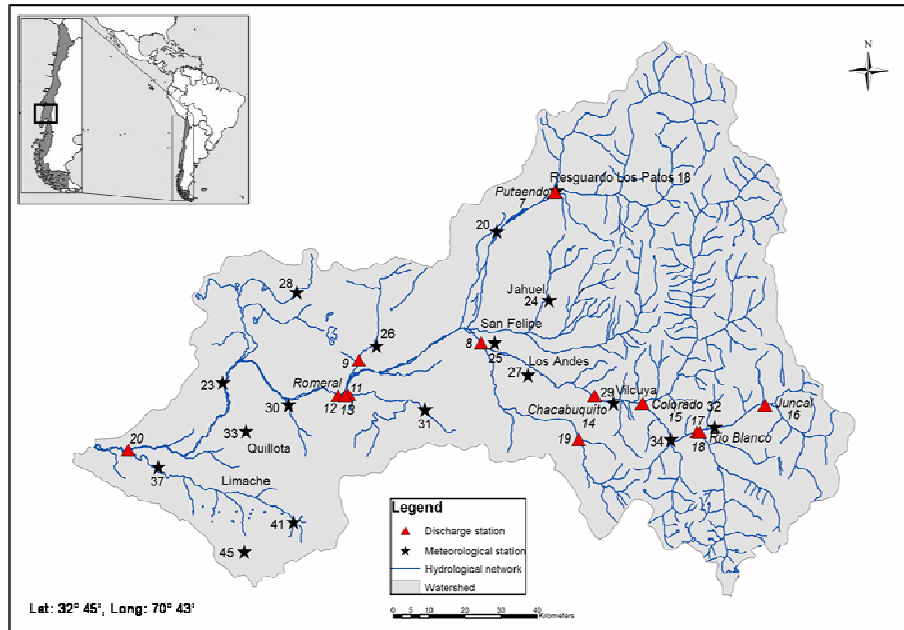


Figure 4: Spatial distribution of streamflow and meteorological stations in the Aconcagua basin

Most of these stations had a record of 34 years from 1970 until 2003 but at the same time many years within this period were missing in several stations, as we can see in table 4. In the subsequent analysis only stations with most complete records were used and stations with more than one year without data were discarded.

Table 4: Number of missing years within the period 1970 and 2003 for streamflow and meteorological stations

N° of missing years	Streamflow Stations (DGA number)	Precipitation Stations (DGA number)	Temperature Stations (DGA number)
0	14	18, 25, 26, 29, 34	29
1	13, 16, 17, 18, 19, 15	27	-
2	7	30	-
3	8, 11	-	-
4	-	37	-
6	-	-	33
8	-	45	-
9	-	33	45
12	-	-	37
16	9	-	-
26	12	-	-
19	-	24	-
20	-	20, 31, 41	-

3.2 Data base quality

Data quality assessment is an important requirement before conducting any statistical analysis since erroneous and missing values can have a serious impact on trends. In this context data for all the remaining stations were analyzed to identifying two problems:

- 1) Discontinuity or data gaps periods within the initial available record 1970 – 2003. This was the case for all the variables: streamflow, precipitation and temperature at all the stations.
- 2) Suspicious data jumps, outliers and other artefacts. This was the case of streamflow at stations: 13, 15 and 19. In figure 5 we can see an example:

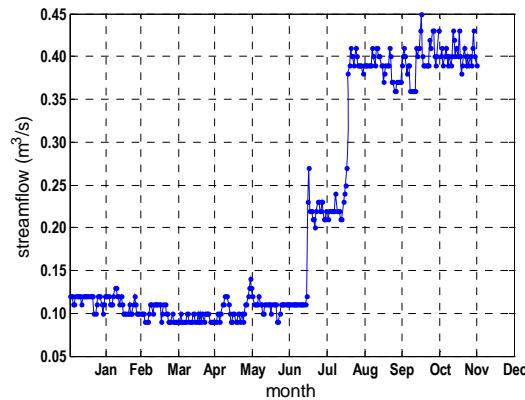


Figure 5: Streamflow at Station 19 for year 1970

Considering this problem and the fact that these stations did not add more information to our question of glacier impact on streamflow changes; stations 13, 15 and 19 were also eliminated. In this way only reliable data was used in order to achieve good results. The remaining stations after the last selection are presented in table 5 and 6 in which the data gaps were filled by a procedure described in the following section.

Table 5: Streamflow stations used for the analysis

Name of Station	DGA number	Altitude (metres)	Latitude (UTM)	Longitude (UTM)	Period (years)
Rio Aconcagua en Chacabucuito	14	1030	6364600	358650	1970-2003
Rio Juncal en Juncal	16	1800	6362500	390250	1970-2003
Rio Aconcagua en Rio Blanco	17	1420	6358450	378100	1970-2003
Rio Blanco en Rio Blanco	18	1420	6358150	378650	1970-2003

Table 6: Meteorological stations used for the analysis

Name of Station	DGA number	Altitude (metres)	Latitude (UTM)	Longitude (UTM)	Period (years)
Resguardo Los Patos	18	1220	6403236	351793	1970-2003
San Felipe	25	640	6374869	340319	1970-2003
Catemu	26	440	6374300	318221	1970-2003
Los Andes	27	820	6368858	346567	1970-2003
Vilcuya (*)	29	1100	6363575	362480	1970-2003
Riecillos	34	1290	6356815	373286	1970-2003

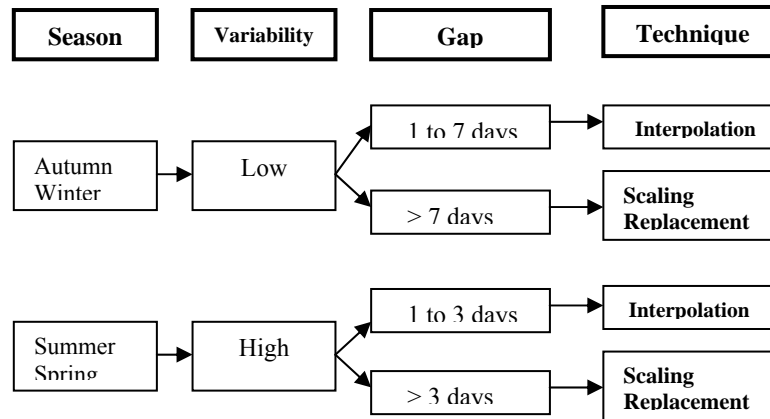
(*) Station where temperature was also recorded

3.3 Data Filling Procedure

3.3.1 Streamflow

Infilling missing runoff data was carried out using two techniques: (a) linear interpolation and (b) Scaling replacement method. One of these techniques was chosen to filling a gap depending on the durations of the gap and variability of the season. This process is outlined in the next scheme (See Fig. 6).

Figure 6: Runoff data filling procedure



3.3.1.1 Linear interpolation

As mentioned above, the interpolation was used in all four seasons for short gaps. In autumn (March, April and May) and winter (June, July and August) when flow variability was low, compared to the rest of the seasons, gaps until 7 days duration were filled by this method. In some years the presence of streamflow peaks due to winter precipitation, have caused a high variability of the data in the months of June and July, in these specific cases the scale factor method was used instead. On the other hand, gaps in summer and spring were completed by interpolation only if their duration was less than or equal to 3 days.

3.3.1.2 Scaling Replacement Method

This method uses measured data of the closest station, with the biggest cross correlation, to fill in data. Every gap was filled in using data for the missing period, the replacement series was linearly scaled in such a way that the beginning and end of the missing data period coincided with observed data. The goal of this technique was to preserve the distribution of the series on a seasonal basis.

Table 6-a: Scaling replacement equation and parameters

Linear scale equation	Parameter	
$Q_m = A \cdot Q_a + B \cdot t$	$A = Q_{mo} / Q_{ao}$	$B = (Q_{mT} - A \cdot Q_{aT}) / T$
t : day within the gap varying from 1 to T T : total duration of the gap in days Q_m : runoff value of the gap in day t in station with missing data periods Q_a : runoff value in day t in station with available data Q_{mo} : last observed runoff value before the gap ($t=0$) in station with missing data periods Q_{ao} : runoff value in the same day as Q_{mo} ($t=0$) in station with available data Q_{mT} : first observed runoff value after the gap ($t=T+1$) in station with missing data periods Q_{aT} : runoff value in the same day as Q_{mT} ($t=T+1$) in station with available data		

Factors A and B made that the observed and generated data were equal at the beginning ($t = 0$) and at the end ($t = T$) of the missing period respectively. Figure 7 outlines this method.

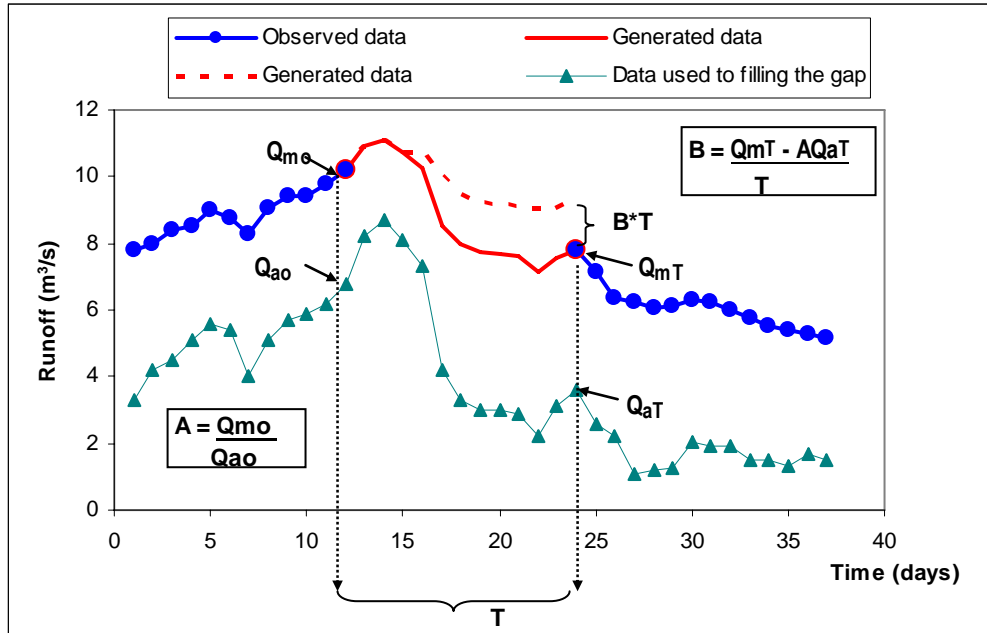


Figure 7: Data gap at a runoff station and the scaling replacement parameters

To select the station that was used to fill in the gaps of the others, the cross correlation between all stations was calculated. Also the proximity of those stations was taken into consideration. In table 7 a cross correlation matrix of the runoff stations is presented. The correlation coefficient is reported for data before and after the infilling, while in figure 8 we can see a part of the Aconcagua basin where the streamflow stations are located.

Table 7: Cross correlation matrix of runoff stations

STATION	14		16		17		18	
	BFD	AFD	BFD	AFD	BFD	AFD	BFD	AFD
14	1.0000	1.0000	0.8144	0.8133	0.8817	0.8829	0.8734	0.8717
16	0.8144	0.8133	1.0000	1.0000	0.8557	0.8583	0.8755	0.8699
17	0.8817	0.8829	0.8557	0.8583	1.0000	1.0000	0.9522	0.9519
18	0.8734	0.8717	0.8755	0.8699	0.9522	0.9519	1.0000	1.0000

BFD: Before filling data AFD: After filling data

From table 7 we can notice that correlations among all the stations were good, being larger than 0.8 in all the cases, in addition the values were almost the same before and after the in filling process. In order to corroborate the importance of the proximity of the stations, one can see that the highest correlation was obtained between stations 17 and 18, with a value around 0.95. In general the gaps of one station were filled in using the data of other one with best cross correlation while it had available data for the gap period; otherwise another station with similar correlation was used. In figure 9 the correlation of runoff data after filling process for each couple of stations is plotted. The obtained scaling factors A and B for all the gaps and each station are listed in appendix 1.

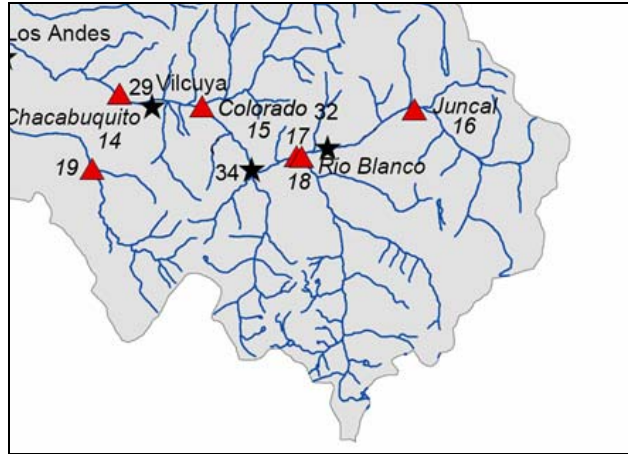


Figure 8: Spatial distribution of the streamflow stations used for the Analysis

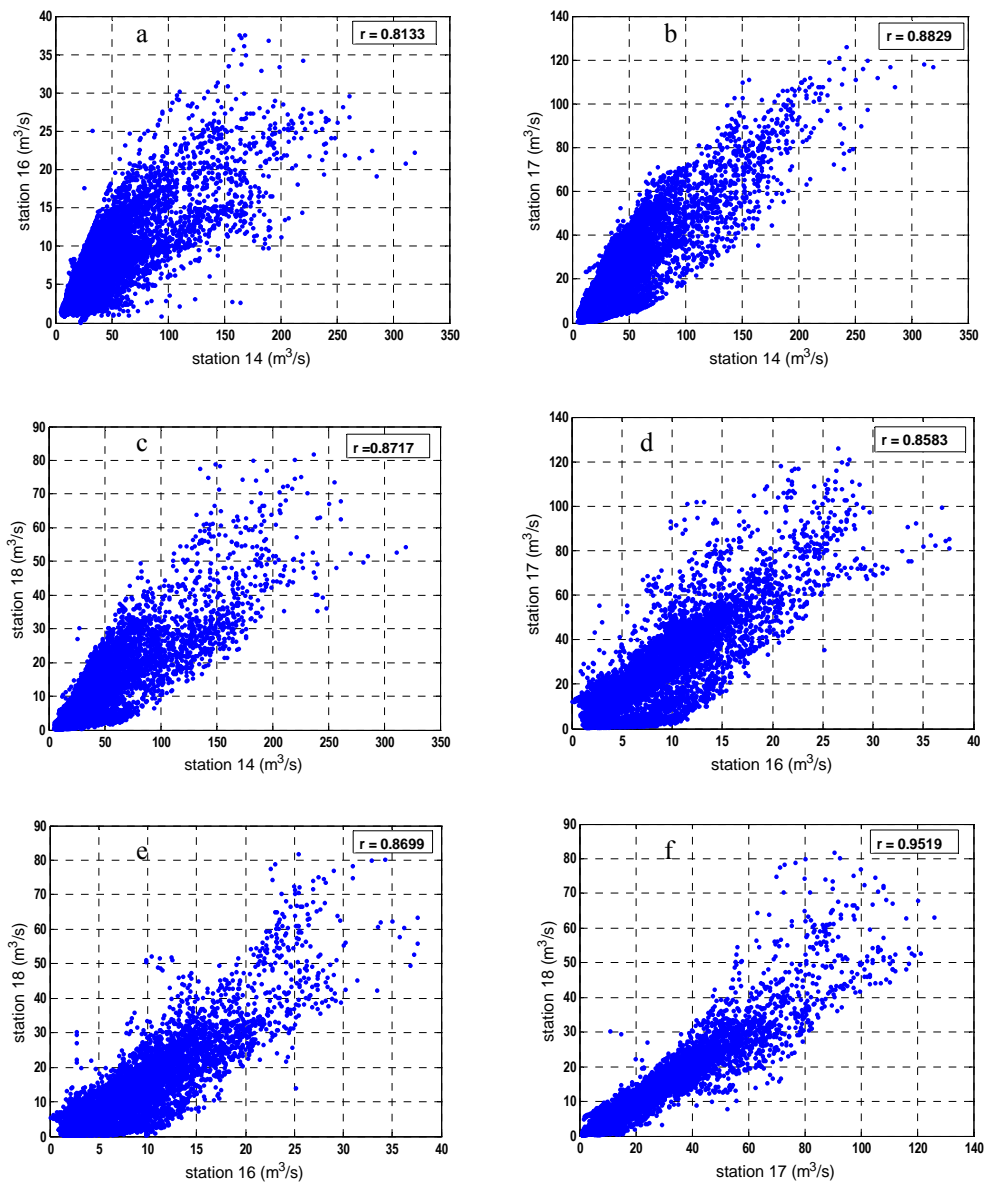


Figure n° 9: (a) Scatter plot between daily streamflow between station 14 and station 16. (b) Between station 14 and station 17. (c) Between station 14 and 18. (d) Between station 16 and 17. (e) Between station 16 and 18. (f) Between station 17 and 18. The cross correlation coefficient r is shown for each plot.

3.3.1.3 Data variability

Finally after the data filling process, the variance of the series was tested. It remained almost identical for all the seasons (see table 8). It is clear also that summer and spring yielded higher variability in comparison with autumn and winter at all the stations. The distribution of data series presents similar behaviour before and after the filling process (see figures 10, 11, 12 and 13) corroborating that it was not affected while completing the gaps.

Table 8: Seasonal Variance for station 14, 15, 16 and 17, computed before and after the filling data process for the period 1970 to 2003

Station	14		16		17		18	
Season	BFD	AFD	BFD	AFD	BFD	AFD	BFD	AFD
Summer	2175.833	2179.450	29.348	28.517	566.876	548.001	189.122	184.861
Autumn	117.903	118.511	7.853	7.796	88.004	89.458	20.790	20.327
Winter	142.468	142.576	0.325	1.460	28.696	27.016	6.501	6.713
Spring	839.210	833.912	9.570	10.235	176.199	182.575	52.361	51.602

BFD: Before filling data AFD: After filling data

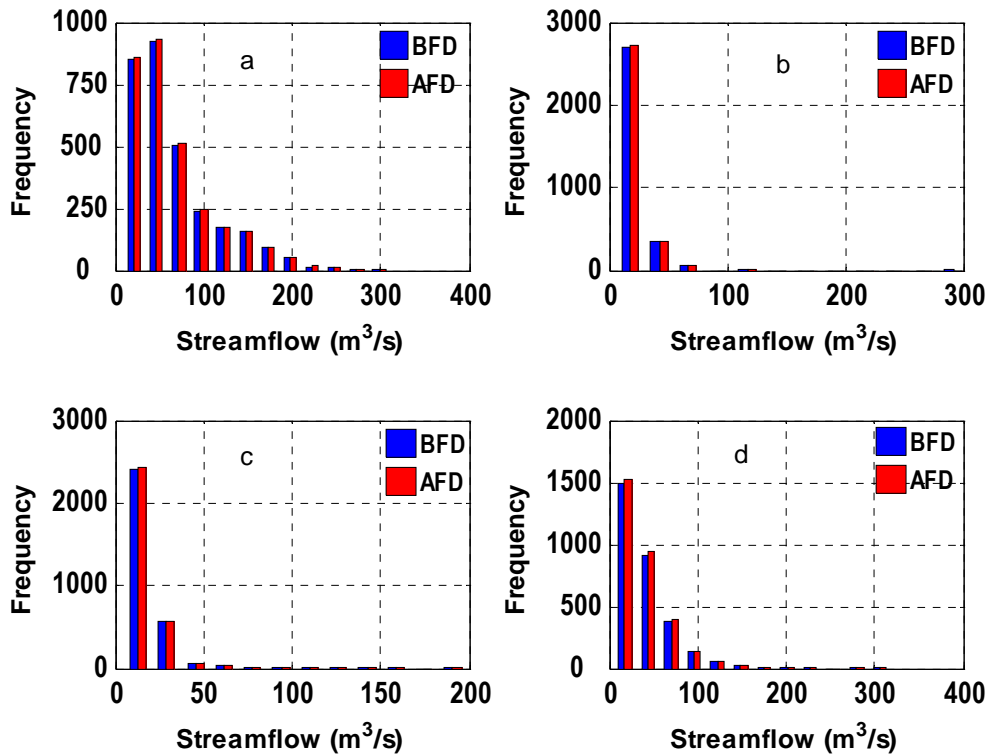


Figure 10: Frequency of daily streamflow at station 14 for period 1970-2003. (a) Summer. (b) Autumn. (c) Winter. (d) Spring. (BFD): Before filling data. (AFD): After filling data.

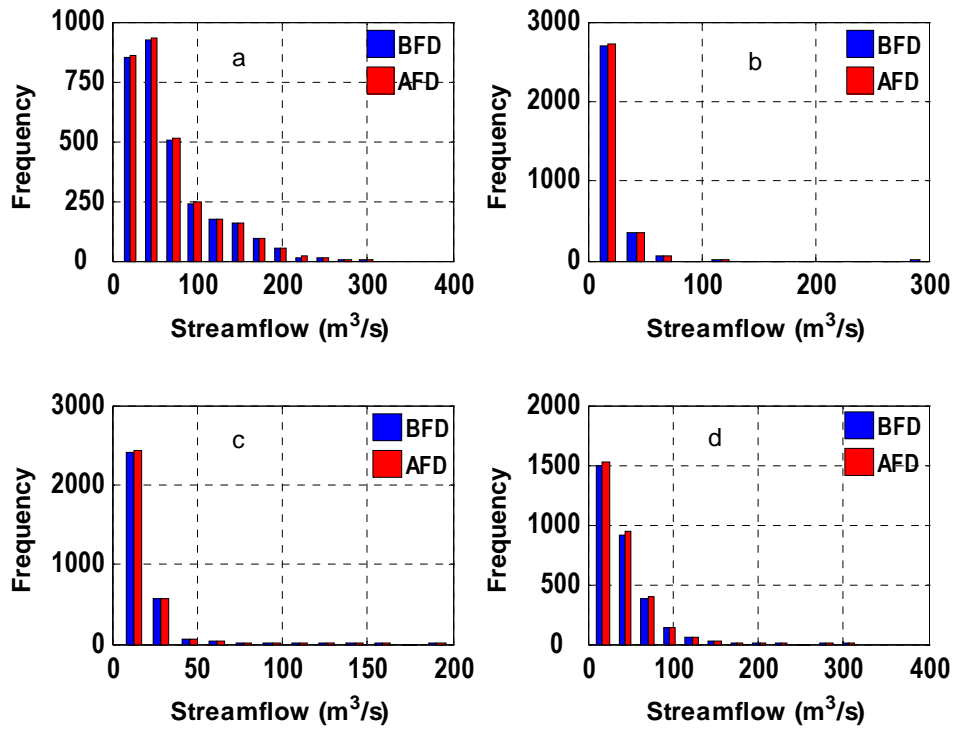


Figure 11: Frequency of daily streamflow at station 16 for period 1970-2003.
(a) Summer. (b) Autumn. (c) Winter. (d) Spring. (BFD) Before filling data.
(AFD) After filling data.

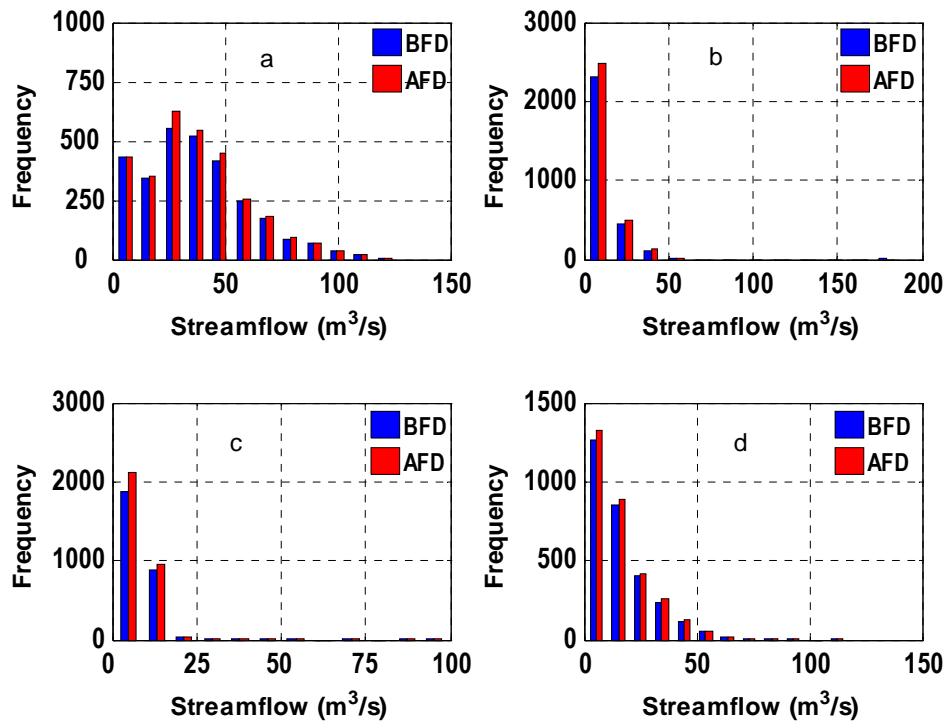


Figure 12: Frequency of daily streamflow at station 17 for period 1970-2003.
(a) Summer. (b) Autumn. (c) Winter. (d) Spring. (BFD) Before filling data.
(AFD) After filling data.

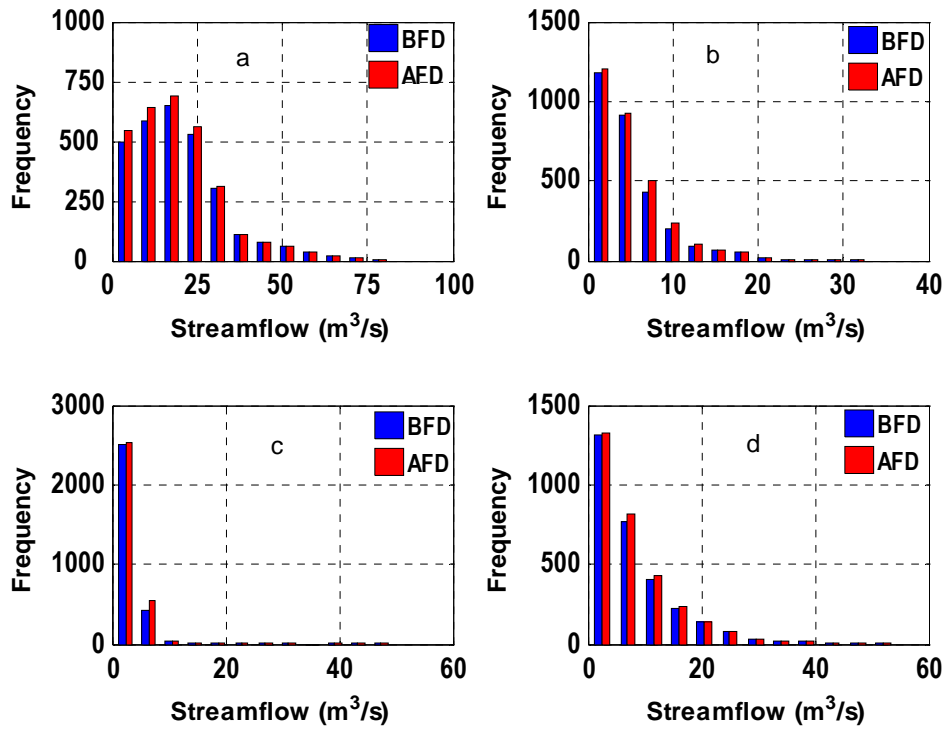


Figure 13: Frequency of daily streamflow at station 18 for period 1970-2003.
(a) Summer. (b) Autumn. (c) Winter. (d) Spring. (BFD) Before filling data.
(AFD) After filling data.

3.3.2 Precipitation

Precipitation missing data was completed using the Linear Regression technique on a seasonal basis. In this method linear regression was conducted between two stations and this equation was used to fill in data. Proximity among the stations was considered and altitude of their locations as well. The assumption in this case was that precipitation in both stations occurred at the same time having, zero or some amount of precipitation simultaneously in both gages, with this the linear equation was:

$$Y = A_i * X$$

Where:

Y = Precipitation value in station with gaps in season i

X = Precipitation value in station with available data in season i

A_i = Dependant variable of the linear equation

The station with which the best linear correlation coefficient (r^2) was obtained, was used to infill the gaps as much the availability of data permitted it, for that reason the linear equation was calculated for several couples of stations including some additional ones that were not selected for the trend analysis nevertheless their data was useful for some gaps in this process. Those

additional stations used just for the infilling process were 20, 24, 28, 30 and 31. The values of parameter A_i and the linear correlation coefficient (r^2) are listed in table 9.

Table n° 9: Linear regression parameter A_i and correlation coefficient (r^2) for autumn winter and spring at all the precipitation stations

SEASON	STATION Y	18		25		26		27		29		34	
		A	r^2	A	r^2	A	r^2	A	r^2	A	r^2	A	r^2
AUTUMN	18			0.721	0.636			0.807	0.674	0.959	0.702	1.487	0.601
	20	1.039	0.734	0.901	0.835	0.899	0.492	1.022	0.844	1.226	0.791	1.679	0.423
	24	0.949	0.710	0.823	0.790			0.929	0.788	1.103	0.689	1.494	0.291
	25	1.103	0.624			0.901	0.390	1.007	0.782	1.177	0.615	1.897	0.443
	26			0.747	0.431			0.811	0.371				
	27	1.032	0.698	0.879	0.810					1.112	0.772	1.769	0.539
	28					0.571	0.596						
	29	0.878	0.742	0.683	0.681			0.793	0.786			1.518	0.677
	30					0.574	0.583						
	31			0.875	0.719	0.989	0.784	0.960	0.664				
	34	0.529	0.627	0.379	0.531			0.429	0.557	0.538	0.662		
WINTER	18			0.712	0.643			0.718	0.508	0.955	0.687	1.313	0.299
	20	1.024	0.825	0.894	0.793	0.945	0.574	0.943	0.760	1.059	0.710	1.383	0.328
	24	1.007	0.668	0.849	0.717			0.950	0.762	1.060	0.640	1.349	0.166
	25	1.119	0.620			0.961	0.474	0.977	0.766	1.169	0.633	1.500	0.119
	26			0.755	0.506			0.801	0.421				
	27	1.067	0.562	0.906	0.805					1.162	0.696	1.566	0.307
	28					0.547	0.540						
	29	0.889	0.728	0.701	0.697			0.732	0.705			1.365	0.564
	30					0.608	0.601						
	31			0.770	0.469	0.970	0.574	0.832	0.469				
	34	0.511	0.378	0.399	0.298			0.425	0.328	0.572	0.562		
SPRING	18			0.550	0.319			0.627	0.298	0.838	0.268	0.941	0.059
	20	1.028	0.303	0.581	0.609	0.802	0.590	0.689	0.503	0.828	0.105	0.845	0.045
	24	0.866	0.142	0.519	0.394			0.635	0.305	0.758	0.145	0.814	0.039
	25	1.153	0.306			1.034	0.570	1.070	0.783	1.273	0.317	1.395	0.172
	26			0.764	0.599			0.840	0.543				
	27	1.055	0.366	0.836	0.822					1.108	0.534	1.232	0.178
	28					0.519	0.435						
	29	0.823	0.449	0.554	0.495			0.696	0.579			1.046	0.350
	30					0.542	0.619						
	31			0.734	0.674	1.072	0.775	0.838	0.481				
	34			0.498	0.432			0.542	0.354	0.683	0.420		

Summer season was excluded from the precipitation analysis because there are very few days with recorded precipitation in this season.

The correlation coefficient in general ranges from 0.49 to 0.89 in autumn and winter seasons, but in spring the value drops to 0.04 to 0.78 being mostly around 0.4, because that season is generally dry with few data to correlate. In addition station 34 (last column of table 9) yields the lowest correlation coefficient when it is linearly correlated with the other stations because it is located at the highest level (1290 metres), only in autumn and winter r^2 factor reaches 0.5 to 0.6 with station 29 that is closest and at 1100 metres of altitude.

In Figures 14, 15, 16, 17, 18 and 19 precipitation data before filling process is plotted for stations 18, 25, 26, 27, 29 and 34 on the Y axis and the station used for filling data on the X axis.

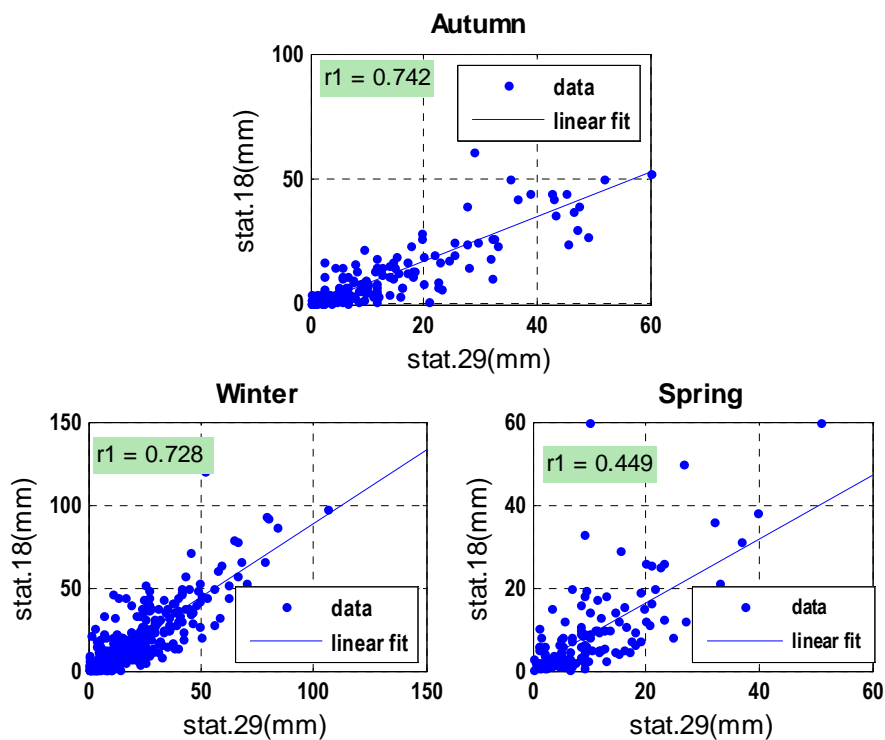


Figure 14: Station 18 correlated with station 29 used to fill its data, ($r_1=r^2$).
(a) Autumn. (b) Winter. (c) Spring

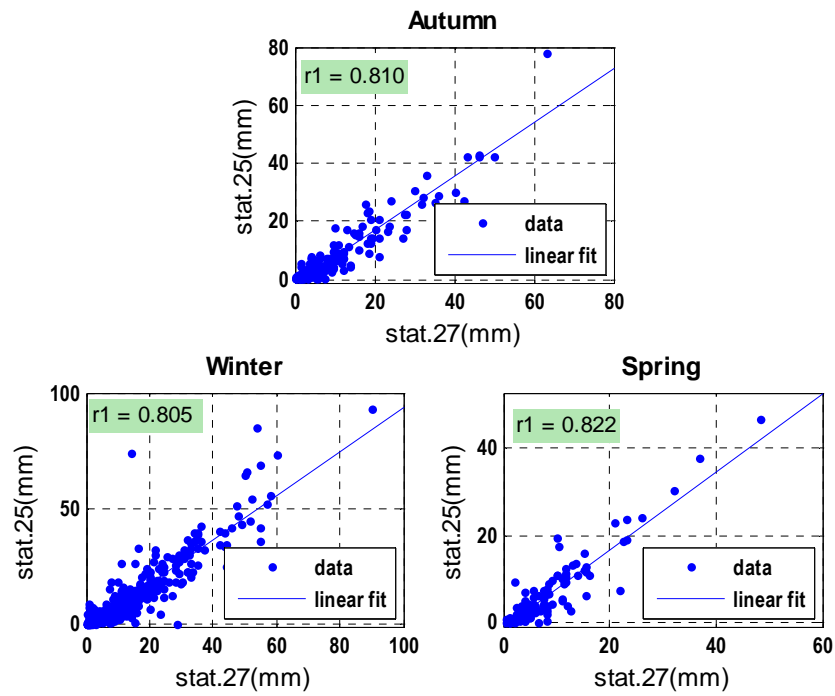


Figure 15: Station 25 correlated with station 27 used to fill its data, ($r1=r^2$)
(a) Autumn. (b) Winter. (c) Spring

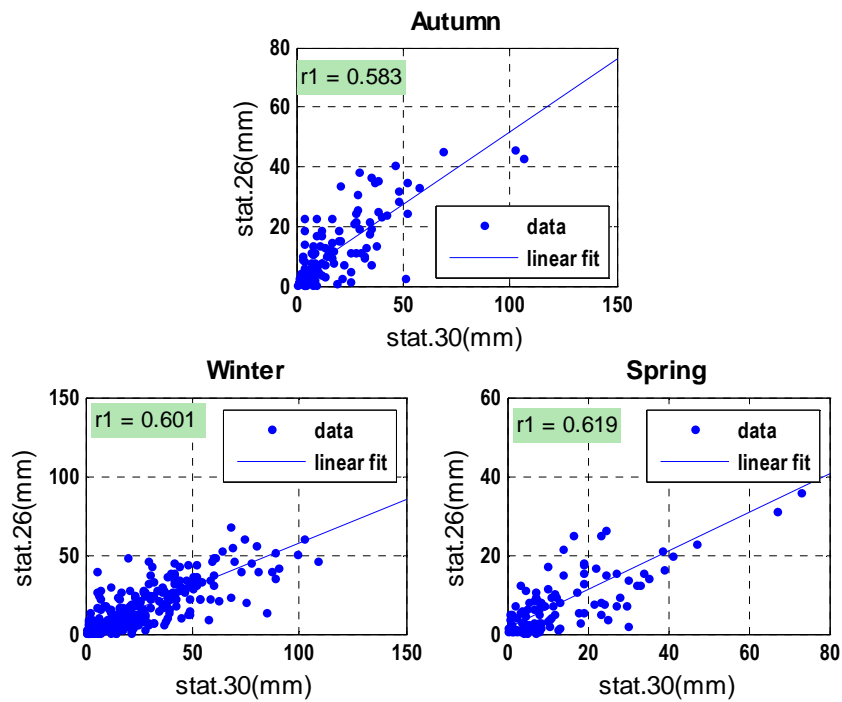


Figure 16: Station 26 correlated with station 30 used to fill its data, ($r1=r^2$)
(a) Autumn. (b) Winter. (c) Spring

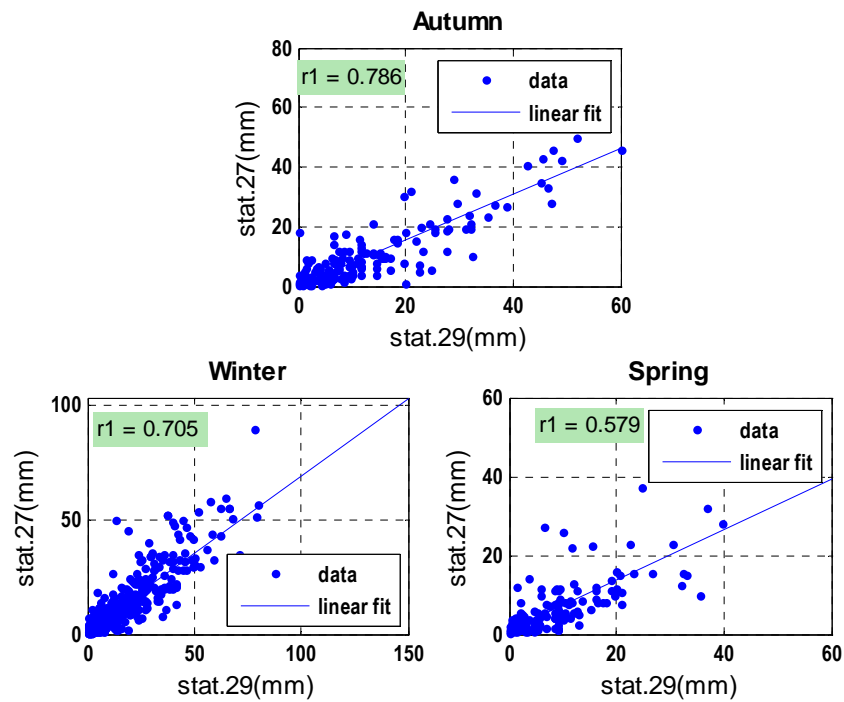


Figure 17: Station 27 correlated with station 29 used to fill its data, ($r1=r^2$)
(a) Autumn. (b) Winter. (c) Spring

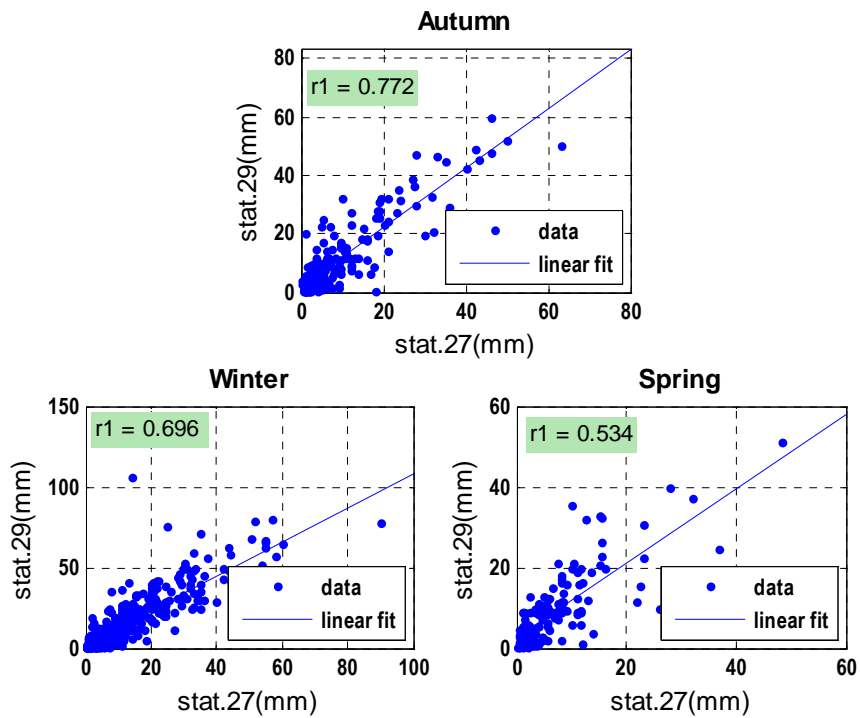


Figure 18: Station 29 correlated with station 27 used to fill its data, ($r1=r^2$)
(a) Autumn. (b) Winter. (c) Spring

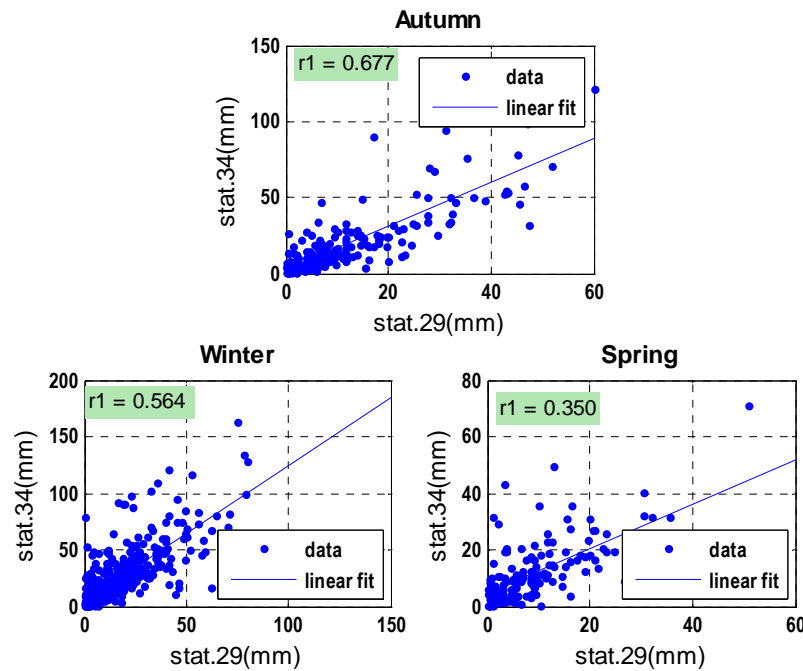


Figure 19: Station 34 correlated with station 29 used to fill its data, ($r1=r^2$).
(a) Autumn. (b) Winter. (c) Spring

3.3.3 Temperature

For temperature data the same procedure as for runoff was followed, it means: linear interpolation, and scaling replacement method. In this case the variability of data was high and similar during the whole year, for that reason the interpolation method was used for gaps with length ≤ 3 days.

The scaling replacement method was used for larger gaps taking stations 33 and 45 data for both minimum and maximum temperature. The criteria for this method consisted also in the analysis of the cross correlation between stations. The correlation was good, with values larger than 0.6 (see table 10). On the other hand, the scarcity of the data did not allow using the closest gages. The location of stations 33 and 45 are close to the basin outlet (see figure 9 in section 3.1 above). Nevertheless the cross correlation coefficients were good enough to consider those stations for filling data. Finally the variability of series among station 29 and those used to fill its data was slightly different specially for temperature maximum (see table 11) in autumn, winter and spring; while for temperature minimal the variance was similar in all the seasons (see table 11).

In appendix 2 the gaps duration are listed and the stations used to fill them as well.

Table 10: Cross correlation matrix of temperature stations

STATION	TEMPERATURE	33	45
29	Maximum	0.727	0.785
	Minimum	0.676	0.705

Table 11: Variance of minimum and maximum temperature at station 29 for period 1970-2003.
The variance of data in stations 33 and 45 are also shown

Station	Daily maximum temperature				Daily minimum temperature			
	29		33	45	29		33	45
Season	BFD	AFD			BFD	AFD		
Summer	7.160	7.485	9.368	9.354	5.449	5.492	5.819	4.500
Autumn	28.885	28.860	16.587	21.318	9.897	9.911	11.596	7.903
Winter	27.289	27.530	13.012	14.270	12.902	13.252	12.310	8.204
Spring	28.839	28.951	17.136	21.751	11.148	11.081	9.012	7.334

BFD: before filling data. AFD: after filling data

After the temperature data filling procedure, the distribution of the data remained unchanged. See figures 20 and 21.

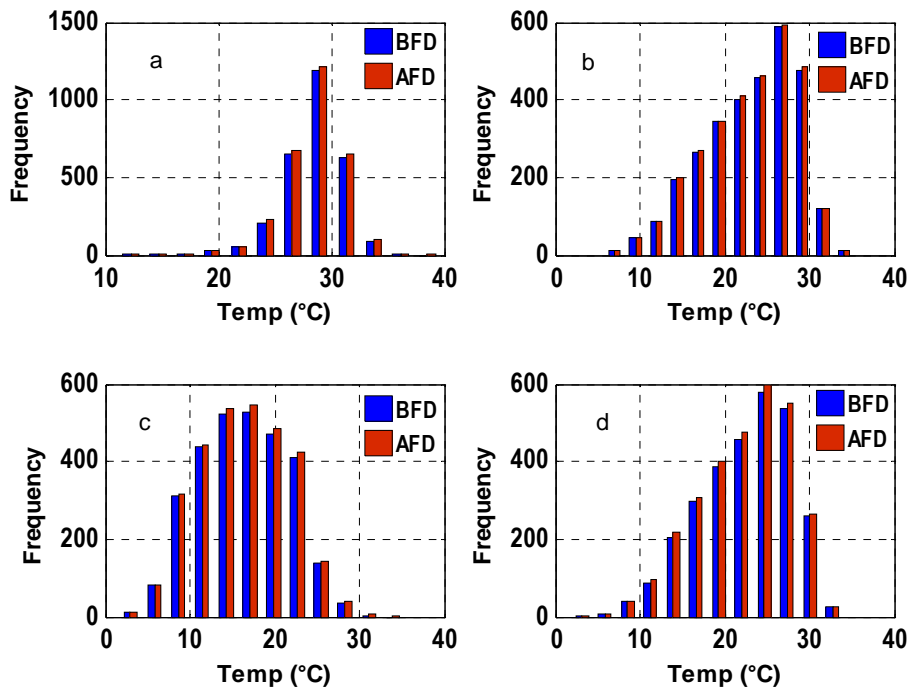


Figure 20: Frequency of daily temperature maximum at station 29 for period 1970-2003.
(a) Summer. (b) Autumn. (c) Winter. (d) Spring. (BFD): Before filling data. (AFD): After filling data.

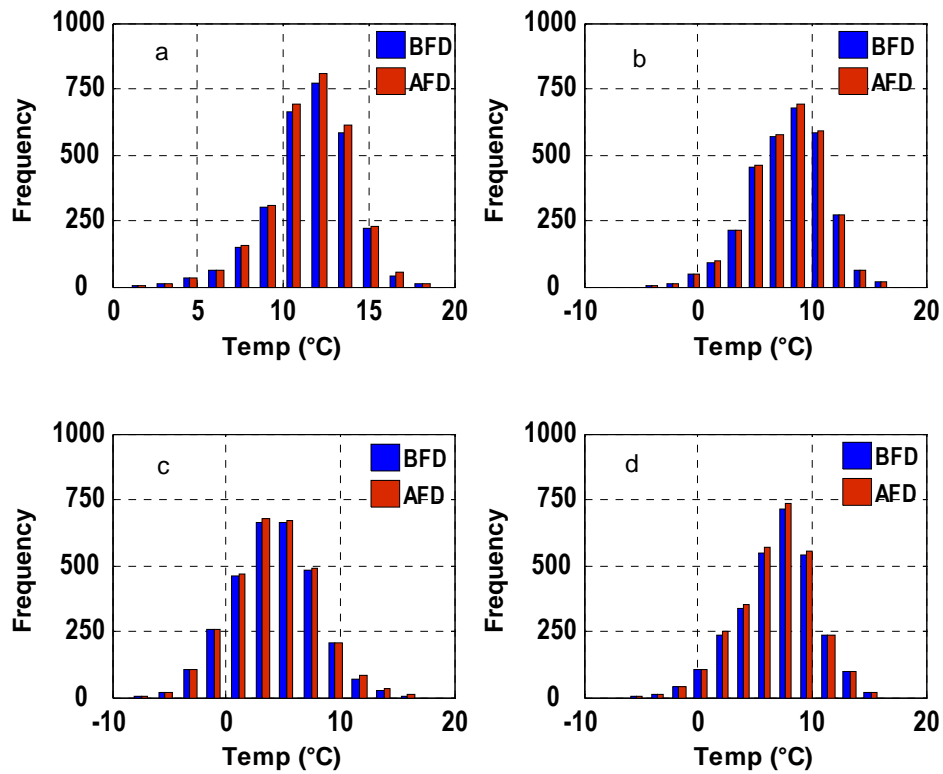


Figure n° 21: Frequency of daily temperature minimum at station 29 for period 1970-2003.
 (a) Summer. (b) Autumn. (c) Winter. (d) Spring.
 (BFD): Before filling data. (AFD): After filling data.

CHAPTER 4

TREND ANALYSIS

The analysis in the Aconcagua basin was carried out on a seasonal basis, because streamflow and precipitation in this area change notably by season, for instance important amounts of precipitation appear in winter, generating peaks in runoff in some years, on the other hand snow melt produces high quantities of streamflow in summer and spring. Autumn and winter are generally the seasons with lowest flows.

Is important to remark here that seasons in the southern hemisphere are distributed like:

SUMMER: December, January and February

AUTUMN: March, April and May

WINTER: June, July and August

SPRING: September, October and November

For the subsequent analysis the following abbreviations will be used to designate each season:

DJF: Summer

MAM: Autumn

JJA: Winter

SON: Spring

4.1 Parameters or indices

4.1.1 Streamflow

For trend analysis in streamflow, the use of percentiles was used in order to understand better gradual changes in the distribution of data throughout time. Table 12 lists the percentiles used and their descriptions.

Table n°12: Indices used in streamflow trend analysis

Indicator name	Abbreviation	Definition	Units
Percentile “0”	P0	Seasonal minimum daily streamflow	m ³ /s
Percentile “25”	P25	Seasonal first quartile of daily streamflow	m ³ /s
Percentile “50”	P50	Seasonal second quartile or median daily streamflow	m ³ /s
Percentile “75”	P75	Seasonal third quartile daily streamflow	m ³ /s
Percentile “90”	P90	Seasonal 9 decile of daily streamflow	m ³ /s
Percentile “100”	P100	Seasonal maximum daily streamflow	m ³ /s

In this study Q90 was also selected to have information about the high flows, because Q100 is too sensitive to variability between years and seasons during the observation record.

4.1.2 Precipitation

For this hydroclimatic variable the analysed parameters were the amount, the frequency and the extreme events were (see table 13):

Table 13: Indices used in precipitation trend analysis

Indicator name	Abbreviation	Definition	Units
Precipitation totals	P totals	Seasonal sum of daily precipitation amount	(mm)
Frequency of dry days	Freq (P=0)	Seasonal probability of zero daily precipitation (threshold "0" precipitation)	-
Maximum precipitation	Pmax	The most intense precipitation if duration 1 day	(mm)

4.1.3 Temperature

The selected temperature indices for this study and their definitions are show in table 14:

Table 14: Indices Used in Temperature trend Analysis

Indicator name	Abbreviation	Definition	Units
Minimum Temperature	Tmin	Seasonal average of daily minimum temperature	(°C)
Maximum Temperature	Tmax	Seasonal average of daily maximum temperature	(°C)
Diurnal Range	DR	Seasonal average of the difference between Tmax and Tmin	(°C)
Frequency of minimum temperature >0	Freq (Tmin>0)	Seasonal probability of daily minimum temperature >0°C	-

4.2 Time series analysis

4.2.1 Streamflow

The seasonal average of each of the six percentiles throughout the record 1970 to 2003 were computed for all runoff stations and then plotted in figure 22. It is clear that the quantity of runoff varies by station, for instance data of station 14 has the highest values, since it is located downstream of the others, receiving the contribution of three tributaries: Blanco, Colorado and Juncal rivers; in second place of magnitude is station 17 that is upstream on the Aconcagua river. Station 18 is close to 17 but the runoff measured there is lower because it is located on the tributary Blanco River. Finally the lowest flows were measured in station 16 that is in Juncal River in the upper part of the basin (see map in figure 4 of section 3.1).

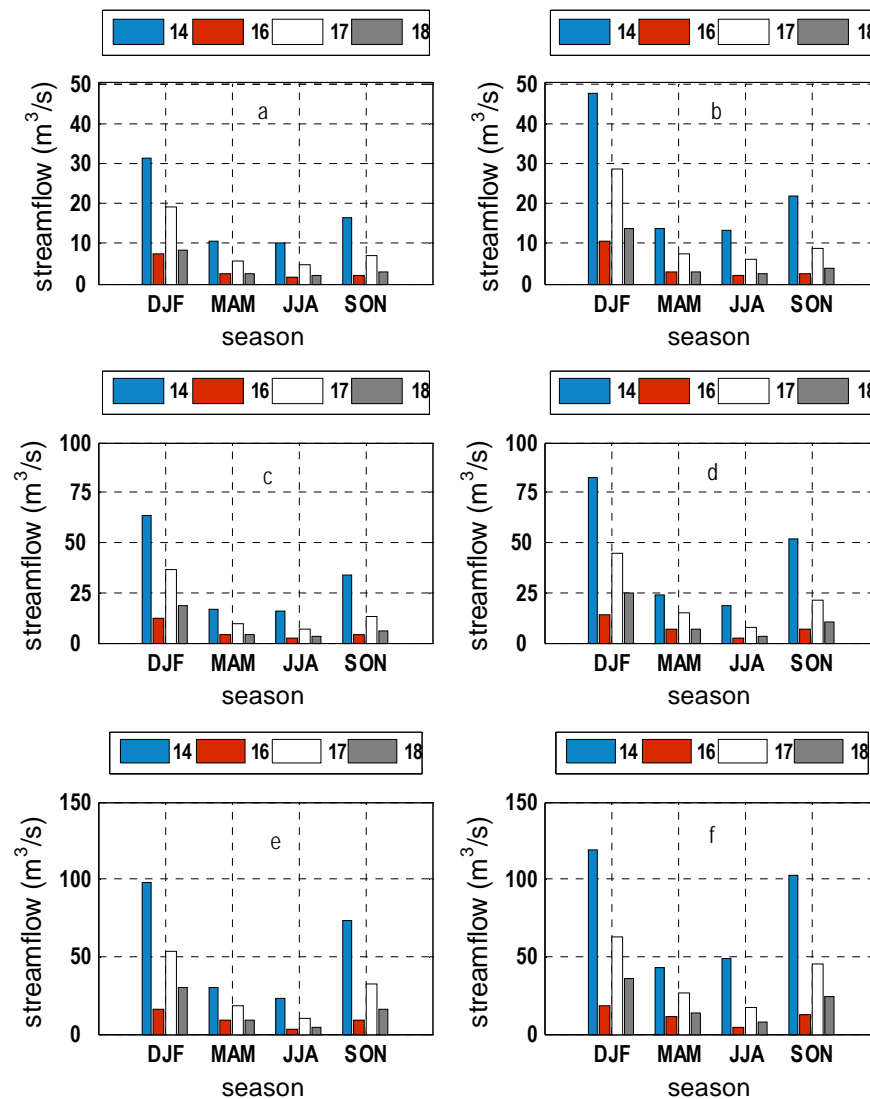


Figure 22: Seasonal average of streamflow aercentiles throughout the record 1970-2003 for stations 14, 16, 17 and 18 (a) Percentile 0. (b) Percentile 25. (c) Percentile 50. (d) Percentile 75. (e) Percentile 90. (f) Percentile 100.

To see the proportion of runoff amount by season and for all the period of record, the seasonal percentage for each station was calculated and is shown in table 15

Table 15: Seasonal runoff percentage in the analysed stations
Period 1970-2003

Season	Station 14	Station 16	Station 17	Station 18
SON	46 %	51 %	51 %	54 %
MAM	14 %	21 %	16 %	14 %
JJA	12 %	9 %	10 %	9 %
SON	28 %	20 %	23 %	23 %

Analysing the variation on a seasonal basis we can observe that in general the percentiles follow this decreasing order: summer, spring, autumn and winter for the four stations. Nevertheless there are notable exceptions in station 16 percentiles 0, 25 and 50 have higher values in autumn than in spring (see the mean in table 16 and figure 22 a,b,c), indicating that these low flows are mainly products of precipitation that fall mostly in autumn (and winter) and not from the snow melting commonly in spring (and summer). It is clear because station 16 is located at the highest point of the river network (see map in figure 4 of section 3.1) where precipitation is most likely to occur as snow, therefore does not directly contribute to high flows. Second exception was station 14, where percentile 100 has larger values in winter than autumn (see the mean in table 16 and figure 22 f) showing that this station has recorded larger peaks in winter. This station is located at 1030 metres; an altitude at which the flow regime of the river begins to change from pluvio-nival to nival⁽¹⁾, so in that context the largest amount of precipitation that appear in winter has to be felt like rainfall contributing directly to runoff peaks. For the rest of the stations (higher altitudes and regimen nival) larger peaks were recorded in autumn, when is possible to have precipitation as rainfall as well.

(1)Source: Dirección General de Aguas DGA

Table 16: Mean, maximum and minimum value of the streamflow percentiles (m^3s^{-1}) throughout the record 1970-2003

Percentile 0						Percentile 25					
Season	Station	14	16	17	18	Season	Station	14	16	17	18
DJF	Max	70.70	13.50	43.60	20.10	DJF	Max	126.0	18.50	69.30	32.10
	Mean	31.49	7.45	18.98	8.50		Mean	47.50	10.49	28.56	13.70
	Min	9.02	2.02	0.83	0.53		Min	14.30	4.29	1.09	0.72
MAM	Max	20.40	4.29	13.10	5.90	MAM	Max	28.30	4.90	15.09	6.85
	Mean	10.79	2.37	5.54	2.29		Mean	13.68	3.09	7.24	3.02
	Min	5.02	1.29	0.76	0.31		Min	7.29	1.55	0.84	0.39
JJA	Max	18.50	3.64	10.30	5.06	JJA	Max	23.05	3.81	12.55	5.95
	Mean	10.11	1.64	4.77	1.97		Mean	13.14	1.93	6.05	2.49
	Min	4.94	0.87	0.76	0.35		Min	6.19	1.31	0.83	0.47
SON	Max	33.20	3.70	14.50	7.63	SON	Max	41.15	4.10	16.92	9.24
	Mean	16.56	1.83	6.76	3.06		Mean	21.70	2.41	8.57	4.02
	Min	4.70	0.01	0.77	0.36		Min	6.78	1.08	0.87	0.43
Percentile 50						Percentile 75					
Season	Station	14	16	17	18	Season	Station	14	16	17	18
DJF	Max	161.0	24.20	81.00	54.10	DJF	Max	195.0	28.40	97.40	63.00
	Mean	63.60	12.47	36.32	18.89		Mean	82.23	14.38	44.68	24.48
	Min	16.20	5.45	1.27	0.84		Min	19.70	6.28	1.89	1.32
MAM	Max	32.20	7.54	21.00	8.91	MAM	Max	50.55	12.00	38.95	18.95
	Mean	16.92	4.43	9.38	4.03		Mean	23.58	6.54	14.60	6.44
	Min	9.40	2.07	0.95	0.47		Min	11.65	3.38	1.09	0.61
JJA	Max	30.85	3.94	14.60	6.41	JJA	Max	49.70	4.38	18.35	7.94
	Mean	15.59	2.08	6.89	2.86		Mean	18.69	2.35	8.01	3.41
	Min	6.97	1.40	0.85	0.49		Min	7.56	1.51	0.89	0.53
SON	Max	56.30	8.95	24.20	12.40	SON	Max	92.20	11.74	40.30	21.60
	Mean	33.34	3.98	12.96	6.14		Mean	51.97	6.59	21.43	10.26
	Min	8.54	2.29	1.05	0.48		Min	11.48	3.41	1.18	0.61
Percentile 90						Percentile 100					
Season	Station	14	16	17	18	Season	Station	14	16	17	18
DJF	Max	234.00	33.20	111.00	72.30	DJF	Max	311.00	37.60	126.00	81.80
	Mean	97.94	16.05	52.80	29.63		Mean	119.32	18.47	63.13	35.62
	Min	21.40	6.86	2.37	1.90		Min	24.00	8.04	4.10	2.84
MAM	Max	67.02	14.66	47.62	28.09	MAM	Max	118.00	25.10	56.60	33.10
	Mean	30.18	8.33	18.72	9.01		Mean	42.37	11.02	26.59	13.35
	Min	14.73	4.51	1.29	0.68		Min	19.20	6.16	2.63	1.50
JJA	Max	63.26	7.62	24.38	10.13	JJA	Max	199.00	36.82	99.50	49.50
	Mean	23.02	2.61	9.48	3.94		Mean	48.33	4.00	17.43	7.50
	Min	7.90	1.62	0.93	0.56		Min	9.19	1.75	1.01	0.62
SON	Max	170.60	17.91	73.64	40.62	SON	Max	319.00	22.70	117.00	54.30
	Mean	73.00	9.37	31.71	16.17		Mean	102.40	12.16	45.58	23.87
	Min	13.40	4.12	1.26	0.85		Min	15.50	5.27	1.39	0.97

4.2.1.1 Station 14

Figure 23 represent the time series of the data in summer, autumn, winter and spring respectively.

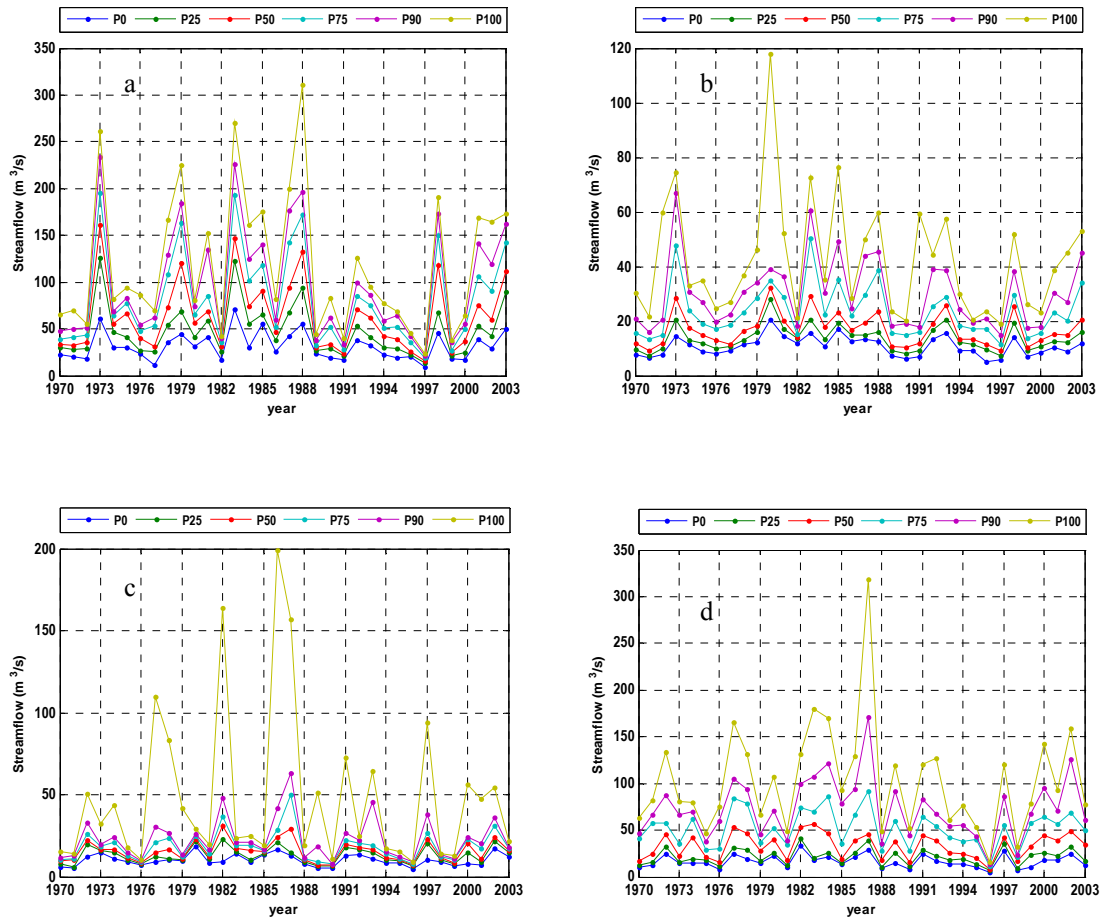


Figure 23: Streamflow series at station 14. The data is presented for the percentiles P0, P25, P50, P75, P90 and P100 (a) SUMMER (b) AUTUMN (c) WINTER (d) SPRING

Observations

- ✓ The peaks:
In autumn: $118 \text{ m}^3/\text{s}$ in 1980 (see figure 23-b)
Winter: $110 \text{ m}^3/\text{s}$ in 1977, $164 \text{ m}^3/\text{s}$ in 1982 and $199 \text{ m}^3/\text{s}$ in 1986 (see figure 23-c)
Spring: $319 \text{ m}^3/\text{s}$ in 1987 (see figure 23-d)
- ✓ The variation of the percentiles during the record 1970 to 2003 present an apparently positive trend in the first half until 1988 afterwards is possible to observe a shift or fall in the values until 1997 year from when the data seems to recover the increasing tendency. This behaviour is similar in all the seasons (see figure 23-a, 23-b, 23-c and 23-d).

4.2.1.2 Station 16

In the same way than for station 14, the series were plotted for each season and they are listed in figure 24

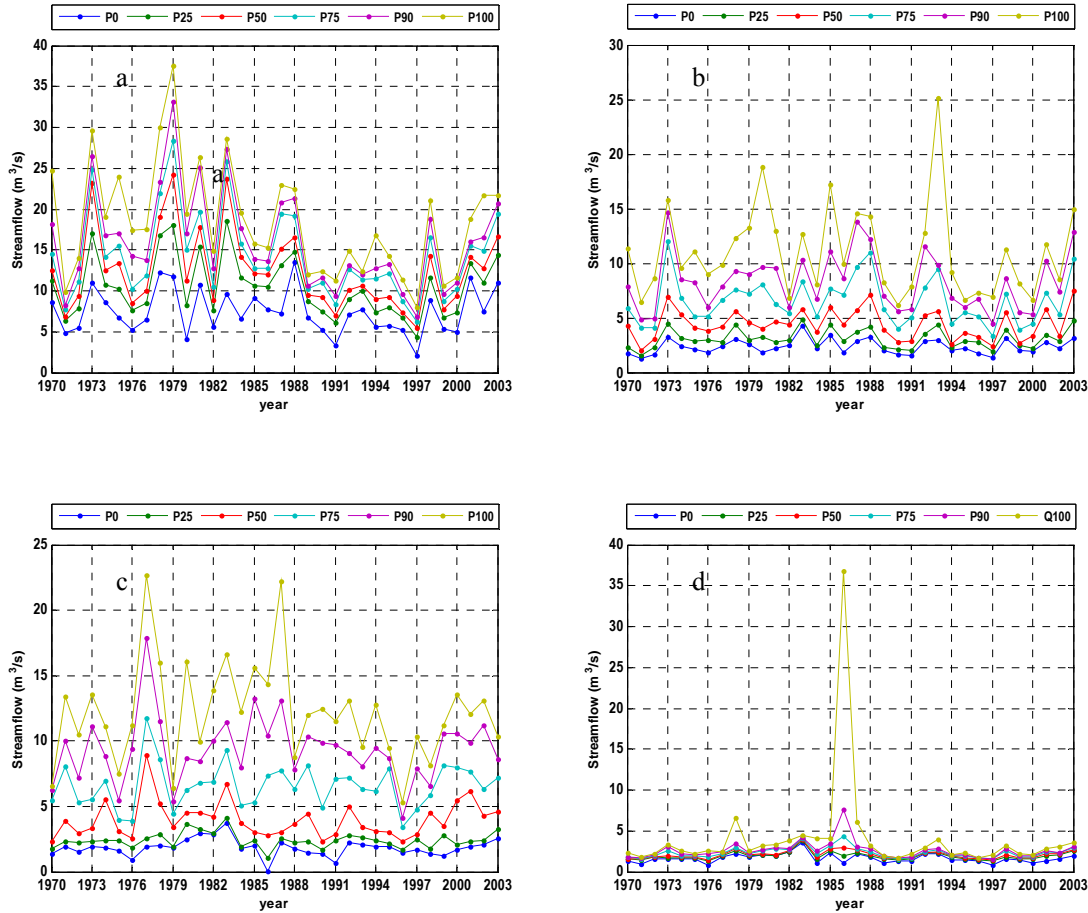


Figure 24: Streamflow series at station 16. The data is presented for the percentiles P0, P25, P50, P75, P90 and P100 (a) SUMMER (b) AUTUMN (c) WINTER (d) SPRING

Observations

- ✓ The peaks:
 - In summer: 37.6m³/s in 1979 (see figure 24-a)
 - In autumn: 25.1m³/s in 1993 (see figure 24-b)
 - Winter: 36.8m³/s in 1986 (see figure 24-c)
 - Spring: 22.7m³/s in 1977 and 22.2m³/s in 1987 (see figure 24-d)
- ✓ It is remarkable that this station has recorded the lowest flows for winter for all the percentiles, being all of them below 5m³/s during the entire record. They are percentiles 100 in year 1978 and 1986 and percentile 90 in 1986 (see figure 24-c)
- ✓ No shifts can be noticed

4.2.1.3 Station 17

For the analysis in this station, the plots are shown by figure 25.

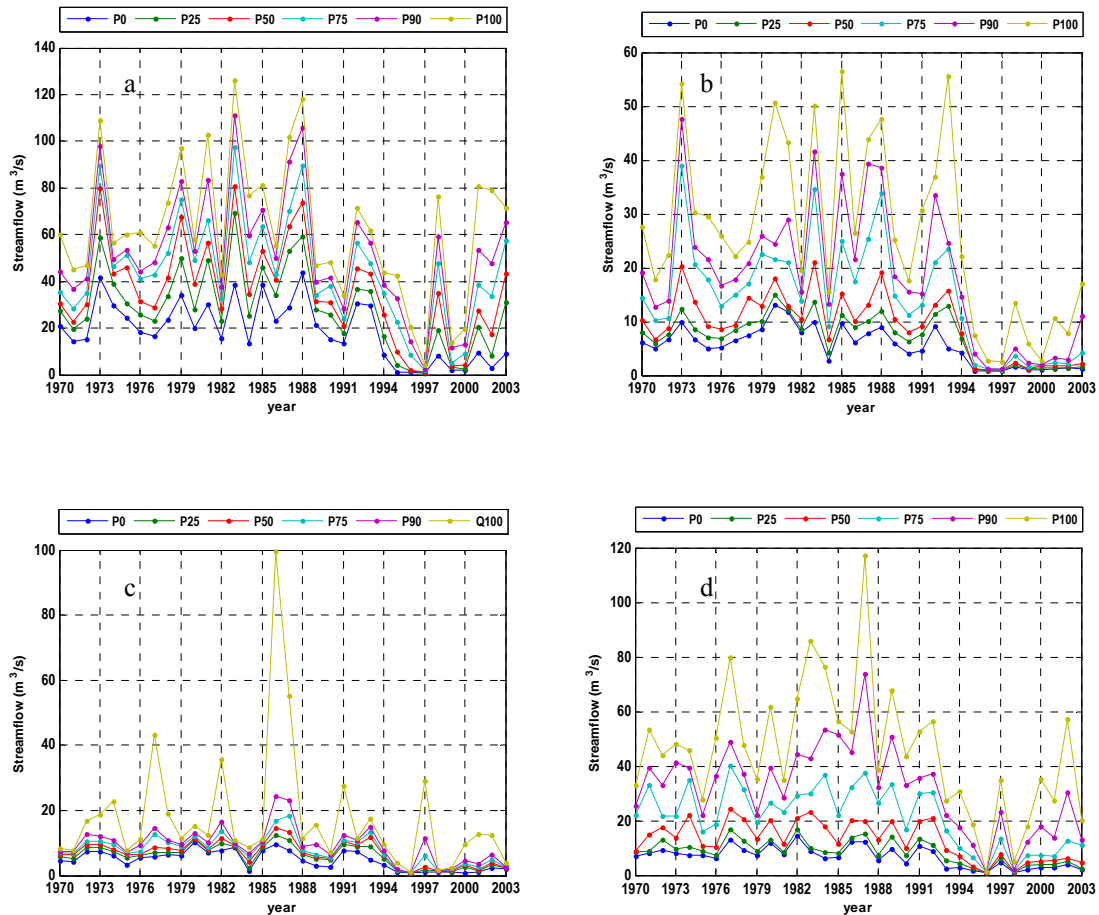


Figure 25: Streamflow series at station 17. The data is presented for the percentiles P0, P25, P50, P75, P90 and P100 (a) SUMMER (b) AUTUMN (c) WINTER (d) SPRING

Observations:

- ✓ The peaks:
Winter: $99.5 \text{ m}^3/\text{s}$ in 1986 (see figure 25-c)
Spring: $117.43 \text{ m}^3/\text{s}$ in 1987 (see figure 25-d)
- ✓ At this station we can observe a decrease in the last 10 years of the record in all the season and for all the percentiles. In summer this drop seems to start in 1988 with a slight increase in 1992 to drop down again since 1994 (see figure 25-a). In autumn is clear that the shift starts in 1995 (see figure 25-b). In winter the values decrease from 1995 (see figure 25-c) and finally in spring the shift begins in 1993 (see figure 25-d).

4.2.1.4 Station 18

Time series for station 18 are in figure 26

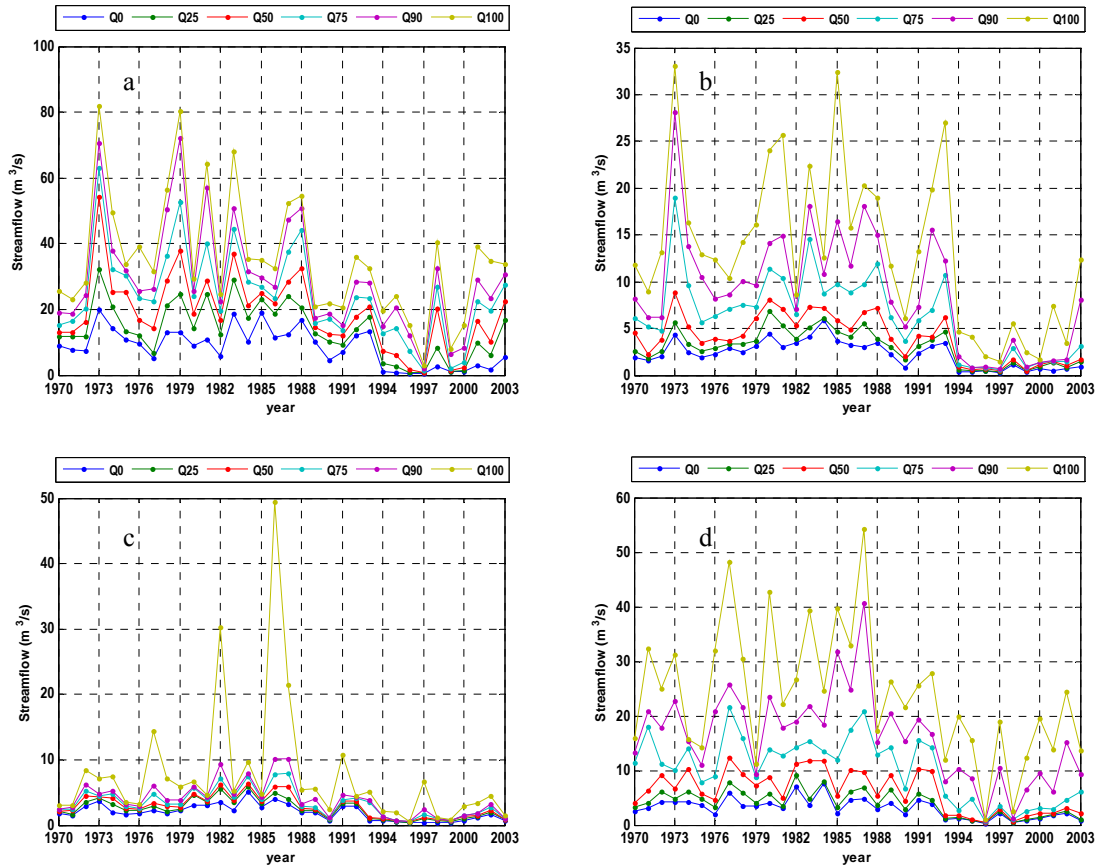


Figure 26: Streamflow series at station 18. The data is presented for the percentiles P0, P25, P50, P75, P90 and P100 (a) SUMMER (b) AUTUMN (c) WINTER (d) SPRING

Observations:

- ✓ The peaks:
Winter: 30.3 m³/s in 1982 and 49.5 m³/s in 1986 and (see figure 26-c)
Spring: 117.43 m³/s in 1987 (see figure 26-d)
- ✓ At this station we can observe a decrease in the last 10 years of the record in all the season and for all the percentiles. In summer this drop seems to start in 1988 with a slight increase in 1992 to drop down again since 1994 (see figure 26-a). In autumn it is clear that the shift starts in 1995 (see figure 26-b). In winter the values decrease from 1995 (see figure 26-c) and finally in spring the shift begins in 1993 (see figure 26-d).

4.2.2. Precipitation

The average of seasonal precipitation totals of the 34 years of the period of record was plotted in figure 27(a). Those values and also the minimum and maximum are shown in table 17. From the plot we can observe that the wettest season was winter being recorded it for all the stations, autumn and spring have much less precipitation (spring is slightly dryer than autumn) for all the stations. On the other hand the quantity of precipitation changes from one station to another. In this case it is station 34 that yields largest values, and from table 6 (section 3.2) we can see that this station is located at the highest altitude (1290 metres) compared to the others. The two other stations that are also at high altitudes are 29 (1100 m) and 18(1220 m) and from the plot we can see that the amount of precipitation measured at these stations are also considerable. Stations 26 (440 m) and 27 (820m) have collected similar values in the three seasons, but less than the stations mentioned before. Station 26 is located 40 km (approximately) downstream from station 27 (see map in figure 4 section 3.2) in the central part of the basin where the amount of precipitation is generally low because of its relief ⁽¹⁾. Finally the lowest quantity of precipitation was registered at station 25 (640m) that is also located int the central part of the watershed. The highest precipitation total was 993.17mm in winter measured by station 34 and the lowest was 0 mm (no precipitation) in autumn recorded by station 26. See table 17.

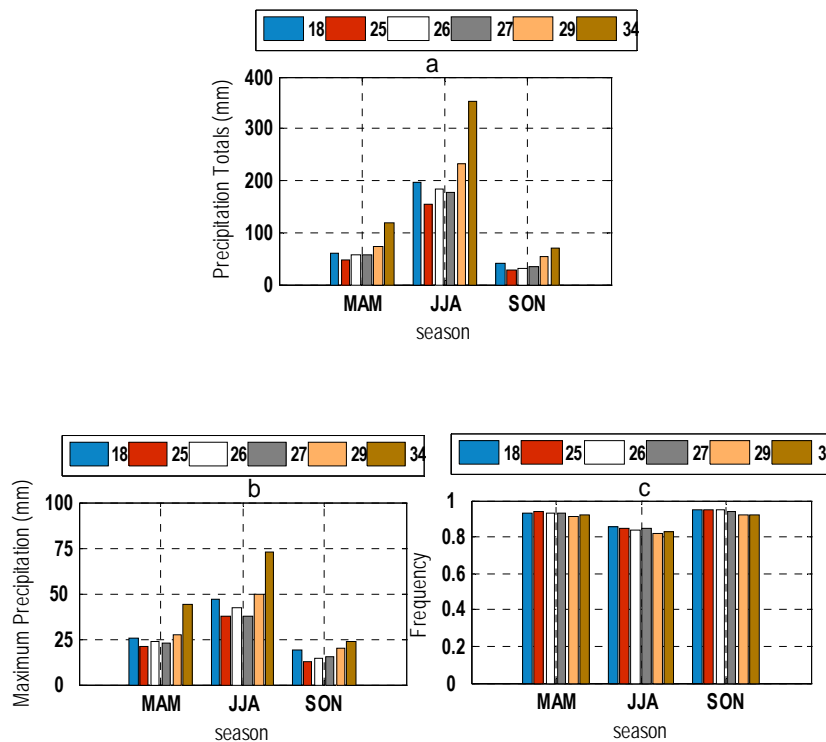


Figure 27: Precipitation parameters in stations 18, 25, 26, 27, 29 and 34. (a) Seasonal Precipitation Totals, averaged for period 1970-2003. (b) Seasonal frequency of dry days, averaged for period 1970-2003. (c) Seasonal maximum precipitation averaged for record 1970-2003

(1)Source: Dirección General de Aguas DGA

In table 17 the percentages of seasonal precipitation totals is summarized for all the stations and for the period of record. We can observe that winter precipitation is around 65% of the total annual amount in autumn it is about 20% and spring around 13% of the annual precipitation for all the analysed meteorological stations.

Table 17: Seasonal percentage of precipitation totals in the analysed stations
Period 1970-2003

Season	Station 18	Station 25	Station 26	Station 27	Station 29	Station 34
MAM	20.21	20.28	21.07	20.98	20.25	21.79
JJA	65.78	67.44	67.17	65.76	64.69	65.23
SON	14.01	12.28	11.76	13.26	15.06	12.99

The frequency of dry days was also analysed for the set of stations, in table 18 the maximum, minimum and mean values for the period of record are shown and in figure 27 (b) the mean was plotted. From this figure the first important observation is that autumn and spring present similar precipitation frequencies with a mean around 0.93 at all the stations, while winter is varying around 0.84 (see table 18) for all the stations as well. This is expected since winter is the season with more events in general. On the other hand regarding the behaviour among stations it is possible to remark that station 29 and 34 have the lowest values of precipitation in the three seasons although they are only slightly different from the others. These two stations are located at high altitudes (1100 and 1290 metres respectively) where the gauges had to record more precipitation.

The highest reported value was 1.0 (no precipitation) in autumn at station 26 and the lowest one was 0.620 in winter recorded by station 27 (see table 18).

The third parameter maximum precipitation (1 day duration) was also analysed for all the stations, the information that can be taken for the figure 27 (c) where its average for the record period was plotted, is basically the same as in figure 27 (a) here precipitation totals is shown. The variation by seasons and by stations follows the same behaviour. Winter has the highest values followed by autumn and finally by spring. The magnitude of the values at the stations, in decreasing order was: station 34, 29, 18, 26, 27 and 25.

The highest maximum precipitation value was 163.6 mm in winter recorded at station 34 and the lowest was 0 mm (no precipitation) in autumn recorded by station 26. See table 18 for details.

Table 18: Mean, maximum and minimum value of precipitation parameters for the period 1970-2003

Precipitation Totals							
Season	Station	18	25	26	27	29	34
MAM	Max	186.50	136.10	152.10	178.00	209.50	432.20
	Mean	60.92	46.21	57.37	56.17	72.86	118.00
	Min	2.50	3.50	0.00	6.50	10.20	9.20
JJA	Max	730.90	523.50	495.50	533.43	743.50	993.17
	Mean	198.32	153.70	182.91	176.10	232.80	353.28
	Min	19.00	5.90	15.60	8.50	22.50	21.50
SON	Max	141.01	83.27	106.10	90.16	148.00	210.10
	Mean	42.24	27.99	32.03	35.51	54.21	70.34
	Min	3.50	0.60	3.00	4.61	7.10	3.10
Frequency of dry days							
Season	Station	18	25	26	27	29	34
MAM	Max	0.989	0.978	1.000	0.989	0.978	0.978
	Mean	0.932	0.938	0.931	0.934	0.915	0.920
	Min	0.837	0.870	0.880	0.848	0.804	0.815
JJA	Max	0.967	0.978	0.946	0.978	0.957	0.957
	Mean	0.856	0.851	0.836	0.845	0.820	0.831
	Min	0.717	0.663	0.696	0.620	0.663	0.641
SON	Max	0.989	0.989	0.989	0.989	0.978	0.989
	Mean	0.946	0.947	0.946	0.939	0.921	0.924
	Min	0.879	0.890	0.835	0.846	0.813	0.780
Maximum precipitation							
Season	Station	18	25	26	27	29	34
MAM	Max	83.00	77.80	65.00	63.00	60.00	140.00
	Mean	25.68	20.44	23.98	22.91	27.62	43.85
	Min	2.00	3.10	0.00	5.00	5.00	5.00
JJA	Max	120.00	92.80	130.00	90.00	106.50	163.60
	Mean	46.63	37.34	42.05	37.80	49.64	72.78
	Min	12.40	3.00	8.80	5.00	12.50	14.50
SON	Max	60.00	46.60	48.50	48.50	51.00	71.00
	Mean	18.77	12.92	14.11	14.99	19.88	23.55
	Min	2.00	0.60	2.00	3.00	4.60	3.10

4.2.2.1 Station 18

Figure 28 represent the time series of the data in summer, autumn, winter and spring respectively.

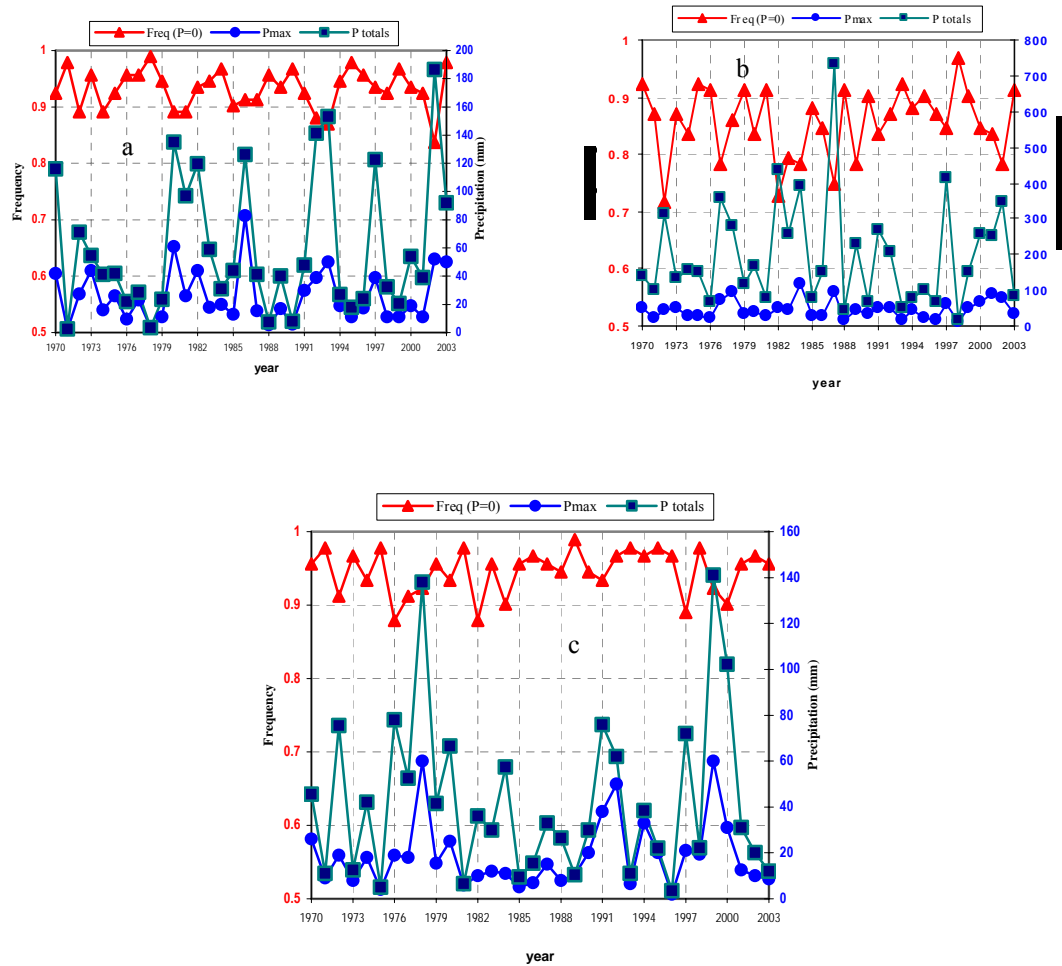


Figure 28: Precipitation series at station 18. The data is presented for Ptotal, Pmax and Freq (P=0). (a) AUTUMN. (b) WINTER (c) SPRING.

Observations:

- ✓ In general no tendency, shifts and seasonality can be noticed in the series in any of the three seasons; only a slightly positive trend seems to appear in Ptotal in autumn (see fig. 28-a).
- ✓ The maximum precipitation (duration 1 day) series behaves similar to precipitation total throughout time. It is better noticeable in autumn and spring because having few wet days, P total does not differ so much from the maximum one day precipitation since the latter contributes significantly to the amount of the total precipitation.

4.2.2.2 Station 25

Figure 29 represent the time series of the data in summer, autumn, winter and spring.

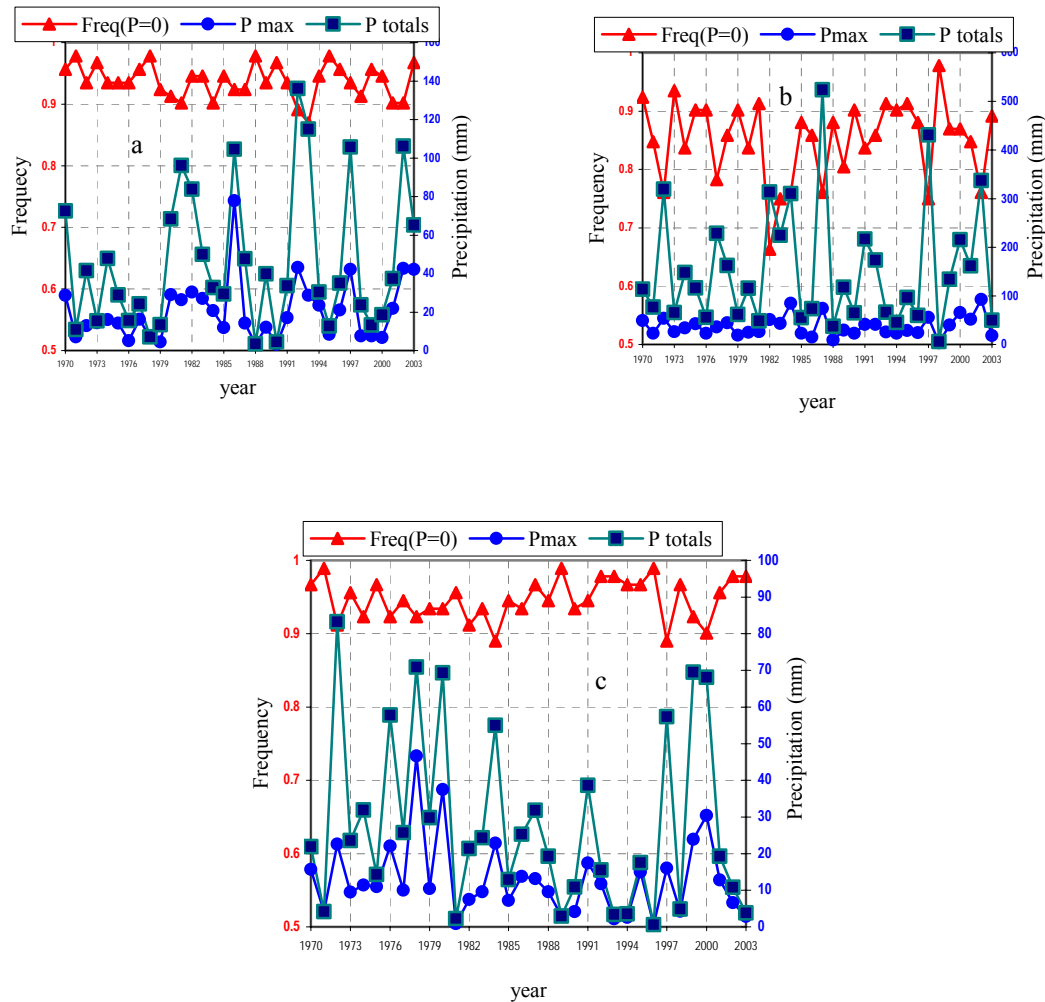


Figure 29: Precipitation series at station 25. The data is presented for Ptotal, Pmax and Freq (P=0). (a) AUTUMN. (b) WINTER (c) SPRING.

Observations:

- ✓ No tendency shifts and seasonality can be noticed in the series in any season.
- ✓ Ptotal and Pmax follow similar distribution throughout time.
- ✓ There are 3 years consecutives in winter when the frequency of dry days was low (more rainy days), they are 1982, 1983 and 1984 (See figure 29-b) although the amount of precipitation or P total in those years were not the highest peaks (smaller than peaks of 1987 and 1997) indicating that precipitation were less intense but with longer duration.

4.2.2.3 Station 26

Figure 30 represent the time series of the data in summer, autumn, winter and spring.

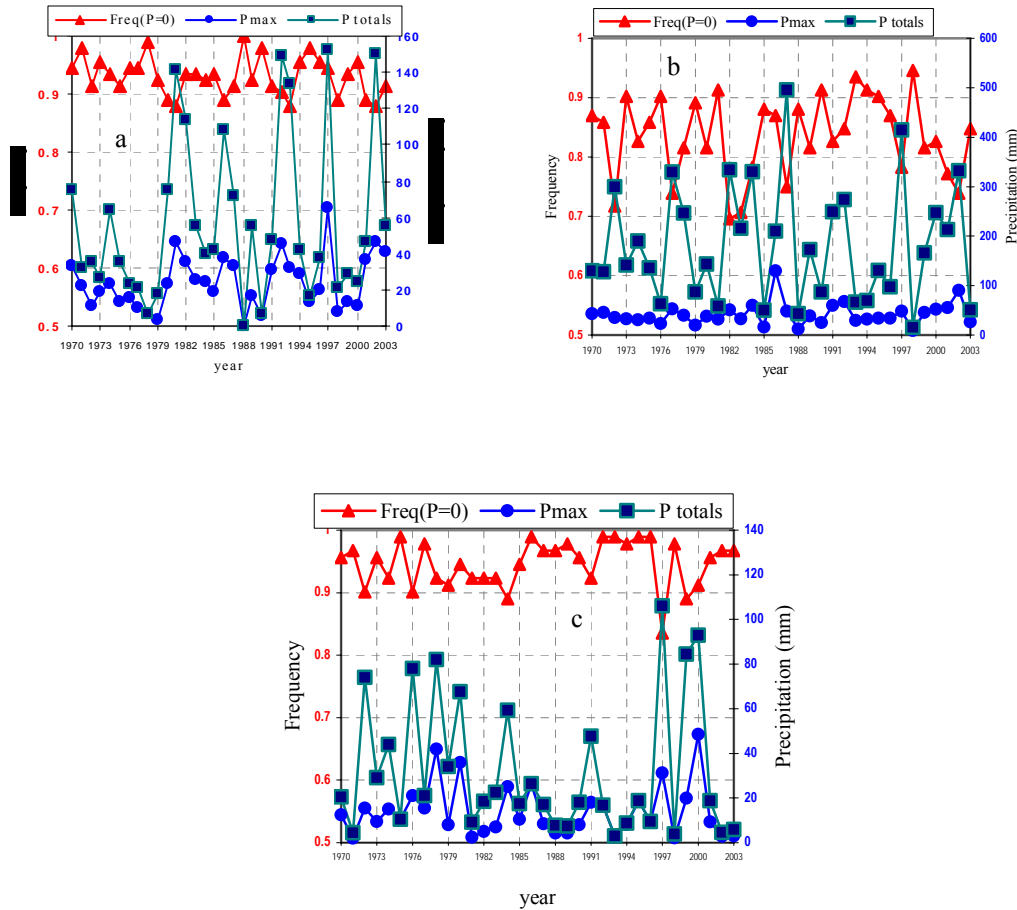


Figure 30: Precipitation series at station 26. The data is presented for Ptotal, Pmax and Freq (P=0). (a) AUTUMN. (b) WINTER. (c) SPRING

Observations:

- ✓ No shifts and seasonality can be noticed in the series
- ✓ A slightly positive trend seems to be in Ptotal and Pmax in autumn (see fig. 30-a)
- ✓ In year 1988 there was not precipitation for the autumn season, so in figure 43 we can see Ptot = 0mm, Pmax=0mm and Freq(P=0) = 1.

4.2.2.4 Station 27

Figures 31 represent the time series of the data in summer, autumn, winter and spring.

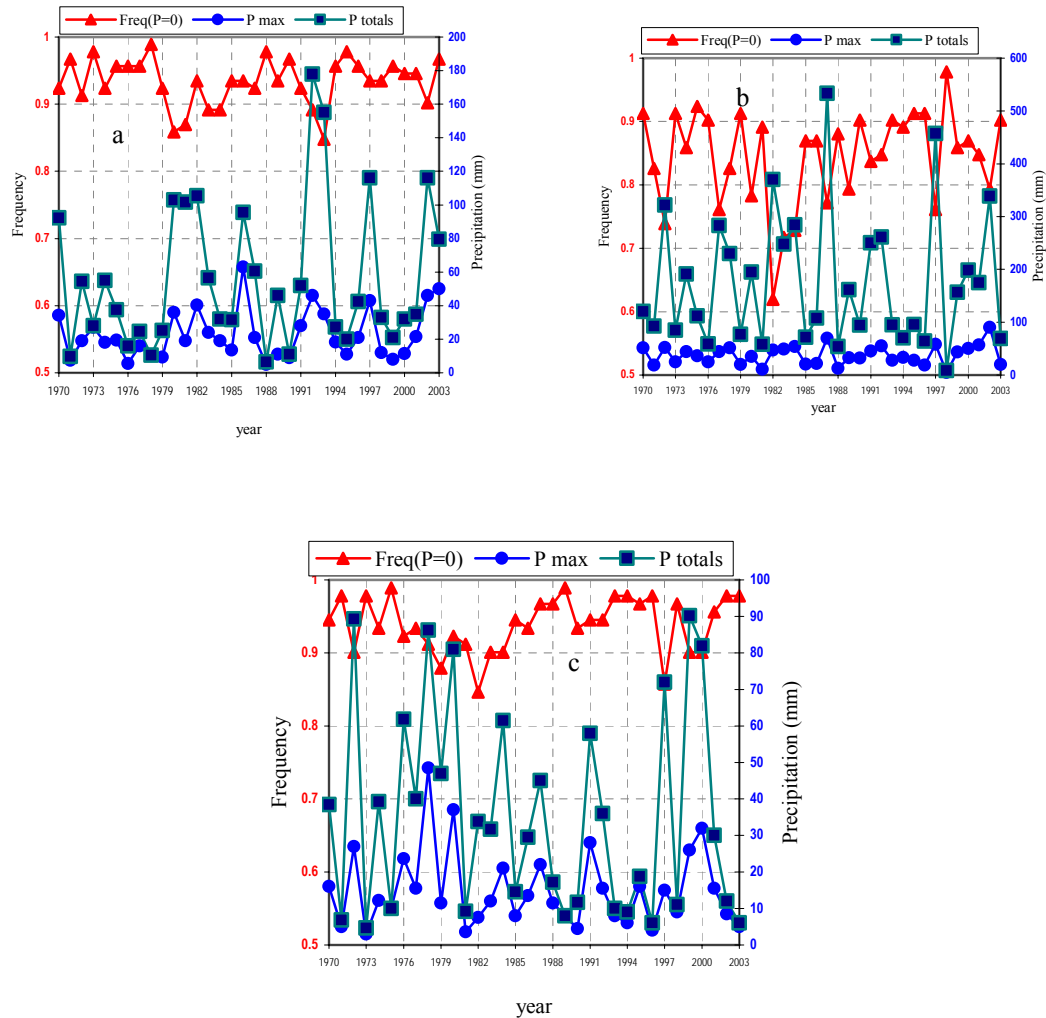


Figure 31: Precipitation series at station 27. The data is presented for Ptotal, Pmax and Freq (P=0). (a) AUTUMN. (b) WINTER. (c) SPRING

Observations:

- ✓ No shifts and seasonality can be noticed in the series
- ✓ In winter of 1982 the lowest value of Frequency of dry days (0.62) can be observed, indicating it was the most raining season throughout the record of period. (see fig. 31-b)

4.2.2.5 Station 29

Figure 32 represent the time series of the data in summer, autumn, winter and spring.

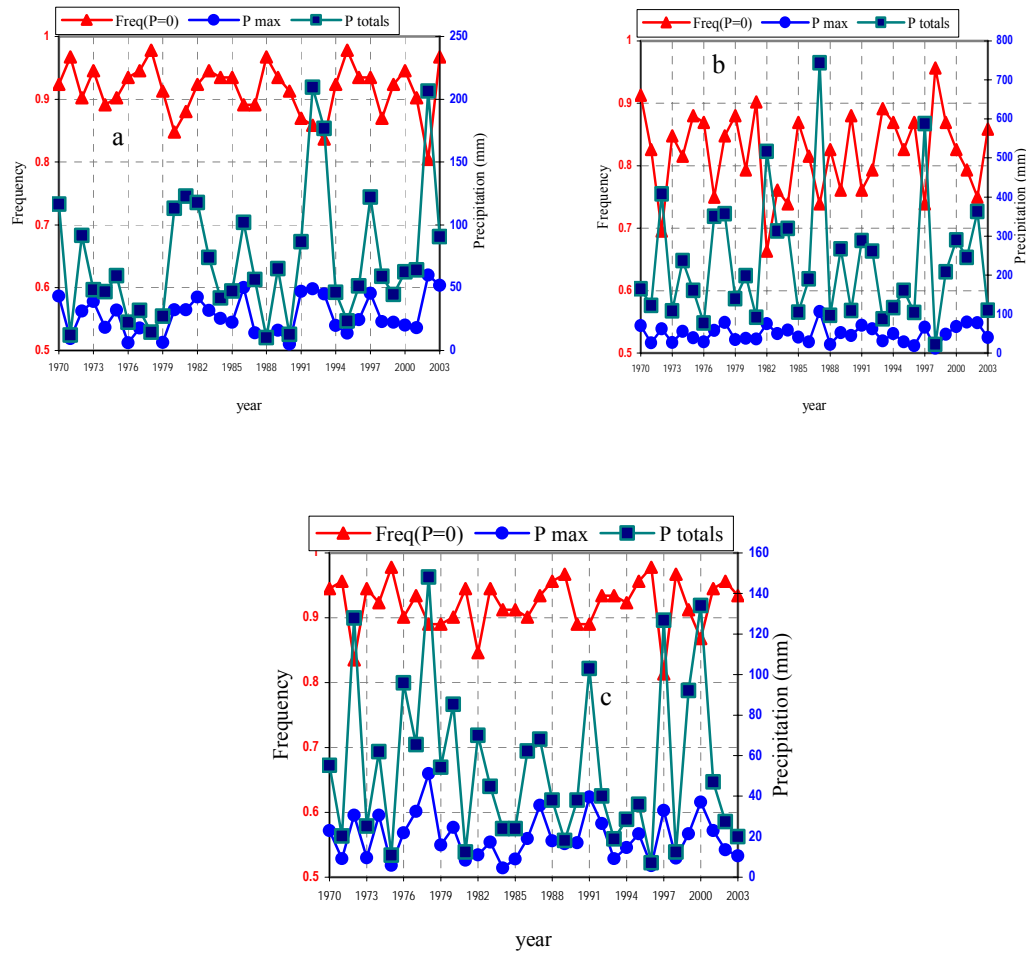


Figure 32: Precipitation series at station 29. The data is presented for Ptotal, Pmax and Freq (P=0). (a) AUTUMN. (b) WINTER. (c) SPRING

Observations:

- ✓ No shifts and seasonality can be noticed in the series
- ✓ Some positive tendency can be noticed in autumn for Ptotal and Pmax (see fig. 32-a).

4.2.2.6 Station 34

Figure 33 represent the time series of the data in summer, autumn, winter and spring.

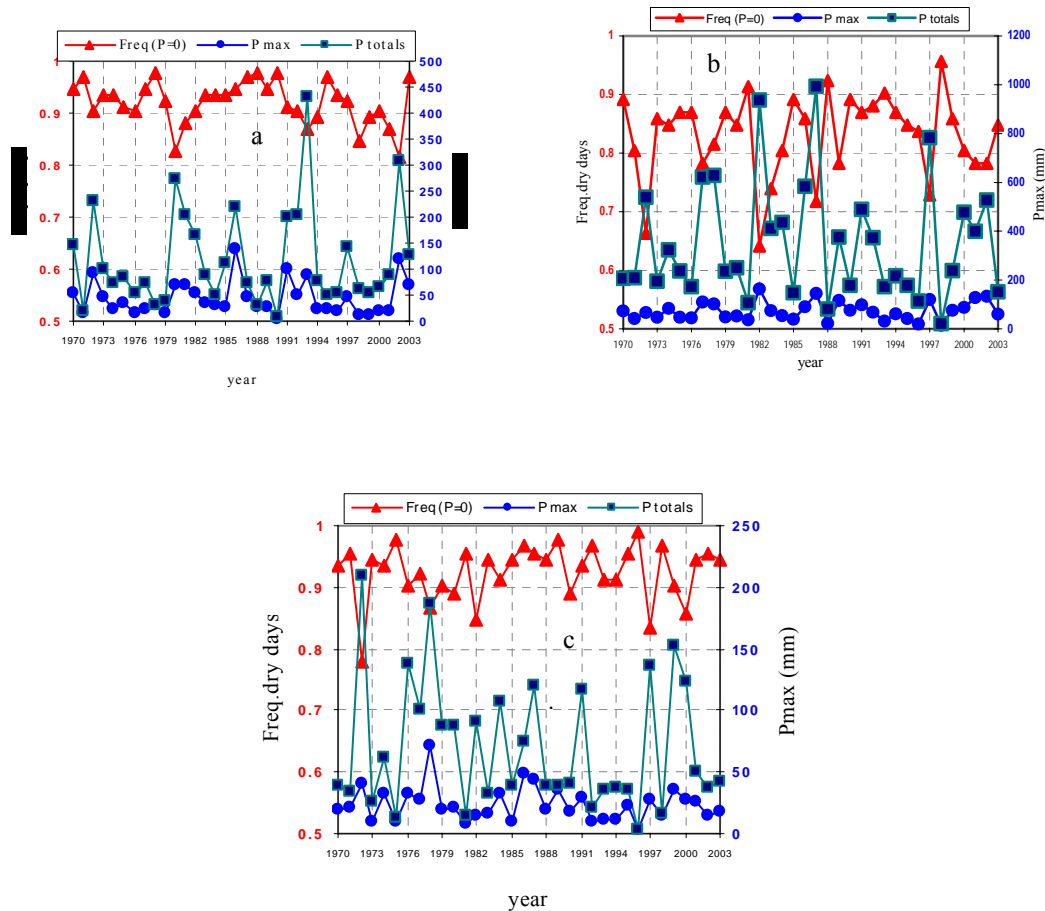


Figure 33: Precipitation series at station 34. The data is presented for Ptotal, Pmax and Freq (P=0). (a) AUTUMN. (b) WINTER. (c) SPRING

Observations:

- ✓ No tendency shifts and seasonality can be noticed in the series
- ✓ In winter of year 1982 the most intense precipitation of duration 1 day was recorded by this station, with Pmax = 163.6mm.

Finally the presence of peaks in a repetitive way was observed in all the stations, the years when they were measured were:

In Autumn: 1980, 1986, 1993, 1997 and 2002

In Winter: 1982, 1987 and 1997

In Spring: 1972 and 1978

4.2.3 Temperature

The temperature parameters were averaged for the period of record and then plotted in figure 34, to see their variability by season. Temperatures maximum and minimum vary in this decreasing order: summer, autumn, spring and winter. Nevertheless the difference between autumn and spring is small (see table 19). The frequency of $T_{min} > 0$ (see figure 19-b) follows the same decreasing order. The diurnal range is largest in summer, in autumn and spring it is almost the same, while in winter it is the (see figure 35-a). It is possible to see also that winter presents a frequency larger than 0.85, so that indicates that T_{min} in the basin is in general larger than zero.

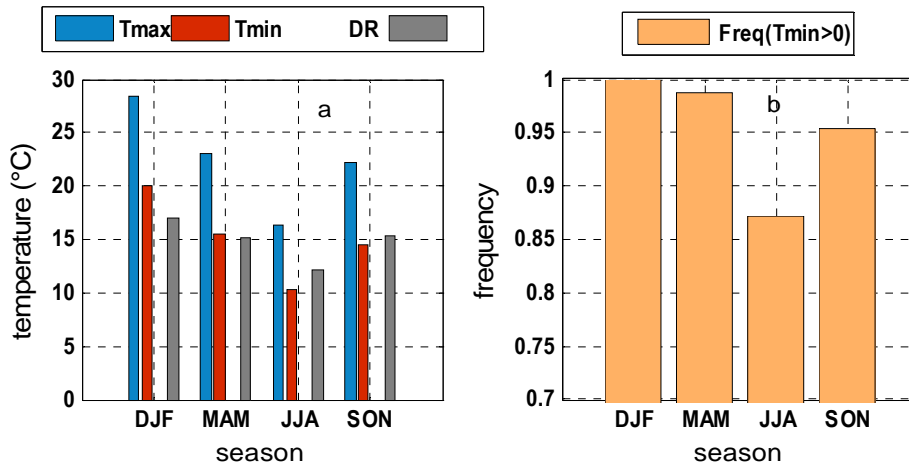


Figure 34: Temperature parameters at station 29 averaged for period 1970-2003. (a) Temperature maximal, minimal and Diurnal Range. (b) Frequency of $T_{min} > 0$

Table 19: Mean, Maximum and Minimum value of Temperature Parameters for the period 1970-2003

season		Tmax	Tmin	DR	Freq($T_{min} > 0$)
DJF	Max	30.11	13.82	19.98	1.00
	Mean	28.44	11.48	16.96	1.00
	Min	26.80	7.16	14.66	1.00
MAM	Max	24.94	9.73	19.68	1.00
	Mean	23.03	7.91	15.12	0.99
	Min	20.95	4.40	12.73	0.93
JJA	Max	19.61	6.28	15.58	0.99
	Mean	16.29	4.20	12.09	0.87
	Min	14.29	0.67	9.23	0.58
SON	Max	25.40	9.14	19.63	1.00
	Mean	22.22	6.87	15.35	0.95
	Min	19.04	2.39	12.06	0.69

4.2.3.1 Station 29

Figure 35 represents the time series of the data in summer, autumn, winter and spring.

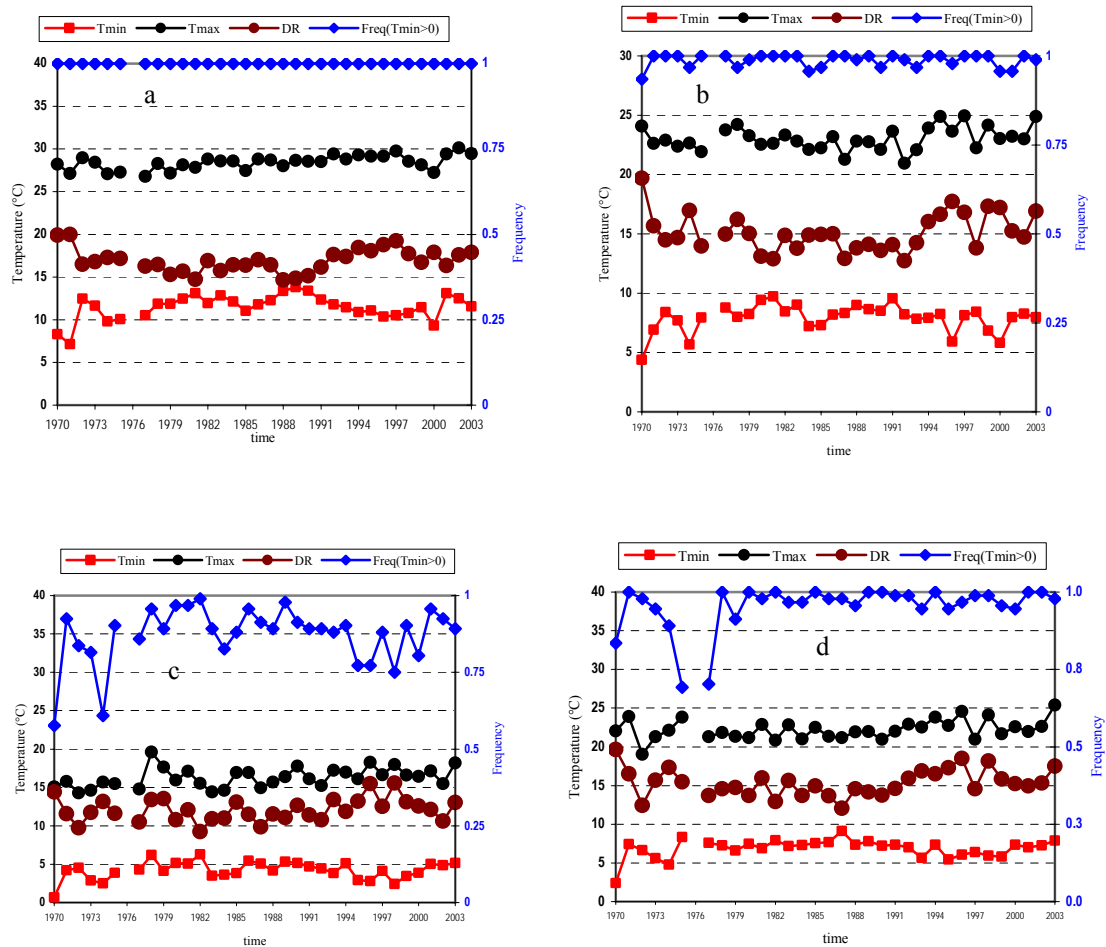


Figure 35: Temperature series at station 29 for the SUMMER season. Data is presented for temperature maximum, minimum, the diurnal range and frequency of $T_{min} > 0$. (a) SUMMER. (b) AUTUM. (c) WINTER. (d) SPRING

Observations:

- ✓ We can observe that year 1976 is completely missing from the record; no data were available for that year at this station and neither in the stations used to fill, so this year was taken out for temperature analysis.
- ✓ No shifts and seasonality can be noticed in the series
- ✓ In summer there seem to be an increasing tendency in all the series, in autumn this positive trend is noticeable for Tmax and DR. In winter is Tmax, Tmin, DR and Freq.(Tmin>0) that tend to increase.
- ✓ Tmin is larger than 0°C for all 4 seasons on the average.

4.3 Trend Analysis Statistics

To carry out the trend analysis an importation observation was taken into account. Regarding the streamflow series, a shift was observed in last 10 years (approximately) of the period of record, which was most noticeable at stations 17 and 18 (see figure 25 and 26). Information was found about the presence of water abstraction for hydropower production purposes. Two abstraction points were located upstream of stations 17 and 18 on rivers Juncal and Blanco. The hydropower plants were run-of-river type and their operations are in such a way that they extract the water upstream of these mentioned stations and transport it to 2 small hydropower plants located in Colorado and Aconcagua river upstream of station 14. Finally the water is released downstream of station 14. The year of starting operation of the hydropower plants system was between 1993 and 1994 for that reason, the trend statistics were only computed for the period 1970 to 1992 to analyse the natural change in the climatic variables.

4.3.1 Method

The methodology used to detect the trend in the series was the nonparametric Mann-Kendall (MK) test; this method was widely used in hydrological studies. This test is a rank-based procedure especially suitable for non-normally distributed data, data containing outliers and non-linear trends (e.g Helsel and Hirsch, 1992)

The null and alternative hypotheses of the MK test for trend in the random variable x are:

$$H_0: \Pr(x_j > x_k) = 0.5, j > i,$$

$$H_A: \Pr(x_j > x_k) \neq 0.5, j > i, \text{ (two-sided test) } \dots (a)$$

The Mann-Kendall statistics S is calculated as:

$$S = \sum_{k=1}^{n-1} \sum_{j=k+1}^n \text{sgn}(x_j - x_k) \dots (b)$$

Where x_j and x_k are data values in years j and k , respectively, with $j > k$, and $\text{sgn}()$ is the function:

$$\text{sgn}(x_j - x_k) = \begin{cases} 1, & \text{if } x_j - x_k > 0 \\ 0, & \text{if } x_j - x_k = 0 \\ -1, & \text{if } x_j - x_k < 0 \end{cases} \dots (c)$$

Under the null hypothesis the distribution of S can be approximated well by a normal distribution (for large sample sizes n), with μ_s and variance σ_s^2 given by:

$$\mu_s = 0, \\ \sigma_s^2 = [n(n-1)(2n+5) - \sum_{i=1}^m t_i(i-1)(2i+5)]/18 \dots (d)$$

Eq.(d) gives the variance of S with a correction for ties in data with t_i denoting the number of ties of extent i. The standard normal variance is then used for hypothesis testing, and is called here the trend test statistic Z.

$$Z = \begin{cases} (S-1)/\sigma_s & \text{if } S>0 \\ 0 & \text{if } S=0 \\ (S+1)/\sigma_s & \text{if } S<0 \end{cases}$$

For a two-tailed test, the null hypothesis is rejected at significance level α (Type I error) if $|Z|>Z_{\alpha/2}$ where $Z_{\alpha/2}$ is the value of the standard normal distribution with an exceed probability $\alpha/2$.

4.3.2 Streamflow:

The lag-1 autocorrelation coefficients were computed for each series and for all the stations and are listed in table 20. We can observe that they are generally low and conclude that the series are not autocorrelated. The highest values were:

- ✓ Station 14: -0.39 for percentile 25 in spring
- ✓ Station 16: 0.39 percentile 75 in winter
- ✓ Station 17: -0.34 percentile 25 in spring
- ✓ Station 18: -0.46 percentile 25 in spring

Prewhitening was not applied for that reason and also because it was reported in previous works (e.g. Pellicciotti, 2006 and Birsan et al., 2005) that the differences between original and pre-whitening data is not large.

Table 20 Lag-1 autocorrelation coefficient of the seasonal streamflow series at stations 14, 16, 17 and 18 for period of record 1970-1992

Station	14						16					
season	P0	P25	P50	P75	P90	P100	P0	P25	P50	P75	P90	P100
DJF	-0.15	-0.09	-0.08	-0.06	-0.10	-0.10	-0.09	-0.01	0.01	0.08	0.10	0.15
MAM	0.38	0.28	0.14	-0.06	-0.08	-0.05	0.03	-0.03	0.11	0.09	0.01	0.02
JJA	0.20	0.10	0.07	0.02	-0.01	0.06	0.02	0.17	0.30	0.39	0.25	0.07
SON	-0.30	-0.39	-0.14	-0.18	-0.06	-0.05	0.23	0.07	0.01	-0.12	-0.02	-0.12
Station	17						18					
season	P0	P25	P50	P75	P90	P100	P0	P25	P50	P75	P90	P100
DJF	-0.19	-0.12	-0.09	-0.13	-0.09	-0.12	-0.02	0.08	0.04	0.04	0.04	-0.03
MAM	0.19	0.00	-0.11	-0.14	-0.17	-0.21	0.41	0.42	0.38	0.06	0.01	-0.02
JJA	0.12	0.16	0.23	0.25	0.27	0.18	0.19	0.26	0.26	0.19	0.13	0.07
SON	-0.21	-0.34	-0.23	-0.23	0.03	-0.06	-0.39	-0.46	-0.14	-0.07	0.00	-0.15

The trend analysis using the Mann-Kendall (MK) test, was applied for all the series, (that means for the 6 seasonal percentiles: P0, P25, P50, P75, P90 and P100) and in the 4 stations, they are shown in table 21 and plotted in figure 36. None of the trends were statistically significant at 5% of significance level, but they show us anyway a tendency. For instance, in station 14 (figure 36-a) all the percentiles tend to increase and for all seasons, same situation can be observed for

station 17 (figure 36-c). In station 16 we can see a decreasing in all the percentiles in summer and of percentile 50 in spring, while in the rest of seasons the percentiles tend to increase (see figure 36-b). Finally in station 18 percentiles 50, 75, 90, 100 show a downward tendency in summer while low flows like percentile 0 and 25 increase slightly in the same season. In the rest of the seasons all percentiles presents an upward tendency for this station (see figure 36-d).

Table 21: Trend test statistics Z at 5% of significance level for seasonal streamflow series
Period of record 1970-1992

Station	14						16					
season	P0	P25	P50	P75	P90	P100	P0	P25	P50	P75	P90	P100
DJF	0.63	0.24	0.40	0.53	0.63	0.74	-0.26	-0.42	-0.42	-0.55	-0.98	-1.45
MAM	1.06	0.87	0.79	0.90	0.58	0.34	0.69	0.05	0.53	0.90	1.21	0.16
JJA	0.50	0.40	0.58	0.42	0.63	0.69	1.22	0.90	1.48	1.08	1.21	1.16
SON	0.82	0.37	0.18	0.26	0.85	0.79	0.21	0.63	-0.21	0.95	0.79	0.95

Station	17						18					
season	P0	P25	P50	P75	P90	P100	P0	P25	P50	P75	P90	P100
DJF	0.32	0.63	0.48	0.63	0.85	0.32	0.11	0.05	-0.13	-0.21	-0.40	-0.53
MAM	0.21	0.69	0.53	0.74	0.79	0.53	1.37	1.16	0.42	0.69	1.06	0.48
JJA	0.82	1.00	0.58	0.42	0.26	0.66	1.16	0.69	0.55	0.69	0.71	0.58
SON	0.37	0.24	0.66	1.06	1.43	1.64	0.37	0.21	0.98	0.85	0.63	0.42

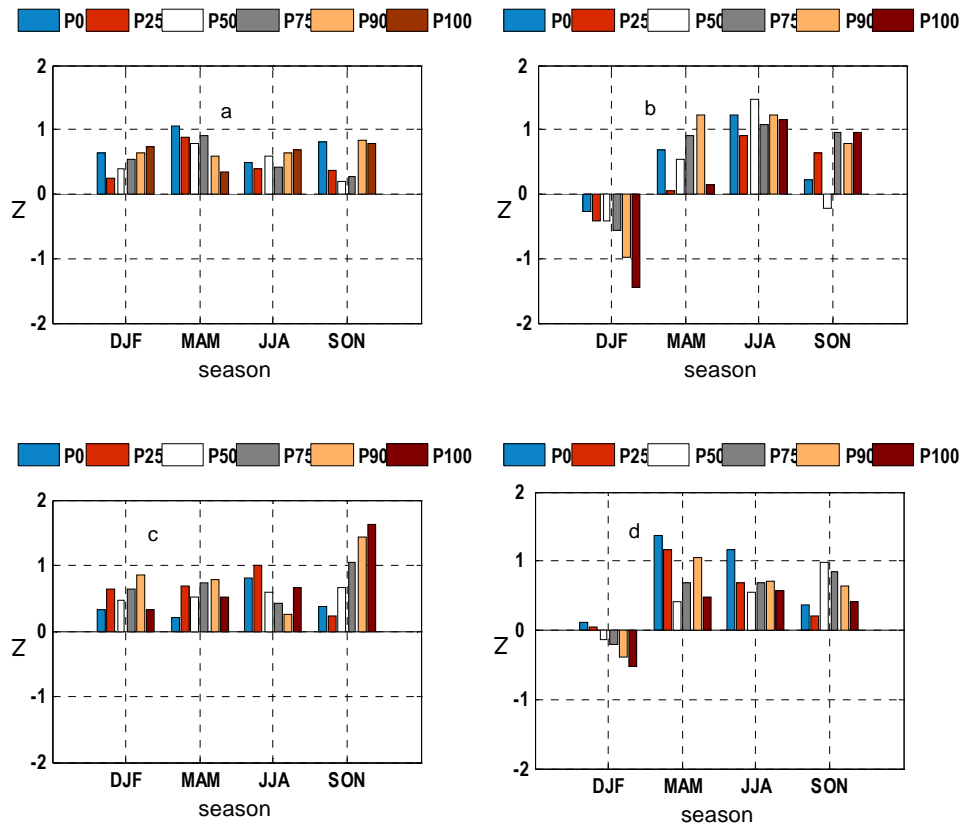


Figure 36: Trend test statistics Z at 5% of significance level for seasonal streamflow series for the period of record 1970-1992. The sign of Z indicates trend direction. (a) Station 14, (b) Station 16, (c) Station 17, (d) Station 18. No statistically significant trends

4.3.2 Precipitation

The lag-1 autocorrelation coefficients for the precipitation series were calculated and are listed in table 22. In this case we can also appreciate low values for all series and seasons, the highest values were:

- ✓ Station 18: -0.29 for Freq(P=0) in winter
- ✓ Station 25: -0.30 for Pmax in winter
- ✓ Station 26: 0.31 for Pmax in autumn
- ✓ Station 27: -0.36 for Pmax in winter
- ✓ Station 29: -0.42 for Pmax in winter
- ✓ Station 34: 0.38 for Ptotal in autumn

Table 22: Seasonal lag-1 autocorrelation coefficient of precipitation series at stations 18, 25, 26, 27, 29 and 34 for the period of record 1970-1992

Station	18			25			26		
season	Ptotal	Pmax	Freq(P=0)	Ptotal	Pmax	Freq(P=0)	Ptotal	Pmax	Freq(P=0)
MAM	-0.01	-0.17	0.11	0.02	0.00	0.14	-0.01	0.31	0.27
JJA	-0.23	-0.18	-0.29	-0.08	-0.30	-0.29	-0.15	-0.16	-0.26
SON	-0.28	0.20	-0.05	-0.15	-0.27	-0.28	-0.11	-0.17	-0.24

Station	27			29			34		
season	Ptotal	Pmax	Freq(P=0)	Ptotal	Pmax	Freq(P=0)	Ptotal	Pmax	Freq(P=0)
MAM	0.23	0.00	0.15	0.25	0.06	0.15	0.38	-0.06	0.09
JJA	0.02	-0.36	-0.32	-0.21	-0.42	-0.28	-0.09	-0.23	-0.17
SON	0.27	-0.26	-0.27	-0.26	0.02	-0.24	-0.19	-0.16	-0.23

Taking into account the low autocorrelation coefficient, prewhitening was not applied to the series. The results of the Mann-Kendall (MK) test trend analysis are shown in table 23, NO statistically significant trends were found for precipitation series. From figure 37 where the Z statistics is plotted for all the series we can see that Ptotal present in general an upward trend in autumn and winter and a downward one in spring in all the gauging stations, but specifically in station 34 (figure 37-f) there is no trend for winter. Pmax doesn't follow the same approach than Ptotal in all the cases. Generally Pmax is increasing in autumn for all the stations, the exception is found in station 18 (figure 37-a) where it is possible to notice a small negative Z. In winter Pmax is also increasing in all the gauging stations but not at the station 16 (figure 37-b), there this parameter presents a downward trend. In spring there is not a general tendency, for instance it is increasing at station 18 (figure 37-a) and 29 (figure 37-e), decreasing in stations 25 (figure 37-b), 26 (figure 37-c), and 34 (figure 37-f) and no tendency in station 27 (figure 37-d). Finally the frequency of dry days or Freq. (P=0) has a downward trend in autumn and winter and an upward one in spring for stations 18, 25, 26 and 27 (figure 37- a, b, c and d respectively). At station 29 (figure 37-e) it decreases for all the seasons and at station 34 (figure 37-f) it has a positive tendency for all the seasons.

Table 23: Trend test statistics Z at 5% of significance level for seasonal precipitation series period of record 1970-1992

Station	18			25			26		
season	Ptotals	Pmax	Freq(P=0)	Ptotals	Pmax	Freq(P=0)	Ptotals	Pmax	Freq(P=0)
MAM	0.26	-0.11	-0.40	0.58	0.29	-1.40	0.53	0.61	-1.32
JJA	0.32	0.48	-0.79	0.05	-0.48	-0.85	0.53	0.63	0.00
SON	-0.29	0.08	0.42	-1.00	-0.71	0.55	-1.32	-0.11	1.03

Station	27			29			34		
season	Ptotals	Pmax	Freq(P=0)	Ptotals	Pmax	Freq(P=0)	Ptotals	Pmax	Freq(P=0)
MAM	0.69	0.40	-0.58	0.48	0.08	-1.22	0.00	0.16	0.61
JJA	0.48	0.37	-0.69	0.37	0.77	-1.00	0.58	1.00	0.77
SON	-0.48	0.00	0.32	-0.34	0.40	-0.37	-0.16	-0.32	1.06

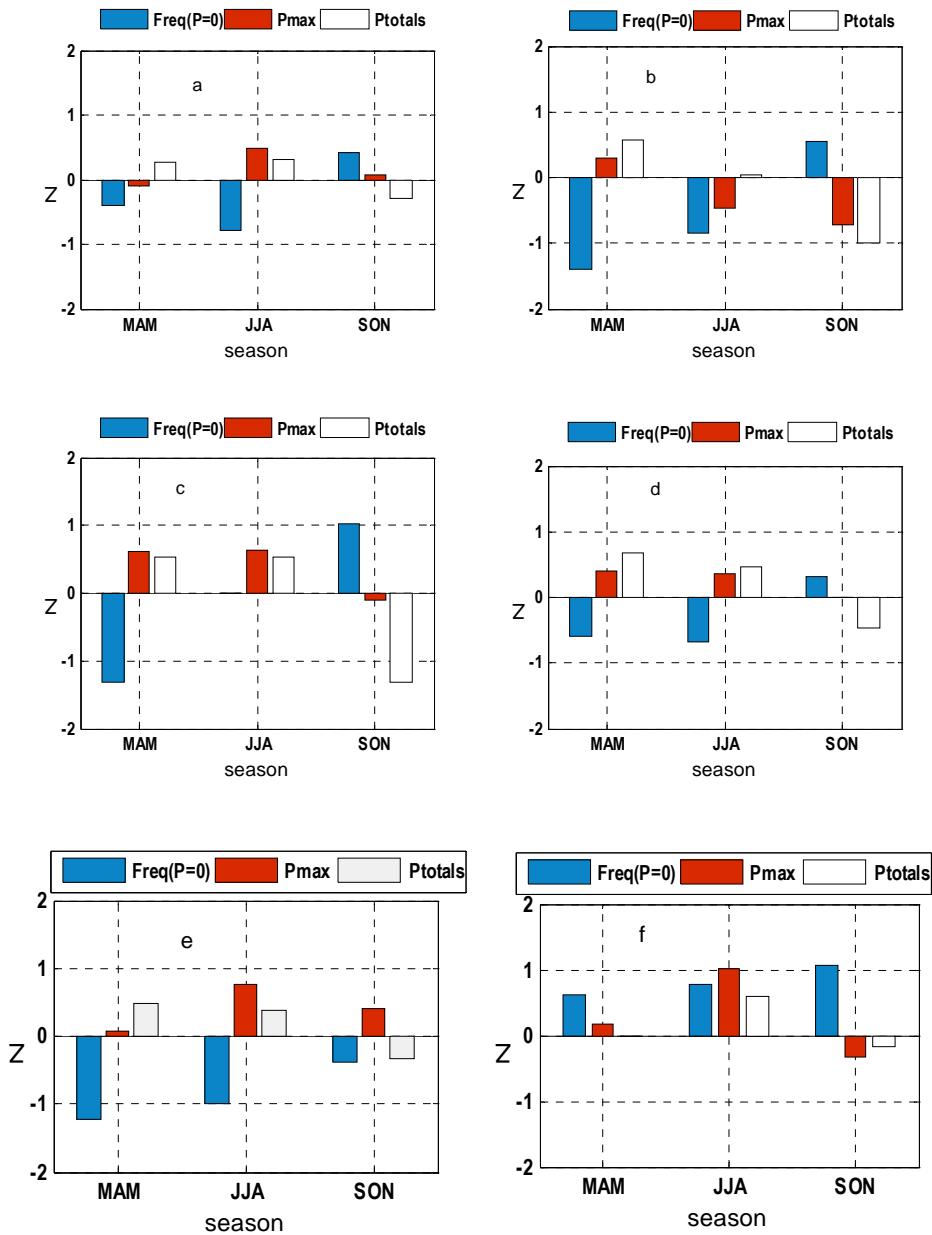


Figure 37: Trend test statistics Z for seasonal precipitation series for the period of record 1970-1992. The sign of Z indicates trend direction. (a) Station 18, (b) Station 25, (c) Station 26, (d) Station 27, (e) Station 29, (f) Station 34. No trends are statistically significant at the 5% significance level.

4.3.3 Temperature

The lag-1 autocorrelation coefficients for temperature series are listed in table 24. They are lower than 0.6, for instance the highest value of 0.51 was reported for the Tmax series in summer, we can also mention 0.43 reported by Tmin and 0.48 by Diurnal Range (DR) in the same season. Freq (Tmin>0) is 1 in the whole summer for that reason no autocorrelation coefficient is presented.

Table 24: Seasonal lag-1 autocorrelation coefficient of temperature series in 29
Period of record 1970-1992

Station	29			
season	Tmax	Tmin	DR	Freq (Tmin>0)
DJF	0.51	0.43	0.48	-
MAM	0.31	0.18	0.19	-0.11
JJA	0.17	0.27	-0.02	0.11
SON	0.06	-0.25	0.06	0.42

No prewhitening was applied in the temperature series. The trend test statistic Z was computed and the results are listed in table 25 and plotted in figure 38. Tmax increases in summer and winter, being significant in summer, but in autumn we can observe a negative and no significant tendency, while in spring there is a slightly decreasing. Temperature minimum is increasing in all the seasons; this reduction is significant in summer and autumn. On the other hand the diurnal range (DR) has a downward tendency in the four seasons with significance in summer and autumn. Finally Frequency of Tmin >0 series present no tendency in summer, slightly decreasing trend in autumn and increasing tendencies in winter and spring. In general we can say that changes in summer are most important.

Table 25: Trend test statistics Z at 5% of significance level for seasonal temperature series
Period of record 1970-1992

Station	29				
season	Tmax	Tmin	Tmed	DR	Freq (Tmin>0)
DJF	2.03	3.05	3.78	-2.20	0.00
MAM	-1.41	2.31	0.45	-2.59	-0.03
JJA	1.18	1.86	1.75	-0.96	1.55
SON	-0.11	1.64	2.09	-1.47	1.72

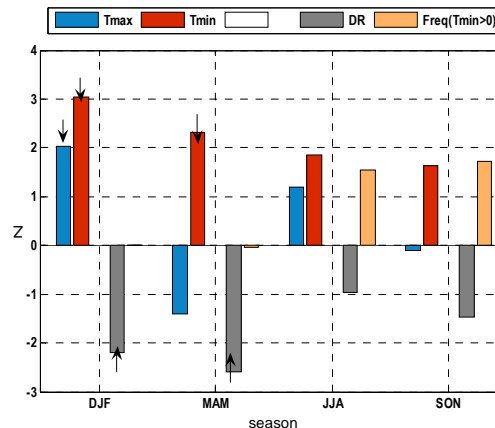


Figure 38: Trend test statistics Z for seasonal temperature series in station 29 for the period of record 1970-1992. The sign of Z indicates trend direction. The arrows indicate significant trends at 5% of significance level.

CHAPTER 5

CORRELATION ANALYSIS WITH LARGE-SCALE CIRCULATION PATTERNS

In order to investigate the influence of global atmospheric circulation patterns on trends in the hydroclimatic variables, correlation with indices of the general circulation of the atmosphere was carried out. Using established definitions, El Niño is the warm ocean current frequently observed in the eastern equatorial Pacific on the coast of Ecuador. In contrast to the El Niño, La Niña refers to an anomaly of unusually cold sea surface temperatures found in the eastern tropical Pacific. The large scale fluctuations in air pressure associated with the El Niño and La Niña ocean temperature changes are referred to as the Southern Oscillation (SO). The SO phase is negative during El Niño and positive during La Niña episodes. A review of the different existent definitions of the El Niño phenomena can be found in Trenberth, (1997).

For instance a quantitative definition was created by the Japan Meteorological Agency (JMA):

“Warms events or El Niño are periods during which, 5 month running means of the monthly Sea Surface Temperature (SST) anomalies are $+0.5^{\circ}\text{C}$ or more for at least six consecutive months in the region Niño 3”

The Sea Surface Temperature (SST) data were downloaded from JMA website. The data were used to obtain the correlation of the phenomena with the climatic variables of the basin; they were also plotted with the purpose to observe the relationship of the warm and cold events with the peaks in runoff, precipitation and temperature. The El Niño periods found within the record 1970-1992 were:

- ✓ May 1972 to February 1973
- ✓ July 1976 to January 1977
- ✓ June 1982 to August 1983
- ✓ October 1986 to January 1988
- ✓ May 1991 to Jun 1992

5.1 Correlation with Streamflow

From table 26 it is possible to see that the correlation between streamflow and SST is in general positive. At station 14 we can observe high values in summer and spring for all 3 percentiles while in winter only for percentiles 50 and 100.

Summer presents high values in general for the four stations that may indicate that El Niño cause an increase in summer precipitation. We can see as well that at station 16 and 18 that are located in glaciated sub basin the correlation is high for percentiles P50 and P100, that could indicate that SST influence on the air temperature producing more melting of the glaciers and therefore an increase in runoff. In autumn the correlation is low at all the stations. In winter stations 14 and 17 have high values, revealing the increase of winter precipitation which results into an increase of runoff. In spring the correlation is important at station 14 and, at station 17 only for percentile 0, El Niño may be causing the increase of spring precipitation and then of runoff.

Observing the plot in figure 39 is possible to see that peaks have appeared during the El Niño events at all the stations, but one exception is the peak presented in year 78-79 that is not within one of the “El Niño” periods.

Table 26: Correlation coefficients between mean seasonal streamflow percentiles: P0, P50, P100 and seasonal standardised Sea Surface Temperature (SST) for “Niño 3”. Period of record 1970-1992

Station	14			Station	16		
Season	P0	P50	P100	Season	P0	P50	P100
DJF	0.532	0.587	0.557	DJF	0.295	0.541	0.462
MAM	0.237	0.269	0.244	MAM	0.370	0.109	0.105
JJA	0.304	0.573	0.423	JJA	0.320	0.303	0.075
SON	0.645	0.484	0.455	SON	-0.053	-0.067	0.262
Station	17			Station	18		
Season	P0	P50	P100	Season	P0	P50	P100
DJF	0.422	0.571	0.594	DJF	0.336	0.461	0.457
MAM	0.231	0.264	0.204	MAM	0.187	0.189	0.092
JJA	0.436	0.507	0.320	JJA	0.192	0.371	0.331
SON	0.576	0.357	0.327	SON	0.310	0.395	0.269

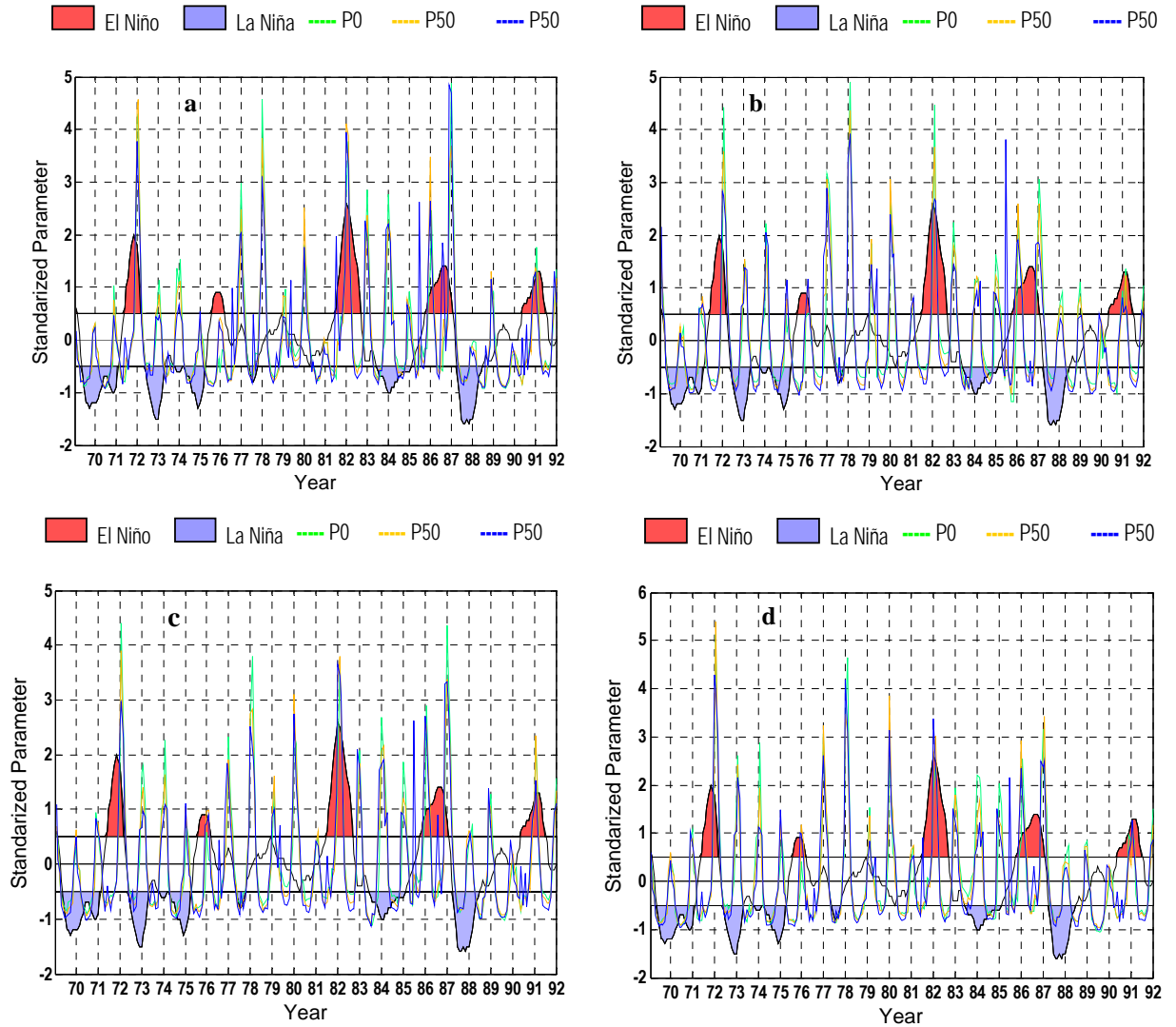


Figure 39: Time series of standardised 5 months running means of the Sea Surface Temperature (SST) for "Niño 3" and of standardised monthly streamflow percentiles: P0, P50 and P100 for period of record 1970-1992. (a) Station 14. (b) Station 16. (c) Station 17. (d) Station 18. El Niño events are indicated by the red curves above the threshold $+0.5^{\circ}\text{C}$

5.2 Correlation with Precipitation

Correlation with P_{total} is positive and high in winter for all the stations (see table 27), values vary from 0.544 at station 18 and 26 up to 0.629 at station 27, showing the strong influence of el Niño in winter precipitation that was reported in previous studies (e.g. Montecinos & Aceituno, 2003). Important values of correlation with P total can be observed in spring for stations 27, 29 and 34 as well, so the phenomena may be influencing precipitation in this season. As well from figure 40 we can see that high precipitation coincides with the El Niño periods (red curves) in all the stations, nevertheless there are exceptions e.g. the high precipitation year 1984 did not coincide with a period of El Niño; similar case was the event of 1978 recorded by stations 29 and 34 (see figure 40 (e) and (f) respectively).

On the other hand the frequency of dry days or $P=0$, present negative correlation with SST as was expected. High values can be observed in winter for all stations varying from -0.515 at station 18 up to -0.612 at station 34. In spring we can see also high correlations at stations 18, 27, 29, and 34 that are located at high altitudes.

Table 27: Correlation coefficients between mean seasonal precipitation parameters: Freq. ($P=0$) and P_{total} and seasonal standardised Sea Surface Temperature (SST) for “Niño 3”. Period of record 1970-1992

Station	18		25			26		
Season	Freq($P=0$)	P total	Season	Freq($P=0$)	P total	Season	Freq($P=0$)	P total
MAM	-0.187	0.315	MAM	-0.294	0.346	MAM	-0.291	0.292
JJA	-0.590	0.544	JJA	-0.576	0.610	JJA	-0.558	0.544
SON	-0.505	0.306	SON	-0.374	0.372	SON	-0.340	0.315

Station	27		29			34		
Season	Freq($P=0$)	P total	Season	Freq($P=0$)	P total	Season	Freq($P=0$)	P total
MAM	-0.407	0.411	MAM	-0.325	0.407	MAM	-0.156	0.246
JJA	-0.515	0.629	JJA	-0.571	0.603	JJA	-0.612	0.596
SON	-0.574	0.472	SON	-0.757	0.573	SON	-0.566	0.623

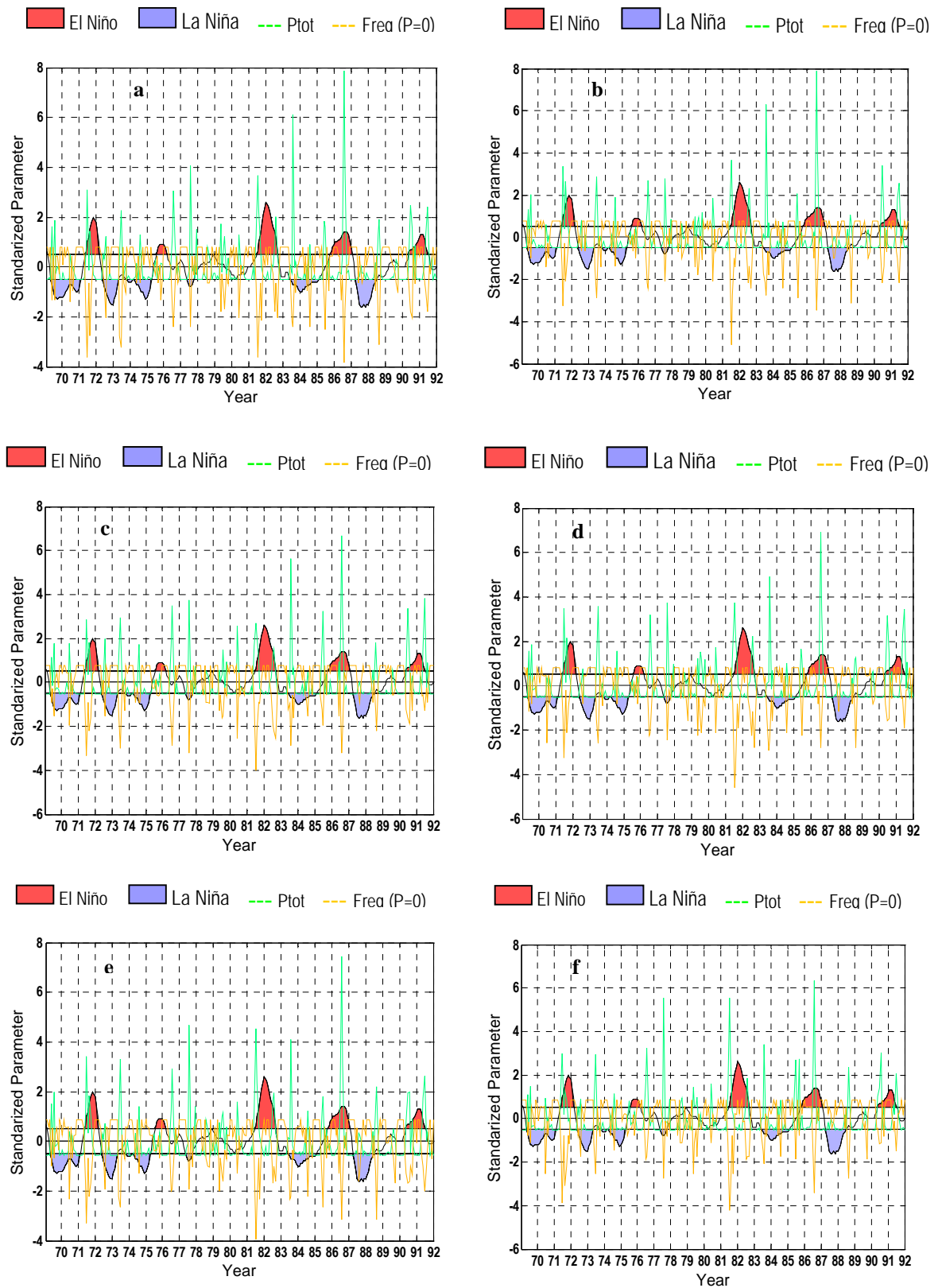


Figure 40: Time series of standardised 5 months running means of the Sea Surface Temperature (SST) for "Niño 3" and of standardised monthly precipitation parameters: Freq(P=0) and Ptotal for period of record 1970-1992. (a) Station 18. (b) Station 25. (c) Station 26. (d) Station 27. (e) Station 29. (f) Station 34. El Niño events are indicated by the red curves above the threshold +0.5°C

5.3 Correlation with Temperature

Correlations between SST and air temperature at station 29 are generally low, only Tmax presents a negative and important correlation of -0.576 in spring (see table n°28). In figure 41 no important variations or events can be observed during the El Niño periods.

Table 28: Correlation coefficients between mean seasonal temperature parameters: Tmin and Tmax and seasonal standardised Sea Surface Temperature (SST) for “Niño 3”. Period of record 1970-1992

Station	29	
Season	Tmin	Tmax
DJF	0.209	0.325
MAM	0.342	-0.220
JJA	0.397	-0.201
SON	0.356	-0.576

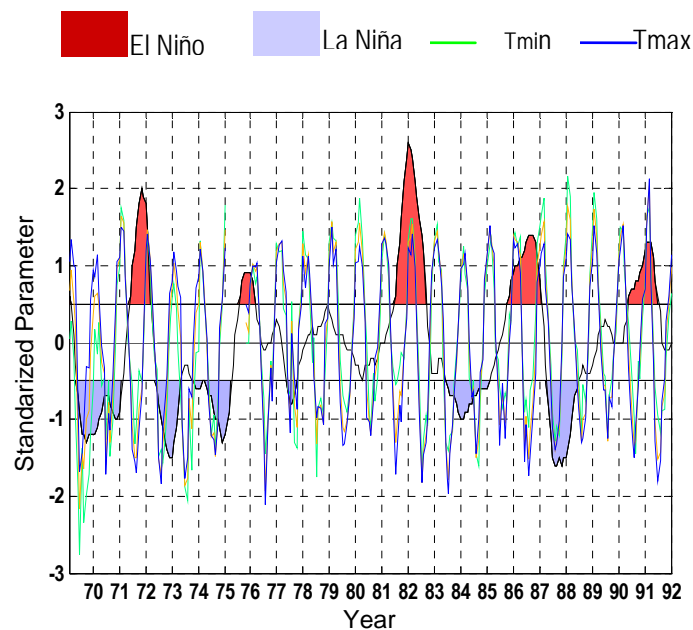


Figure 41: Time series of standardised 5 months running means of the Sea Surface Temperature (SST) for “Niño 3” and of standardised monthly temperature parameters: Tmin and Tmax for period of record 1970-1992 in station 29. El Niño events are indicated by the red curves above the threshold +0.5°C

CHAPTER 6

GLACIER COVERAGE

The drainage area was computed for the watershed upstream of each streamflow station. It is shown in figure 42 where the glaciers in the region are also indicated, some properties of those watersheds such as: area, mean altitude and mean slope are shown in table 29. To map the watersheds and the glaciers, a Digital Elevation Model (DEM) of 90 metres resolution was used. It was downloaded from The Consortium for Spatial Information (CGIAR-CSI) website. Using the Arc Map tools the flow directions throughout the watershed were calculated, following the steps such as: skin filling, slope and aspect of filled DEM to finally obtain flow directions and flow accumulation. Then the streamflows watersheds were extracted. Using ASTER images of the glaciers in the Aconcagua basin (provided by Chilean Direccion General de Aguas) was possible to map them in order to observe their special distribution on the watersheds.

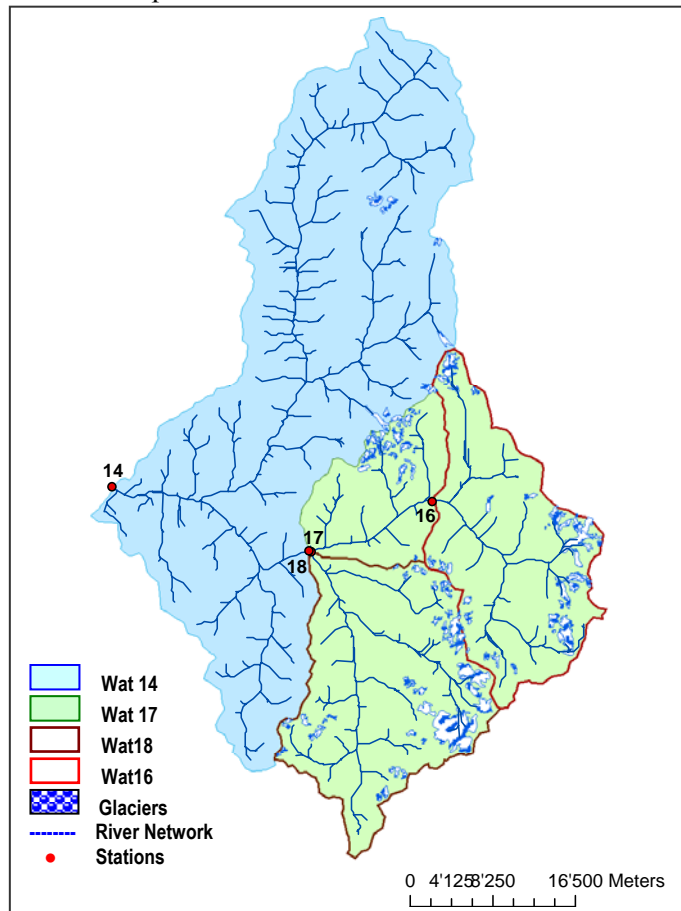


Figure 42 Watershed of streamflow stations 14, 16, 17 and 18

Table 29: Properties of the Streamflow stations Watershed

Watershed of station	Area (m ²)	Mean altitude (m)	Mean Slope (degrees)
14	2.1038 x 10 ⁹	3177.36	24.45
16	3.378 x 10 ⁸	3643.97	27.46
17	8.8724 x 10 ⁸	3462.11	27.10
18	3.867 x 10 ⁸	3477.03	26.22

On the other hand the frequency distribution of altitude within each watershed was plotted in each watershed (see figure 43, 44, 45 and 46) and the minimum, maximum and mean altitude of the glaciers were calculated (see table 30) at stations 16 and 18, using the spatial analysis tools of Arc Map with the ASTER image of glaciers and glacier data inventory. In these two watersheds the percentage of area occupied by glaciers is: 11.41% and 13.09% respectively.

Observing figures 46 and 47 we can see that glacierized areas are distributed at lower altitudes in watershed of station 16 than in watershed of station 18. It is also clear if we observe the altitudes in table 69. Glaciers in watershed of station 16 vary from 2956 m to 5835 m with a mean altitude of 3974 m while in watershed of station 18 from 3209 m to 5443 m. We can argue that glaciers at watershed of station 16 may be more vulnerable to the warming changes considering their low altitude distribution.

Table 30: Properties of Glaciers in Watershed of stations 16 and 18

Glaciers in Watershed of station	Area (Km ²)	Maximum Altitude (m)	Mean Altitude (m)	Minimum Altitude (m)
16	38 550 000	5835	3974	2956
18	50 640 000	5443	4058	3209

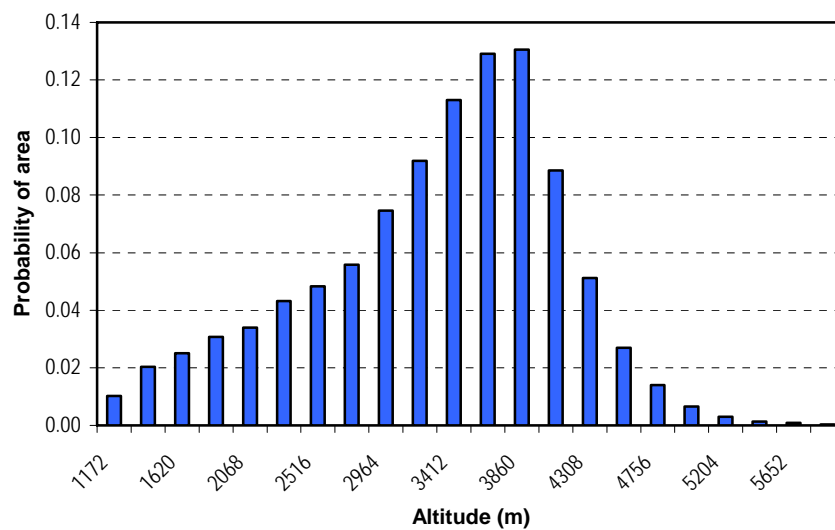


Figure 43: Histogram of altitude in the watershed of station 14

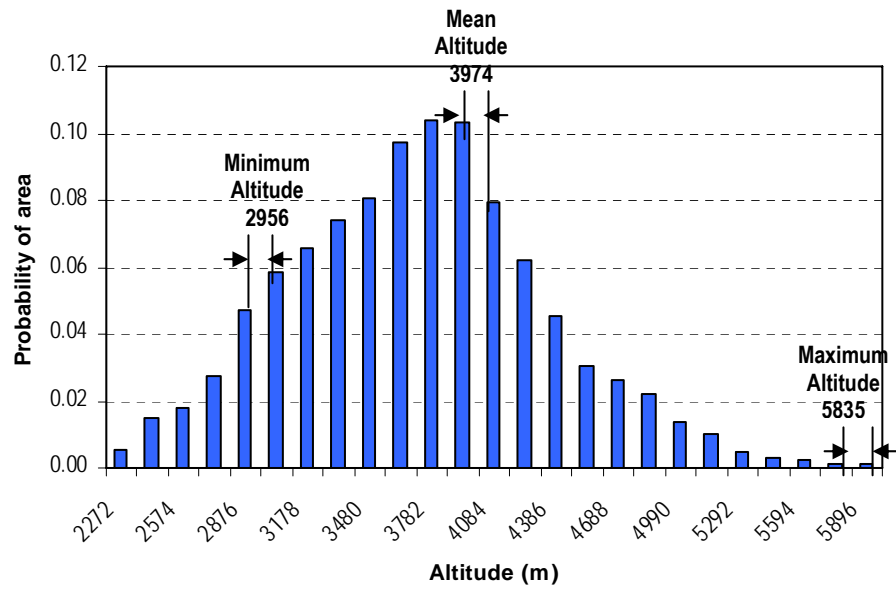


Figure 44: Histogram of altitude in the watershed of station 16. Minimum, maximum and mean altitudes of the areas covered by glaciers are indicated

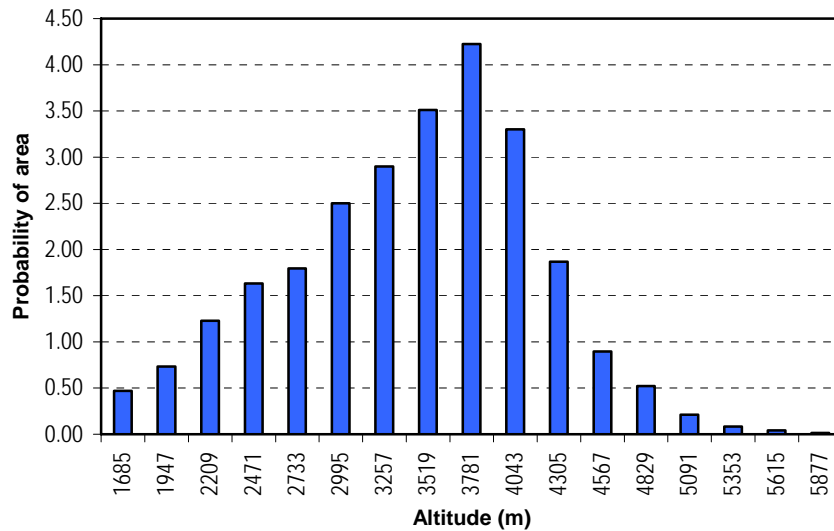


Figure 45: Histogram of altitude in the watershed of station 17.

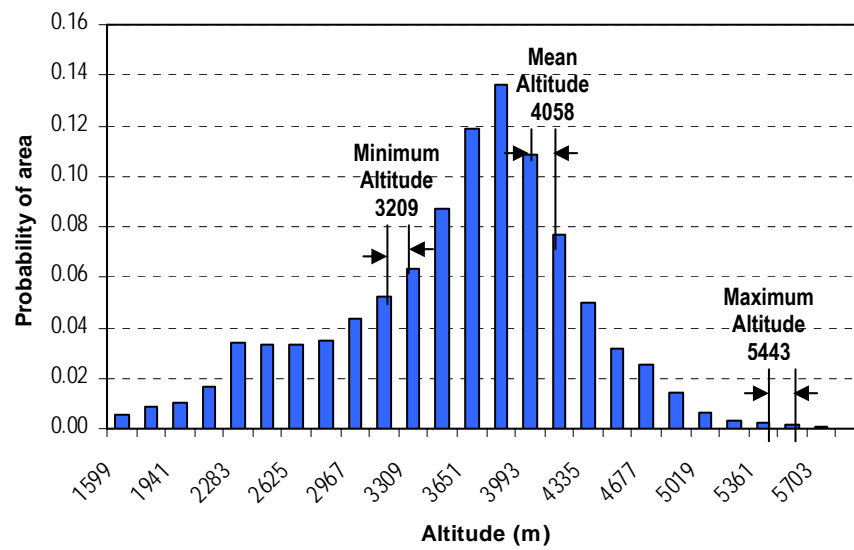


Figure 46: Histogram of altitude in the watershed of station 18. Minimum, maximum and mean altitudes of the areas covered by glaciers are indicated

CHAPTER 7

DISCUSSION

The analyses of the trends in streamflow, precipitation and temperature in the Aconcagua basin have revealed interesting features that are summarized below:

Although no significance was exhibited, in general positive trends were found in autumn, winter and spring streamflow at all the stations and in summer only at stations 14 and 17. The stations located in the upper part of the Aconcagua in the watersheds with an important amount of glacial coverage have revealed a decreasing tendency in summer. It was the case of station 16 and 18. This is the most important finding of this work; they may be explained by the fact that those flows being mainly fed by snow covers and glaciers are vulnerable to their progressive change, which in the area has been reported as a retreat of the glaciers.

This is supported by previous studies such as Casassa (1995), which has reported a retreat of glaciers in Chile due the existence of tropospheric warming observed in the second half of the 20th century. Carrasco et al., (2005) has also concluded that glaciers have been shrinking in the Andes of central Chile during the last 100 years.

As precipitation is the main source of snow and glaciers, its not significant increasing may be an explanation of the snow and glacier reduction. In this work, an upward tendency of amount and frequency of precipitation was found in autumn and winter and a downward one in spring. Carrasco et al., (2005) reported a negative tendency until 1976 and afterwards a positive trend although not significant north of 34°S and a decreasing trend south of 34°S, in the last quarter of the 20th century in Chile.

Temperature trends complement this explanation; this work showed significant positives trends for maximum and minimum temperature in summer and autumn. Minimum temperature exhibits a larger warming compared with the maximum and it is significant in summer and autumn. The maximum temperature and the diurnal range exhibit significance only in summer. The frequency of minimum temperature larger than zero is increasing in winter and spring although not significant. It may supported by Carrasco et al., (2005) where an overall warming of 1.3-2.1°C in minimum near-surface temperature and a warming of 0.2-1.5 C in maximum temperature were reported in central Chile during the period 1961 to 2001.

A positive change in air temperature will likely increase the summer snowmelt and the winter precipitation. The winter precipitation will be as rainfall instead of snow, thus decreasing glacier storage. For the same reasons, it is likely that also the extension and depth of the seasonal snow covers in the area have been decreasing, as it may be inferred also from results of Carrasco et al., (2005), which have shown an increase of the snow line elevation in the last quarter of the 20th century by 127m.

The Sea Surface Temperature has a direct correlation with precipitation in the basin, being the correlation factors at time lag 0 significant in winter (0.54 to 0.629) and spring (0.47 to 0.623) at all the stations. This finding agrees with the evidence produced by a number of other studies that looked at the effect of ENSO events on the region. (e.g. Waylen & Caviedes, 1990, Rutllant & Fuenzalida, 1991, Montecinos and Aceituno, 2003). El Niño years result in a significant increases of winter precipitation producing peaks in runoff and an accumulation of snow that will increase the snowmelt in spring and summer of the same year and a year later. The high values or peaks in runoff and precipitation coincide with most of the El Niño events presents in the period of record 1970-1992. From the correlation coefficients of streamflow and sea surface temperature we can find positives and significant values in summer (0.42 to 0.59), winter (0.42 to 0.57) and spring (0.46 to 0.65). Finally temperature of the air measured at station 29 did not show high values of correlation coefficients with SST; only minimum temperature has shown positive correlation (0.21 to 0.39) at all the seasons with the highest value in winter. The SST is not strongly correlated with air temperature at the upper part of the basin.

CHAPTER 8

CONCLUSION

This study has presented a statistical analysis of trends in daily streamflow, precipitation and temperature records from the Aconcagua basin at four stations for the period of record 1970 – 1992. No statistical significant trends were found neither in streamflow nor in precipitation, but in temperature on a seasonal basis. Identified trends in streamflow were related to observed changes in precipitation and air temperature, and correlated with the El Niño Southern Correlation and then analysed with the glacier coverage of the watershed. The main conclusions of this work are:

1. A negative trend although no significant in summer runoff was observed at stations 16 and 18, located in the upper part of the Aconcagua basin, which are directly fed by glacier and snow melt. In the rest of the seasons and at the others stations 14 and 17, a general increase in runoff was observed although not significant.
2. Trends in daily precipitation total and maximum precipitation were in general positive in autumn and winter but negative in spring. The frequency of zero precipitation has shown in general the opposite trend. No trend was significant.
3. Maximum temperature shows positive and significant trend in summer, while minimum temperature was significant in summer and autumn. The diurnal range had negative and statistically trend in summer and autumn. The main warming was observed in summer.
4. It is not possible to explain trends in streamflow only with the changes in precipitation. Nevertheless the decrease of summer runoff at station 16 and 18 can be explained by the decrease of glacial coverage and reduction of the snow depth in their drainage watershed. This is supported by previous studies that have reported the retreat of glaciers and also by the strong increase of temperature recorded in station 29 that might cause a change of phase in precipitation from snowfall into rainfall, causing less snow storage and increase of liquid precipitation.
5. The ENSO phenomena is affecting the changes in precipitation and streamflow, the results shows that winter and spring precipitation increase during El Niño events, resulting in peaks in winter streamflow and accumulation of snow that increase the snowmelt in spring and

summer within the same year. The effects are not easily noticeable in the highest part of the basin.

6. In comparison with the study by Pellicciotti et al, (2006) which carried out the first step of analysis of the hydroclimatic trends in the Aconcagua basin, this work has added the observation about the summer streamflow reduction in the highest part of the basin, at stations 16 and 18; although trends were no significant. This finding is to be considered because it may provide additional evidence of the retreat of glaciers in the basin.
7. Finally it is also important to consider that the record of period was short, 1970-1992 which is less than 30 years, which is generally used as minimum reference for the trend detection with the Mann-Kendal test. The changes observed in this study may become significant if we could analyse the data for a longer period, until nowadays for instance. It is of high importance that the Chilean Direccion General de Aguas obtain updated high resolution data which can reflect the natural variability in the basin and especially in the watersheds covered by glaciers.

Appendix

A1. Parameters A, B of the scaling replacement method for the streamflow gaps

Station 14

Gap n°	year	A	B	Used Station
1	1970	1.723404	-0.29911	stat17
2	1973	3.449074	0.045441	stat18
3	1974	1.665823	0.07231	stat17
4	1976	1.740484	-0.66558	stat17
5	1977	2.540416	-1.02494	stat17
6	1977	1.936306	-0.04739	stat17
7	1977	2.051948	1.674126	stat17

Station 16

Gap n°	year	A	B	Used Station
1	1970	0.375		
2	1970	0.835106	-0.01131	stat.18
3	1971	1.013605	-0.06949	stat.18
4	1971	0.610236	-0.00025	stat.18
5	1972	0.41048	0.01847	stat.18
6	1972	0.349183	0.025729	stat.18
7	1973	0.374408	0.009283	stat.18
8	1974	0.408219	0.047895	stat.18
9	1974	0.378319	0.02007	stat.18
10	1974	0.428894	0.056242	stat.18
11	1974	0.422481	0.048148	stat.18
12	1975	0.87156	0.029808	stat.18
13	1975	1.40000	-0.05186	stat.18
14	1975	0.801653	-0.01362	stat.18
15	1976	0.823045	-0.00692	stat.18
16	1977	0.947115	-0.44911	stat.18
17	1978	0.362117	-0.01974	stat.17
18	1980	0.836193	-0.32562	stat.18
19	1980	0.443165	-0.12156	stat.18
20	1983	0.415718		stat.17
21	1984	0.20743	-0.03155	stat.14
22	1986	0.302663	0.016765	stat.17
23	1986	0.385744	-0.02892	stat.17
24	1987	0.66426	-0.06551	stat.18
25	1987	0.401786	-0.11646	stat.18
26	1989	0.534545	-0.02931	stat.18
27	1990	0.887324	0.05956	stat.18
28	1990	1.348214	0.058605	stat.18
29	1990	0.824959	-0.07328	stat.18
30	1992	0.782016	-0.05527	stat.18
31	1993	1.022727	0.066507	stat.18
32	1993-1994	0.949721	-0.01672	stat.18
33	1999	0.118578	0.120684	stat.14

Station n° 17

Gap n°	year	A	B	Used Station
1	1970	0.913793		stat.14
2	1973	1.971429	0.011229	stat.18
3	1974	0.514504	0.043264	stat.14
4	1974	0.506757	0.190927	stat.14
5	1975	2.791809	-0.01721	stat.18
6	1976	3.40553	-0.04014	stat.18
7	1977	3.098592	-0.12717	stat.18
8	1979	2.546296	0.163384	stat.18
9	1979	3.28626	-0.03393	stat.18
10	1981	1.876344	-0.43983	stat.18
11	1981	2.179353	-0.29816	stat.18
12	1983-1984	0.477222	-0.01308	stat. 14

Station n° 18

Gap n°	year	A	B	Used Station
1	1970	0.390517		stat.14
2	1976	0.536601	-0.05857	stat.17
3	1976	0.375196	-0.00829	stat.17
4	1977	0.370992	0.076866	stat.17
5	1984-1985	1.445205	0.022509	stat.16
6	1993	0.262896	-0.03337	stat.17
7	1995	0.034328	0.047944	stat.14
8	1996	0.618357	0.172504	stat.17
9	1996	0.473282	-0.00649	stat.17
10	1996	0.382979	0.120091	stat.17
11	1997	0.736318	-0.00891	stat.17

A2. Parameters A and B of the scaling replacement method for the temperature gaps. At station 29 Vilcuya.

Temperature Maximum

Gap n°	year	A	B	Used station
1	1978	1.106195	-0.15068	stat33
2	1978	1.152174	0.26087	stat33
3	1978	1.656716	-0.5966	stat33
4	1979	1.078431	-0.02454	stat33
5	1982	1.176471	-1.13235	stat45
6	1984	0.705882	1.255147	stat45
7	1990	1.038462	-0.00613	stat45
8	1991	1.132231	-0.08199	stat45
9	1992	1.133047	0.166667	stat45

Temperature Minimum

Gap n°	year	A	B	Used station
1	1978	1.575	-0.2125	stat33
2	1978	1.189189	-0.17135	stat33
3	1978	0.425	-0.0127	stat33
4	1979	1.122449	-0.07646	stat33
5	1982	1.117647	0.048039	stat45
6	1984	1.155556	-0.09651	stat45
7	1990	0.891089	0.020761	stat45
8	1991	1.061947	0.079036	stat45
9	1992	1.068702	0.040204	stat45
10	2000	1.079208	0.02452	stat45

A3. Mann-Kendall code, developed in MATLAB

```
D=data;
[R,C]=size(D);
A=[]; S=[]; Var=[]; Z=[]; Ho=[];
man=[];
t=[];
for n=1:C
for j = 2:R
    for k = 1:R-1
        if j>k
            if (D(j,n)==D(k,n))
                A(k,j)=0;
            else
                if (D(j,n)>D(k,n))
                    A(k,j)=1;
                else A(k,j)=-1;
                end
            end
            t=transp(A);
            man= sum(t);
            ss=sum(man);
        end
    end
end
vars=(R*(R-1)*(2*R+5))/18;
%Ties calculation%
count=1;
for i=1:R-1
    if(D(i,n)==D(i+1,n))
        count = count+1;
        if i==(R-1)
            vars = vars-(count*(count-1)*(2*count+5))/18;
        end
    else
        vars = vars-(count*(count-1)*(2*count+5))/18;
        count = 1;
    end
end
end
if ss>0
    ZZ = (ss-1)/vars^0.5; Z=[Z;ZZ];
else
    if ss==0
        ZZ = 0; Z=[Z;ZZ];
    else ZZ = (ss+1)/vars^0.5; Z=[Z;ZZ];
    end
end
end
%alfa      0.2      0.5      1      2.5      5      20
%Zalfa/2    2.99    2.805    2.61    1.15    1.96    1.28
%analysing at significance level of 5 (type error I),Z(?/2)=1.96
Zpositif=((ZZ)^2)^0.5;
if Zpositif > 1.96
    HHo=0; Ho=[Ho;HHo];%rejected-there is a trend%
else
    HHo=1; Ho=[Ho;HHo];%accepted-there is not a trend%
end
S=[S;ss]; Var=[Var;vars];
end
```

Bibliography

Data and basin attributes

- Pellicciotti, F., Burlando, P. and van Vliet, K. (2006): Recent trends in precipitation and streamflow in the Aconcagua River Basin, central Chile. IAHS Publication (In press).
- asassa, G. (1995) Glacier inventory in Chile: current status and recent glacier variations. *Ann. Glaciol.*, 21, 317-322.

Streamflow trend analyses

- Pellicciotti, F., Burlando, P. and van Vliet, K. (2006): Recent trends in precipitation and streamflow in the Aconcagua River Basin, central Chile. IAHS Publication (In press).
- Birsan, M.V., Molnar, P., Burlando, P. & Pfaundler, M. (2005) Streamflow trends in Switzerland. *J Hydrol.*, 314(1-4), 312-329.
- Burn, D.H., and M.A. Hag Elnur, 2002. Detection of hydrologic trends and variability. *J. Hydrol.*, 255, 107-122.
- Waylen, P. R. & Caviedes, C. N. (1990) Annual and seasonal streamflow fluctuations of precipitation and streamflow in the Aconcagua River basin, Chile. *J. Hydrol.*, 120, 79-102.
- Zhang, X, Harvey, K.D., Hogg, W.D., and T.R. Yuzyk, 2001. Trends in Canadian streamflow. *Water Resour. Res.*, 37(4), 987-998.

Precipitation trend analyses

- Pellicciotti, F., Burlando, P. and van Vliet, K. (2006): Recent trends in precipitation and streamflow in the Aconcagua River Basin, central Chile. IAHS Publication (In press).
- Brunetti, M., Colacino, M., Maugeri, M., and T. Nanini, 2001. Trends in the daily intensity of precipitation in Italy. *Int. J. Climatol.*, 21, 299-316.
- Frei, C., and C. Schaer, 2001. Detection probability of trend in rare events: Theory and application to heavy precipitation in the Alpine region. *J. Climate*, 14, 1568-1584.
- Karl, T.R., and R.W. Knight, 1998. Secular trends of precipitation amount, frequency, and intensity in the United States. *Bull. Amer. Meteor. Soc.*, 79(2), 231-241.
- Osborn, T.J., Hulme, M., Jones, P.D., and T.A. Basnett, 2000. Observed trends in the daily intensity of United Kingdom precipitation. *Int. J. Climatol.*, 20, 347-364.
- Widmann, M., and C. Schaer, 1997. A principal component and long-term trend analysis of daily precipitation in Switzerland. *Int. J. Climatol.*, 17, 1333-1356.

Combined trend analyses

- Beighley, R.E., and G.E. Moglen, 2002. Trend assessment in rainfall-runoff behaviour in urbanising watersheds. *J. Hydrol. Eng.*, 7(1), 27-34.
- Groisman, P.Y., Knight, R.W., and T.R. Karl, 2001. Heavy precipitation and high streamflow in the contiguous United States: trends in the twentieth century. *Bull. Amer. Meteo. Soc.*, 82(2), 219-246.
- Molnár, P. & Ramírez, J. G. (2001) Recent trends in precipitation and streamflow in the Rio Puerco basin. *J. Climate*, 14, 2317-2328. Montecinos, A., Díaz, A. & Aceituno, P. (2000) Seasonal diagnostic and predictability of rainfall in subtropical South America based on tropical Pacific SST. *J. Climate*, 13, 746-758.
- Montecinos, A., Díaz, A. & Aceituno, P (2000) Seasonal diagnostic and predictability of rainfall in subtropical South America based on tropical pacific SST. *J. Climate*, 13, 746-758.

SO Southern Oscillation

- Rutllant, J. & Fuenzalida, H. (1991) Synoptic aspects of the central Chile rainfall variability associated with the Southern Oscillation. *Int. J. Climatol.*, 11, 63-76.
- Aceituno, P. (1988) On the functioning of the Southern Oscillation in the South America Sector. Part I: Surface Climate. *Monthly Weather Rev.*, 116, 505-524.
- Cerveny, R. S., Skeeter, B. R. & Dewey, K. F. (1987) A preliminary investigation of a relationship between South American snow cover and the southern oscillation. *Monthly Weather Rev.*, 115, 620-623.

Mann-Kendall trend test applications

- Hamed, K.H., and A.R. Rao, 1998. A modified Mann-Kendall trend test for autocorrelated data. *J. Hydrol.*, 204, 182-196.
- Yue, S., Pilon, P., and G. Cavadias, 2002. Power of the Mann-Kendall and Spearman's rho tests for detecting monotonic trends in hydrological series. *J. Hydrol.*, 259, 254-271.
- Yue, S., Pilon, P., Phinney, B., and G. Cavadias, 2002. The influence of autocorrelation on the ability to detect trend in hydrological series. *Hydrol. Process.*, in press.